ISSN 1948-0210 (online)

World Journal of *Stem Cells*

World J Stem Cells 2022 March 26; 14(3): 219-266

Published by Baishideng Publishing Group Inc

World Journal of Stem Cells

Contents

Monthly Volume 14 Number 3 March 26, 2022

REVIEW

ORIGINAL ARTICLE

Basic Study

LETTER TO THE EDITOR

World Journal of Stem Cells

Monthly Volume 14 Number 3 March 26, 2022

Contents

ABOUT COVER

Editorial Board Member of *World Journal of Stem Cells*, Yun-Bae Kim, DVM, PhD, Professor, College of Veterinary Medicine, Chungbuk National University, 1 Chungdaero, Cheongju, Chungbuk 28644, South Korea. solar93@chungbuk.ac.kr

AIMS AND SCOPE

The primary aim of *World Journal of Stem Cells* (*WJSC*, *World J Stem Cells*) is to provide scholars and readers from various fields of stem cells with a platform to publish high-quality basic and clinical research articles and communicate their research findings online. *WJSC* publishes articles reporting research results obtained in the field of stem cell biology and regenerative medicine, related to the wide range of stem cells including embryonic stem cells, germline stem cells, tissue-specific stem cells, adult stem cells, mesenchymal stromal cells, induced pluripotent stem cells, embryonal carcinoma stem cells, hemangioblasts, lymphoid progenitor cells, *etc*.

INDEXING/ABSTRACTING

The *WJSC* is now indexed in Science Citation Index Expanded (also known as SciSearch®), Journal Citation Reports/Science Edition, Biological Abstracts, BIOSIS Previews, Scopus, PubMed, and PubMed Central. The 2021 Edition of Journal Citation Reports® cites the 2020 impact factor (IF) for *WJSC* as 5.326; IF without journal self cites: 5.035; 5-year IF: 4.956; Journal Citation Indicator: 0.55; Ranking: 14 among 29 journals in cell and tissue engineering; Quartile category: Q2; Ranking: 72 among 195 journals in cell biology; and Quartile category: Q2. The *WJSC*'s CiteScore for 2020 is 3.1 and Scopus CiteScore rank 2020: Histology is 31/60; Genetics is 205/325; Genetics (clinical) is 64/87; Molecular Biology is 285/382; Cell Biology is 208/279.

RESPONSIBLE EDITORS FOR THIS ISSUE

Production Editor: *Yan-Liang Zhang*; **Production Department Director:** *Xu Guo*; **Editorial Office Director:** *Ze-Mao Gong*.

NAME OF JOURNAL
World Journal of Stem Cells

ISSN
ISSN 1948-0210 (online)

LAUNCH DATE
December 31, 2009

FREQUENCY
Monthly

EDITORS-IN-CHIEF
Shengwen Calvin Li, Carlo Ventura

EDITORIAL BOARD MEMBERS
https://www.wjgnet.com/1948-0210/editorialboard.htm

PUBLICATION DATE
March 26, 2022

INSTRUCTIONS TO AUTHORS
https://www.wjgnet.com/bpg/gerinfo/204

GUIDELINES FOR ETHICS DOCUMENTS
https://www.wjgnet.com/bpg/GerInfo/287

GUIDELINES FOR NON-NATIVE SPEAKERS OF ENGLISH
https://www.wjgnet.com/bpg/gerinfo/240

PUBLICATION ETHICS
https://www.wjgnet.com/bpg/GerInfo/288

PUBLICATION MISCONDUCT
https://www.wjgnet.com/bpg/gerinfo/208

ARTICLE PROCESSING CHARGE
https://www.wjgnet.com/bpg/gerinfo/242

STEPS FOR SUBMITTING MANUSCRIPTS
https://www.wjgnet.com/bpg/GerInfo/239

ONLINE SUBMISSION
https://www.f6publishing.com

World Journal of Stem Cells

Submit a Manuscript: https://www.f6publishing.com

World J Stem Cells 2022 March 26; 14(3): 219-230

DOI: 10.4252/wjsc.v14.i3.219

ISSN 1948-0210 (online)

REVIEW

Adult neural stem cells and schizophrenia

Ling Hu, Lei Zhang

Specialty type: Neurosciences

Provenance and peer review: Invited article; Externally peer reviewed.

Peer-review model: Single blind

Peer-review report's scientific quality classification

Grade A (Excellent): 0
Grade B (Very good): B
Grade C (Good): C, C
Grade D (Fair): D
Grade E (Poor): 0

P-Reviewer: Durán Alonso MB, Spain; Gaitanou M, Greece; Khan MM, India; Tanabe S, Japan

Received: April 6, 2021
Peer-review started: April 6, 2021
First decision: June 5, 2021
Revised: June 18, 2021
Accepted: March 7, 2022
Article in press: March 7, 2022
Published online: March 26, 2022

Ling Hu, Department of Laboratory Animal Science and Institutes of Brain Science, Fudan University, Shanghai 200032, China

Lei Zhang, Shanghai Yangzhi Rehabilitation Hospital (Shanghai Sunshine Rehabilitation Center) and Department of Anatomy and Neurobiology, Tongji University School of Medicine, Shanghai 200092, China

Corresponding author: Lei Zhang, PhD, Associate Professor, Shanghai Yangzhi Rehabilitation Hospital (Shanghai Sunshine Rehabilitation Center) and Department of Anatomy and Neurobiology, Tongji University School of Medicine, No. 1239 Siping Road, Shanghai 200092, China. leizhang1120@outlook.com

Abstract

Schizophrenia (SCZ) is a devastating and complicated mental disorder accompanied by variable positive and negative symptoms and cognitive deficits. Although many genetic risk factors have been identified, SCZ is also considered as a neurodevelopmental disorder. Elucidation of the pathogenesis and the development of treatment is challenging because complex interactions occur between these genetic risk factors and environment in essential neurodevelopmental processes. Adult neural stem cells share a lot of similarities with embryonic neural stem cells and provide a promising model for studying neuronal development in adulthood. These adult neural stem cells also play an important role in cognitive functions including temporal and spatial memory encoding and context discrimination, which have been shown to be closely linked with many psychiatric disorders, such as SCZ. Here in this review, we focus on the SCZ risk genes and the key components in related signaling pathways in adult hippocampal neural stem cells and summarize their roles in adult neurogenesis and animal behaviors. We hope that this would be helpful for the understanding of the contribution of dysregulated adult neural stem cells in the pathogenesis of SCZ and for the identification of potential therapeutic targets, which could facilitate the development of novel medication and treatment.

Key Words: Neural stem cells; Adult hippocampal neurogenesis; Schizophrenia; Risk genes; Signaling pathways; Behavior

Core Tip: This review focuses on the role of schizophrenia risk genes and related signaling pathways in adult hippocampal neurogenesis, which has been shown to play an essential role in many psychiatric disorders. We summarize the outcome of adult neural stem cells and animal behavior when these risk genes or the key components in related signaling pathways are dysregulated. We hope this will shed light on the elusive pathogenesis of schizophrenia.

Citation: Hu L, Zhang L. Adult neural stem cells and schizophrenia. *World J Stem Cells* 2022; 14(3): 219-230
URL: https://www.wjgnet.com/1948-0210/full/v14/i3/219.htm
DOI: https://dx.doi.org/10.4252/wjsc.v14.i3.219

INTRODUCTION

Schizophrenia (SCZ) is a devastating brain disorder with a prevalence of 1% worldwide. Patients typically show a subset of positive symptoms including delusions, auditory and visual hallucinations, disorganized speech and thought disorder, negative symptoms including a lack of motivation, interest and emotional blunting, lack of thought and content of speech, and/or cognitive deficits[1-3]. Although SCZ has been extensively investigated in the past few decades, the underlying cellular defects and molecular mechanism of SCZ have not been clearly established. Considerable evidence supports the notion that SCZ is the behavioral outcome of neurodevelopmental disturbance long before the onset of clinical symptoms[4]. However, it is known that neurodevelopment is not confined to the embryonic stages, and is a prolonged process continuing in adults. On the basis that the first psychotic symptoms in most patients occur in late adolescence[3], abnormal adult hippocampal neurogenesis might facilitate the emergence of hippocampal-dependent cognitive and affective deviation.

Adult neurogenesis is a complex and complicated process, which occurs in the subgranular zone (SGZ) of the dentate gyrus (DG) in mammalian brain[5]. Quiescent neural stem cells in the SGZ become activated, proliferate, differentiate, mature into glutamatergic neurons and receive innervations from the entorhinal cortex while projecting axons to the cornu ammonis 3 (CA3) region[6]. The direct evidence that defective adult neurogenesis might be involved in the etiology of SCZ originates from studies on post-mortem samples, in which the number of cells expressing Ki67, the cell proliferation marker, was reduced by 50%-60% in the SGZ[7]. In addition, patients diagnosed with SCZ present with an immature DG with impaired maturation of adult-born neurons[8].

Recently, several risk genes associated with SCZ have been identified through genome-wide association studies (GWAS), some of which are components of important signaling pathways. Given the evidence that numerous genes are implicated in the etiology of SCZ, the disease is currently accepted as a polygenic disorder caused by the complex interplay between genetic and environmental factors[9-11]. In this review, we mainly focus on the roles of some risk genes and key signaling pathways implicated in SCZ, during the process of adult neurogenesis.

SCZ RISK GENES

Disrupted in SCZ 1

Disrupted in SCZ 1 (DISC1), one of the widely-studied risk genes for SCZ, was originally identified in a large Scottish family. A balanced chromosomal translocation t(1;11)(q42.1;q14.3) leads to disruption of the C-terminal region in *DISC1* gene, which is co-segregated with mental disorders such as SCZ and depression[12-15]. Suppression of *Disc1* expression perturbs neural progenitor proliferation during adult neurogenesis through the glycogen synthase kinase 3β (Gsk-3β)/β-catenin pathway. Furthermore, Gsk-3 inhibitors attenuate progenitor proliferation and behavioral defects caused by *Disc1* suppression [16]. Various studies have shown that alteration of *Disc1* expression impedes the maturation of new-born neurons including aberrant morphological development, mis-positioning of new DG granule cells, enhanced dendritic outgrowth and defects in axonal targeting[17-20]. In addition, Disc1 works as a scaffold protein and interacts with many signaling effectors to regulate adult neurogenesis. For example, Disc1 directly interacts with Girdin, which regulates the differentiation, maturation, migration, and cytoskeleton organization of adult neural progenitors and inhibits Akt activity[21,22]. Interestingly, the cellular defects and hippocampal-dependent behavioral deficits caused by *Disc1* deficiency can be largely rescued by the administration of rapamycin, an inhibitor of mammalian target of rapamycin (mTOR), which is the Akt downstream effector[23]. In addition, an interplay between intrinsic Disc1 and extrinsic γ-amino butyric acid (GABA) signaling also contributes to dendritic growth and synapse formation in immature neurons *via* the Akt-mTOR pathway[24-26]. Collectively, *DISC1* regulates multiple steps of adult neurogenesis through interaction with key effectors of various signaling

pathways directly and indirectly.

Neuregulin-1

Neuregulin-1 (NRG1) was identified as a risk factor for SCZ more than a decade ago through a genome-wide scan of SCZ families in Iceland, which was later supported by many associated studies[27-29]. NRG1 binds to ErbB2-4, a family of epidermal growth factor-like tyrosine kinases, and defective NRG1/ErbB4 signaling is found in the prefrontal cortex and hippocampus of SCZ patients[30-32]. Moreover, multiple studies have proven that NRG1 is associated with affective behavior and the pathology of SCZ[33-36]. It has been reported that the administration of Nrg1 displays robust antidepressant-like behaviors accompanied by increased ventral DG cell proliferation and neurogenesis in the caudal DG without alteration of neuronal fate[37]. The finding that it interacts with molecules in the glutamatergic synapse implies a role of Nrg1 in adult plasticity[38,39]. These observations suggest that NRG1/ErbB4 signaling might participate in the process of adult neurogenesis.

Synaptosomal-associated protein, 25 kDa

Synaptosomal-associated protein, 25 kDa (SNAP-25) is a soluble N-ethylmaleimide-sensitive factor attachment protein receptor protein, which plays a crucial role in modulating synaptic exocytosis[40-42]. Genetic studies and genome-wide meta-analyses have revealed its close association with multiple mental diseases including SCZ[43-46]. *Snap-25* mutant mice display histologically and electrophysiologically immature DG neurons, leading to a severe working memory deficit[47]. Interestingly, selective inactivation of *Snap-25* in adult neural stem cells results in enhancement in proximal dendritic branching of new-born neurons in the DG and robust efferent mossy fiber output to the CA3 region[48]. So far, the immature DG phenotype and similar schizophrenic-like behaviors have been found in *Schnurri-2* knockout[49], *Snap-25* mutant[47], and calmodulin-dependent protein kinase II (CaMKII) knockout mice[49]. Importantly, this immature DG phenomenon has also been observed in the post-mortem brains from schizophrenic patients[8,50], suggesting a close link between disrupted maturation of adult-born cells and schizophrenic-like behaviors.

Calcium voltage-gated channel subunit alpha1 C

Calcium voltage-gated channel subunit alpha1 C (CACNA1C) encodes the Cav1.2 subunit of voltage-gated calcium channels, whose genetic variations have been reported to increase the risk of psychiatric disorders including SCZ[51,52]. GWAS have identified several single-nucleotide polymorphisms (SNPs) of the *CACNA1C* gene, which show a close link with SCZ[53-55]. Furthermore, large exome sequencing studies have defined disruptive mutations within calcium ion channels in schizophrenic patients[56]. With regard to the functions of *CACNA1C*, it has received a lot of attention and been studied extensively in animal models. The results obtained from mice have shown that reduced gene dosage of *Cacna1c* leads to behavioral impairments including reduced locomotion and fear learning as well as impaired spatial memory[57-59]. Cacna1c has also been found to mediate brain-derived neurotrophic factor production and thus might also play a role in regulating adult neurogenesis. Indeed, studies on mice with ablation of *Cacna1c* showed that adult neurogenesis was impaired as revealed by decreased proliferation of progenitors and survival of new-born neurons, which coincides with its cognitive deficits[60, 61].

Reelin

Reelin, an extracellular matrix glycoprotein which is mainly synthesized by Cajal-Retzius cells in the cortical marginal zone of the telencephalon at embryonic stages and in a subpopulation of GABAergic interneurons in adulthood, has been shown to play an essential role in embryonic and adult brains[62-66]. Reelin exerts its biological functions by binding to integrin receptors and then triggers phosphorylation of disabled-1 (Dab1). Phosphorylated Dab1 then recruits downstream molecules such as Crk/CrkL, phosphatidylinositol 3-kinase and Nckβ to their functional compartment[67,68]. It has been reported that *Reelin* mRNA and protein levels are reduced by almost 50% in cortical and hippocampal regions in post-mortem brains and serum of schizophrenic patients[69-71]. In the adult brain, Reelin is synthesized and secreted by GABAergic interneurons, and the reduction of glutamic acid decarboxylase 67 (Gad67), an enzyme which catalyzes the transition of glutamate to GABA, has also been observed in the same brains[72]. Thus, the authors postulate that decreases in neuropil and dendritic spines observed in the prefrontal cortex of post-mortem brains may be an outcome of disturbed GABAergic function and an associated decrease in Reelin secretion[73]. In addition, Li *et al* identified six SNPs located in Intron 29 of the *REELIN* gene, which have a significant association with the risk of SCZ in the Chinese population[74]. Similarly, other groups have reported a gender-specific (women) association between SNPs in *REELIN* and SCZ[75-77]. Studies on animal models have also found that heterozygous Reeler mice (*Reelin* mutant) display many neuroanatomic and neurochemical changes similar to those described in patients with SCZ. These changes include altered synaptic plasticity, decreased dendritic spine density, reduced *Gad67* mRNA and protein levels in the frontal cortex and behavioral disturbances in associative memory and prepulse inhibition, whereas supplementation with REELIN can partially restore these abnormalities[78-83]. Inactivation of Reelin signaling

also leads to impaired adult neurogenesis as shown by decreased proliferation, aberrant migration and dendritic development of new-born neurons[84-86]. Taken together, these findings suggest that reduced *REELIN* expression in SCZ might have an impact on adult neurogenesis.

Other molecules

Apart from the susceptibility genes mentioned above, other molecules are also implicated in adult neurogenesis and SCZ, such as miR-19. A recent study revealed that miR-19 is enriched in adult hippocampal neural progenitor cells and regulates the migration of newborn neurons, highlighting its critical role in adult hippocampal neurogenesis[87]. Furthermore, miR-19 is found to be abnormally expressed in neural progenitor cells derived from induced pluripotent stem cells of schizophrenic patients[87], who show aberrant cell migration in brain. Thus, these data suggest that miR-19 may be a molecule associated with adult hippocampal neurogenesis and SCZ.

SCZ AND RELATED SIGNALING PATHWAYS CONTROLLING ADULT NEUROGENESIS

Wnt signaling

Wnt signaling, one of the most conserved molecular pathways, plays a vital role in the neurodevelopmental process and regulates the function and structure of the adult nervous system[88-90]. Wnts comprise a large cohort of secreted glycoproteins which interact with extracellular receptors, Frizzled or Low-density lipoprotein receptors 5/6[91]. Consequently, the activation of scaffold protein Dishevelled (Dvl) leads to inactivation of Gsk-3β. Normally, Gsk-3β promotes the degradation of β-catenin *via* phosphorylation. The inactivation of *Gsk-3β* finally causes the accumulation and translocation of β-catenin to the nucleus where it binds to the transcription factor Tcf/Lef family and activates target genes.

Wnt signaling is involved in brain development during the embryonic stages including cortical patterning, cell adhesion, migration, cell fate determination and proliferation[38,92,93]. In the adult brain, growing evidence indicates that components of Wnt signaling regulate multiple stages of adult neurogenesis including proliferation, fate commitment and synaptic plasticity[90,94,95]. For example, loss of *Wnt7a* expression dramatically reduced the neural stem cell population, increased the rate of cell cycle exit in neural progenitors and dramatically impaired dendritic development in the hippocampal DG of adult mice by modulating the β-catenin-cyclin D1 and β-catenin-neurogenin 2 pathway, respectively[96]. Knockdown of *Wnt5a* impaired neuronal differentiation and dendritic development of adult-born neurons by activating Wnt/c-Jun N-terminal kinase (JNK) and Wnt/CaMKII signaling[97].

Disturbances in components of the Wnt signaling pathway have been reported in post-mortem brains of patients diagnosed with SCZ. These abnormalities include: (1) Reduced GSK-3β levels in the prefrontal cortex, hippocampus and cerebrospinal fluid of patients[98-100]. It is noteworthy that medications which may treat symptoms of SCZ in clinical use, also modulate the levels and activity of AKT, GSK-3 and WNT-related intracellular signaling[101,102]; (2) A reduction in Dickkopf WNT signaling pathway inhibitor 3 (DKK3) mRNA, a suppressive factor of WNT signaling, in the cerebral cortex and an increase in the Adenomatous polyposis coli (APC) expression, acting as an antagonist of the WNT signaling pathway, is found in schizophrenic brain[103]; and (3) The expression of WNT-related genes in canonical WNT signaling was attenuated in whole blood in a sample of SCZ patients using an enzyme immunoassay. Furthermore, plasma levels of soluble DKK1 and SCLEROSTIN were downregulated in patients[104]. Wnt signaling in SCZ was further confirmed in animal studies. One of the first animal models included *Dvl* knockout mice, which exhibited reduced social interaction and deficits in prepulse inhibition of acoustic and tactile startle[105]. In addition, Disc1 exerts its function through Wnt signaling directly or indirectly[17]. Subsequent studies have shown that *Apc* and *β-catenin* knockout mice also display behavioral deviations related to SCZ[106,107]. In addition, the component of Wnt signaling, T-cell factor 4 (Tcf4), has received increased attention as the SNPs in its non-coding regions are associated with an increased risk of SCZ in GWAS[108-111]. *Tcf4* also plays an important role in adult neurogenesis. *Tcf4* heterozygous mice showed a decreased hippocampal neural stem cell pool, and impaired maturation and survival of adult-born neurons[112]. Thus, it is likely that dysregulation of the WNT signaling pathway contributes to adult neurogenesis deficits observed in SCZ patients.

Notch signaling

The Notch signaling pathway plays a crucial role in a wide array of neurodevelopmental processes and adult neurogenesis. Notch receptors are single-pass transmembrane heterodimers and four isoforms (Notch1-4) have been identified. In mammals, there are several types of Notch ligands including three Delta/Delta-like molecules (Dll/Dlk-1, -3, and -4) and two Serrate/Jagged molecules (Jag-1 and Jag-2). The heterodimeric Notch receptor undergoes proteolytic cleavage after binding to one of its ligands. This process liberates the Notch intracellular domain (NICD) which later translocates to the nucleus and interacts with the DNA-binding protein RBPj. The NICD-RBPj conjugation in turn works as a transcriptional activator and stimulates the expression of basic helix-loop-helix transcription factors, such as the

Table 1 Studies of schizophrenia risk genes and related signaling pathways in adult neurogenesis

Genes or signaling pathways	Effects on adult neurogenesis	Behavior deviations	Ref.	Post-mortem or genetic studies
DISC1	Suppression of *Disc1* expression results in accelerated neuronal integration, mispositioning of new DG granule cells, accelerated dendritic development, premature cell cycle exit and differentiation	Hyper-locomotion, depressive-like behavior, cognitive deficits (object place recognition test, Morris water maze test)	[16,18,20,23]	[130-132]
NRG1	NRG1 treatment induces increased ventral DG cell proliferation and neurogenesis.NRG1 regulates both excitatory and inhibitory synaptic transmission in the adult brain and abnormal neurotransmission and/or synaptic plasticity have been observed in the schizophrenic brain	*Nrg1* hypomorphs showed hyperactivity in a number of tests, including the novel open-field test and the alternating-Y maze, impaired social behavior and increased aggression	[36,37,133]	[30-32]
SNAP-25	*Snap-25* mutant mice display histologically and electrophysiologically immature DG neurons. Inactivation of *Snap-25* in adult neural stem cells results in enhancement of proximal dendritic branching of new-born neurons in the DG and robust efferent mossy fiber output to the CA3 region	Working memory deficits, impaired contextual fear-discrimination learning	[47,48]	[43,44]
CACNA1C	*Cacna1c* deletion results in decreased progenitor proliferation and reduced survival of new-born neurons	*Cacna1c* heterozygous mice display reduced locomotion, fear learning, and impaired spatial memory	[57-61]	[53-56]
Reelin	Adult Reeler mutants show decreased proliferation, aberrant migration and dendritic development of new-born neurons	Heterozygous Reeler mice show a significant reduction in contextual fear conditioned learning and an age-dependent decrease in prepulse inhibition of startle	[82-84,86]	[69-71,74-77]
Wnt signaling	Overexpression of stabilized β-catenin leads to enlarged brain and expanded neural precursor population. *Wnt7a* knockout mice show fewer neural stem cells. *Wnt5a* knockdown decreases the number of immature neurons. *Tcf4* heterozygotes show reduced size of neural stem cell pool and impaired maturation and survival of adult-born neurons	*Dvl* knockout mice display reduced social interaction and deficits in prepulse inhibition of acoustic and tactile startle. Forebrain-specific *β-catenin* knockout mice show a depression-like phenotype. *Apc* heterozygote shows hypoactivity and a severe performance deficit in working memory	[90,96,106,107,134,135]	[98-100,112]
Notch signaling	Inactivation of *Notch1* blocks self-renewal of neural stem cells, reduces mitotic progenitors and neurogenesis. Adult deletion of *RBPj* leads to depletion and exhaustion of neural stem cells	*Notch1* heterozygote displays deficits in spatial learning and memory	[100,121,122,128,129]	[116-118]

APC: Adenomatous polyposis coli; CA3: Cornu ammonis 3; CACNA1C: Calcium voltage-gated channel subunit alpha1 c; DG: Dentate gyrus; DISC1: Disrupted in schizophrenia 1; Dvl: Dishevelled; NRG1: Neuregulin-1; SNAP-25: Synaptosomal-associated protein, 25kDa; Tcf4: T-cell factor 4.

Hairy-Enhancer of Split[113-115]. A number of *NOTCH4* variants and haplotypes have been found to be associated with SCZ[116,117]. This finding was subsequently confirmed by large GWAS[118]. Recent studies showed that the plasma levels of secreted NOTCH ligands (DLL1 and DLK-1) were elevated, whereas the levels of PRESENILIN-1, CREB-binding protein and RBPj were decreased in microarray analyses of whole blood from a large sample of SCZ patients[119]. In the study by Xue *et al*[120], Risperidone, one of medications used to treat SCZ, ameliorated cognitive deficits and cell proliferation by modulating the activity of Notch signaling in a murine model of SCZ. Mice deficient in Notch signaling have been shown to display spatial learning and memory impairment[121,122].

Notch signaling has long been identified as a factor which plays a primary role in adult neurogenesis. Notch receptors are expressed in neural stem cells and progenitors in the SGZ (Type-1 cells)[123,124]. In neural stem cells, the components of Notch signaling mainly work together to maintain an undifferentiated, proliferative state and therefore preserve the neural stem cell pool[125-127]. Indeed, inactivation of *Notch1* leads to reduced mitotic progenitors and neurogenesis[128], whereas activation of Notch1 signaling increases neural stem cells and results in the generation of glial cells at the expense of neurons [124]. Adult deletion of *RBPj* results in depletion and exhaustion of neural stem cells[129]. Therefore, NOTCH signaling might be involved in the etiology of SCZ and especially cognitive deficits.

CONCLUSION

Accumulating evidence shows that impaired adult neurogenesis in the hippocampus is implicated in the pathogenesis of SCZ (Table 1). Decreased proliferation of adult neural stem cells in the DG and reduced hippocampal volume often coincide with impaired cognitive and affective functions, which are

commonly identified in animal models and schizophrenic patients. The question of how dysregulation of neurogenesis in the adult brain participates in the progression of SCZ arouses more and more interests. As SCZ is a neurodevelopmental disorder, many risk genes have an impact on both early brain development and adult neurogenesis. Thus, adult neurogenesis provides an attractive model to study the neurodevelopmental process, as it generalizes each step of neuronal development, including proliferation, specification, migration, dendritic branching and synapse formation. Although numerous susceptibility genes/molecules have been uncovered by genetic analysis and high-throughput sequencing, their functions still remain elusive. The studies on the roles of these susceptibility genes/signaling pathways in adult neurogenesis might shed some light on the understanding the etiology of SCZ and identifying potential therapeutic targets, which could facilitate the development of novel medication and treatment.

FOOTNOTES

Author contributions: Hu L and Zhang L wrote the manuscript and prepared the table.

Supported by Shanghai Pujiang Program, No. 20PJ1413300.

Conflict-of-interest statement: Authors declare no conflict of interests for this article.

Country/Territory of origin: China

ORCID number: Ling Hu 0000-0003-4135-4561; Lei Zhang 0000-0001-7242-5292.

S-Editor: Chang KL
L-Editor: A
P-Editor: Chang KL

REFERENCES

1 **Andreasen NC**. Symptoms, signs, and diagnosis of schizophrenia. *Lancet* 1995; **346**: 477-481 [PMID: 7637483 DOI: 10.1016/s0140-6736(95)91325-4]
2 **Jones CA**, Watson DJ, Fone KC. Animal models of schizophrenia. *Br J Pharmacol* 2011; **164**: 1162-1194 [PMID: 21449915 DOI: 10.1111/j.1476-5381.2011.01386.x]
3 **Marder SR**, Cannon TD. Schizophrenia. *N Engl J Med* 2019; **381**: 1753-1761 [PMID: 31665579 DOI: 10.1056/NEJMra1808803]
4 **Birnbaum R**, Weinberger DR. Genetic insights into the neurodevelopmental origins of schizophrenia. *Nat Rev Neurosci* 2017; **18**: 727-740 [PMID: 29070826 DOI: 10.1038/nrn.2017.125]
5 **Gage FH**, Temple S. Neural stem cells: generating and regenerating the brain. *Neuron* 2013; **80**: 588-601 [PMID: 24183012 DOI: 10.1016/j.neuron.2013.10.037]
6 **Toda T**, Parylak SL, Linker SB, Gage FH. The role of adult hippocampal neurogenesis in brain health and disease. *Mol Psychiatry* 2019; **24**: 67-87 [PMID: 29679070 DOI: 10.1038/s41380-018-0036-2]
7 **Reif A**, Fritzen S, Finger M, Strobel A, Lauer M, Schmitt A, Lesch KP. Neural stem cell proliferation is decreased in schizophrenia, but not in depression. *Mol Psychiatry* 2006; **11**: 514-522 [PMID: 16415915 DOI: 10.1038/sj.mp.4001791]
8 **Walton NM**, Zhou Y, Kogan JH, Shin R, Webster M, Gross AK, Heusner CL, Chen Q, Miyake S, Tajinda K, Tamura K, Miyakawa T, Matsumoto M. Detection of an immature dentate gyrus feature in human schizophrenia/bipolar patients. *Transl Psychiatry* 2012; **2**: e135 [PMID: 22781168 DOI: 10.1038/tp.2012.56]
9 **International Schizophrenia Consortium**, Purcell SM, Wray NR, Stone JL, Visscher PM, O'Donovan MC, Sullivan PF, Sklar P. Common polygenic variation contributes to risk of schizophrenia and bipolar disorder. *Nature* 2009; **460**: 748-752 [PMID: 19571811 DOI: 10.1038/nature08185]
10 **Lewis DA**, Lieberman JA. Catching up on schizophrenia: natural history and neurobiology. *Neuron* 2000; **28**: 325-334 [PMID: 11144342 DOI: 10.1016/s0896-6273(00)00111-2]
11 **Owen MJ**, Sawa A, Mortensen PB. Schizophrenia. *Lancet* 2016; **388**: 86-97 [PMID: 26777917 DOI: 10.1016/S0140-6736(15)01121-6]
12 **Blackwood DH**, Fordyce A, Walker MT, St Clair DM, Porteous DJ, Muir WJ. Schizophrenia and affective disorders--cosegregation with a translocation at chromosome 1q42 that directly disrupts brain-expressed genes: clinical and P300 findings in a family. *Am J Hum Genet* 2001; **69**: 428-433 [PMID: 11443544 DOI: 10.1086/321969]
13 **Taylor MS**, Devon RS, Millar JK, Porteous DJ. Evolutionary constraints on the Disrupted in Schizophrenia locus.

Genomics 2003; **81**: 67-77 [PMID: 12573262 DOI: 10.1016/s0888-7543(02)00026-5]
14 **St Clair D**, Blackwood D, Muir W, Carothers A, Walker M, Spowart G, Gosden C, Evans HJ. Association within a family of a balanced autosomal translocation with major mental illness. *Lancet* 1990; **336**: 13-16 [PMID: 1973210 DOI: 10.1016/0140-6736(90)91520-k]
15 **Kuroda K**, Yamada S, Tanaka M, Iizuka M, Yano H, Mori D, Tsuboi D, Nishioka T, Namba T, Iizuka Y, Kubota S, Nagai T, Ibi D, Wang R, Enomoto A, Isotani-Sakakibara M, Asai N, Kimura K, Kiyonari H, Abe T, Mizoguchi A, Sokabe M, Takahashi M, Yamada K, Kaibuchi K. Behavioral alterations associated with targeted disruption of exons 2 and 3 of the Disc1 gene in the mouse. *Hum Mol Genet* 2011; **20**: 4666-4683 [PMID: 21903668 DOI: 10.1093/hmg/ddr400]
16 **Mao Y**, Ge X, Frank CL, Madison JM, Koehler AN, Doud MK, Tassa C, Berry EM, Soda T, Singh KK, Biechele T, Petryshen TL, Moon RT, Haggarty SJ, Tsai LH. Disrupted in schizophrenia 1 regulates neuronal progenitor proliferation *via* modulation of GSK3beta/beta-catenin signaling. *Cell* 2009; **136**: 1017-1031 [PMID: 19303846 DOI: 10.1016/j.cell.2008.12.044]
17 **Wu Q**, Li Y, Xiao B. DISC1-related signaling pathways in adult neurogenesis of the hippocampus. *Gene* 2013; **518**: 223-230 [PMID: 23353011 DOI: 10.1016/j.gene.2013.01.015]
18 **Duan X**, Chang JH, Ge S, Faulkner RL, Kim JY, Kitabatake Y, Liu XB, Yang CH, Jordan JD, Ma DK, Liu CY, Ganesan S, Cheng HJ, Ming GL, Lu B, Song H. Disrupted-In-Schizophrenia 1 regulates integration of newly generated neurons in the adult brain. *Cell* 2007; **130**: 1146-1158 [PMID: 17825401 DOI: 10.1016/j.cell.2007.07.010]
19 **Kang E**, Burdick KE, Kim JY, Duan X, Guo JU, Sailor KA, Jung DE, Ganesan S, Choi S, Pradhan D, Lu B, Avramopoulos D, Christian K, Malhotra AK, Song H, Ming GL. Interaction between FEZ1 and DISC1 in regulation of neuronal development and risk for schizophrenia. *Neuron* 2011; **72**: 559-571 [PMID: 22099459 DOI: 10.1016/j.neuron.2011.09.032]
20 **Faulkner RL**, Jang MH, Liu XB, Duan X, Sailor KA, Kim JY, Ge S, Jones EG, Ming GL, Song H, Cheng HJ. Development of hippocampal mossy fiber synaptic outputs by new neurons in the adult brain. *Proc Natl Acad Sci U S A* 2008; **105**: 14157-14162 [PMID: 18780780 DOI: 10.1073/pnas.0806658105]
21 **Kim JY**, Duan X, Liu CY, Jang MH, Guo JU, Pow-anpongkul N, Kang E, Song H, Ming GL. DISC1 regulates new neuron development in the adult brain *via* modulation of AKT-mTOR signaling through KIAA1212. *Neuron* 2009; **63**: 761-773 [PMID: 19778506 DOI: 10.1016/j.neuron.2009.08.008]
22 **Enomoto A**, Murakami H, Asai N, Morone N, Watanabe T, Kawai K, Murakumo Y, Usukura J, Kaibuchi K, Takahashi M. Akt/PKB regulates actin organization and cell motility *via* Girdin/APE. *Dev Cell* 2005; **9**: 389-402 [PMID: 16139227 DOI: 10.1016/j.devcel.2005.08.001]
23 **Zhou M**, Li W, Huang S, Song J, Kim JY, Tian X, Kang E, Sano Y, Liu C, Balaji J, Wu S, Zhou Y, Parivash SN, Ehninger D, He L, Song H, Ming GL, Silva AJ. mTOR Inhibition ameliorates cognitive and affective deficits caused by Disc1 knockdown in adult-born dentate granule neurons. *Neuron* 2013; **77**: 647-654 [PMID: 23439118 DOI: 10.1016/j.neuron.2012.12.033]
24 **Platel JC**, Stamboulian S, Nguyen I, Bordey A. Neurotransmitter signaling in postnatal neurogenesis: The first leg. *Brain Res Rev* 2010; **63**: 60-71 [PMID: 20188124 DOI: 10.1016/j.brainresrev.2010.02.004]
25 **Kim JY**, Liu CY, Zhang F, Duan X, Wen Z, Song J, Feighery E, Lu B, Rujescu D, St Clair D, Christian K, Callicott JH, Weinberger DR, Song H, Ming GL. Interplay between DISC1 and GABA signaling regulates neurogenesis in mice and risk for schizophrenia. *Cell* 2012; **148**: 1051-1064 [PMID: 22385968 DOI: 10.1016/j.cell.2011.12.037]
26 **Wei J**, Graziane NM, Gu Z, Yan Z. DISC1 Protein Regulates γ-Aminobutyric Acid, Type A (GABAA) Receptor Trafficking and Inhibitory Synaptic Transmission in Cortical Neurons. *J Biol Chem* 2015; **290**: 27680-27687 [PMID: 26424793 DOI: 10.1074/jbc.M115.656173]
27 **Stefansson H**, Sigurdsson E, Steinthorsdottir V, Bjornsdottir S, Sigmundsson T, Ghosh S, Brynjolfsson J, Gunnarsdottir S, Ivarsson O, Chou TT, Hjaltason O, Birgisdottir B, Jonsson H, Gudnadottir VG, Gudmundsdottir E, Bjornsson A, Ingvarsson B, Ingason A, Sigfusson S, Hardardottir H, Harvey RP, Lai D, Zhou M, Brunner D, Mutel V, Gonzalo A, Lemke G, Sainz J, Johannesson G, Andresson T, Gudbjartsson D, Manolescu A, Frigge ML, Gurney ME, Kong A, Gulcher JR, Petursson H, Stefansson K. Neuregulin 1 and susceptibility to schizophrenia. *Am J Hum Genet* 2002; **71**: 877-892 [PMID: 12145742 DOI: 10.1086/342734]
28 **Li D**, Collier DA, He L. Meta-analysis shows strong positive association of the neuregulin 1 (NRG1) gene with schizophrenia. *Hum Mol Genet* 2006; **15**: 1995-2002 [PMID: 16687441 DOI: 10.1093/hmg/ddl122]
29 **Agim ZS**, Esendal M, Briollais L, Uyan O, Meschian M, Martinez LA, Ding Y, Basak AN, Ozcelik H. Discovery, validation and characterization of Erbb4 and Nrg1 haplotypes using data from three genome-wide association studies of schizophrenia. *PLoS One* 2013; **8**: e53042 [PMID: 23301017 DOI: 10.1371/journal.pone.0053042]
30 **Mei L**, Nave KA. Neuregulin-ERBB signaling in the nervous system and neuropsychiatric diseases. *Neuron* 2014; **83**: 27-49 [PMID: 24991953 DOI: 10.1016/j.neuron.2014.06.007]
31 **Barakat A**, Dean B, Scarr E, Evin G. Decreased Neuregulin 1 C-terminal fragment in Brodmann's area 6 of patients with schizophrenia. *Schizophr Res* 2010; **124**: 200-207 [PMID: 20926259 DOI: 10.1016/j.schres.2010.09.001]
32 **Chong VZ**, Thompson M, Beltaifa S, Webster MJ, Law AJ, Weickert CS. Elevated neuregulin-1 and ErbB4 protein in the prefrontal cortex of schizophrenic patients. *Schizophr Res* 2008; **100**: 270-280 [PMID: 18243664 DOI: 10.1016/j.schres.2007.12.474]
33 **Bertram I**, Bernstein HG, Lendeckel U, Bukowska A, Dobrowolny H, Keilhoff G, Kanakis D, Mawrin C, Bielau H, Falkai P, Bogerts B. Immunohistochemical evidence for impaired neuregulin-1 signaling in the prefrontal cortex in schizophrenia and in unipolar depression. *Ann N Y Acad Sci* 2007; **1096**: 147-156 [PMID: 17405926 DOI: 10.1196/annals.1397.080]
34 **Georgieva L**, Dimitrova A, Ivanov D, Nikolov I, Williams NM, Grozeva D, Zaharieva I, Toncheva D, Owen MJ, Kirov G, O'Donovan MC. Support for neuregulin 1 as a susceptibility gene for bipolar disorder and schizophrenia. *Biol Psychiatry* 2008; **64**: 419-427 [PMID: 18466881 DOI: 10.1016/j.biopsych.2008.03.025]
35 **Réthelyi JM**, Bakker SC, Polgár P, Czobor P, Strengman E, Pásztor PI, Kahn RS, Bitter I. Association study of NRG1, DTNBP1, RGS4, G72/G30, and PIP5K2A with schizophrenia and symptom severity in a Hungarian sample. *Am J Med*

Genet B Neuropsychiatr Genet 2010; **153B**: 792-801 [PMID: 19937977 DOI: 10.1002/ajmg.b.31049]

36 **Mei L**, Xiong WC. Neuregulin 1 in neural development, synaptic plasticity and schizophrenia. *Nat Rev Neurosci* 2008; **9**: 437-452 [PMID: 18478032 DOI: 10.1038/nrn2392]

37 **Mahar I**, MacIsaac A, Kim JJ, Qiang C, Davoli MA, Turecki G, Mechawar N. Effects of neuregulin-1 administration on neurogenesis in the adult mouse hippocampus, and characterization of immature neurons along the septotemporal axis. *Sci Rep* 2016; **6**: 30467 [PMID: 27469430 DOI: 10.1038/srep30467]

38 **Toro CT**, Deakin JF. Adult neurogenesis and schizophrenia: a window on abnormal early brain development? *Schizophr Res* 2007; **90**: 1-14 [PMID: 17123784 DOI: 10.1016/j.schres.2006.09.030]

39 **Seshadri S**, Faust T, Ishizuka K, Delevich K, Chung Y, Kim SH, Cowles M, Niwa M, Jaaro-Peled H, Tomoda T, Lai C, Anton ES, Li B, Sawa A. Interneuronal DISC1 regulates NRG1-ErbB4 signalling and excitatory-inhibitory synapse formation in the mature cortex. *Nat Commun* 2015; **6**: 10118 [PMID: 26656849 DOI: 10.1038/ncomms10118]

40 **Jahn R**, Lang T, Südhof TC. Membrane fusion. *Cell* 2003; **112**: 519-533 [PMID: 12600315 DOI: 10.1016/s0092-8674(03)00112-0]

41 **Sudhof TC**. The synaptic vesicle cycle. *Annu Rev Neurosci* 2004; **27**: 509-547 [PMID: 15217342 DOI: 10.1146/annurev.neuro.26.041002.131412]

42 **Karmakar S**, Sharma LG, Roy A, Patel A, Pandey LM. Neuronal SNARE complex: A protein folding system with intricate protein-protein interactions, and its common neuropathological hallmark, SNAP25. *Neurochem Int* 2019; **122**: 196-207 [PMID: 30517887 DOI: 10.1016/j.neuint.2018.12.001]

43 **Lewis CM**, Levinson DF, Wise LH, DeLisi LE, Straub RE, Hovatta I, Williams NM, Schwab SG, Pulver AE, Faraone SV, Brzustowicz LM, Kaufmann CA, Garver DL, Gurling HM, Lindholm E, Coon H, Moises HW, Byerley W, Shaw SH, Mesen A, Sherrington R, O'Neill FA, Walsh D, Kendler KS, Ekelund J, Paunio T, Lönnqvist J, Peltonen L, O'Donovan MC, Owen MJ, Wildenauer DB, Maier W, Nestadt G, Blouin JL, Antonarakis SE, Mowry BJ, Silverman JM, Crowe RR, Cloninger CR, Tsuang MT, Malaspina D, Harkavy-Friedman JM, Svrakic DM, Bassett AS, Holcomb J, Kalsi G, McQuillin A, Brynjolfson J, Sigmundsson T, Petursson H, Jazin E, Zoëga T, Helgason T. Genome scan meta-analysis of schizophrenia and bipolar disorder, part II: Schizophrenia. *Am J Hum Genet* 2003; **73**: 34-48 [PMID: 12802786 DOI: 10.1086/376549]

44 **Ramos-Miguel A**, Barakauskas V, Alamri J, Miyauchi M, Barr AM, Beasley CL, Rosoklija G, Mann JJ, Dwork AJ, Moradian A, Morin GB, Honer WG. The SNAP25 Interactome in Ventromedial Caudate in Schizophrenia Includes the Mitochondrial Protein ARF1. *Neuroscience* 2019; **420**: 97-111 [PMID: 30610939 DOI: 10.1016/j.neuroscience.2018.12.045]

45 **Thompson PM**, Sower AC, Perrone-Bizzozero NI. Altered levels of the synaptosomal associated protein SNAP-25 in schizophrenia. *Biol Psychiatry* 1998; **43**: 239-243 [PMID: 9513732 DOI: 10.1016/S0006-3223(97)00204-7]

46 **Thompson PM**, Egbufoama S, Vawter MP. SNAP-25 reduction in the hippocampus of patients with schizophrenia. *Prog Neuropsychopharmacol Biol Psychiatry* 2003; **27**: 411-417 [PMID: 12691775 DOI: 10.1016/S0278-5846(03)00027-7]

47 **Ohira K**, Kobayashi K, Toyama K, Nakamura HK, Shoji H, Takao K, Takeuchi R, Yamaguchi S, Kataoka M, Otsuka S, Takahashi M, Miyakawa T. Synaptosomal-associated protein 25 mutation induces immaturity of the dentate granule cells of adult mice. *Mol Brain* 2013; **6**: 12 [PMID: 23497716 DOI: 10.1186/1756-6606-6-12]

48 **Gustus KC**, Li L, Chander P, Weick JP, Wilson MC, Cunningham LA. Genetic inactivation of synaptosomal-associated protein 25 (SNAP-25) in adult hippocampal neural progenitors impairs pattern discrimination learning but not survival or structural maturation of newborn dentate granule cells. *Hippocampus* 2018; **28**: 735-744 [PMID: 29995325 DOI: 10.1002/hipo.23008]

49 **Yamasaki N**, Maekawa M, Kobayashi K, Kajii Y, Maeda J, Soma M, Takao K, Tanda K, Ohira K, Toyama K, Kanzaki K, Fukunaga K, Sudo Y, Ichinose H, Ikeda M, Iwata N, Ozaki N, Suzuki H, Higuchi M, Suhara T, Yuasa S, Miyakawa T. Alpha-CaMKII deficiency causes immature dentate gyrus, a novel candidate endophenotype of psychiatric disorders. *Mol Brain* 2008; **1**: 6 [PMID: 18803808 DOI: 10.1186/1756-6606-1-6]

50 **Shin R**, Kobayashi K, Hagihara H, Kogan JH, Miyake S, Tajinda K, Walton NM, Gross AK, Heusner CL, Chen Q, Tamura K, Miyakawa T, Matsumoto M. The immature dentate gyrus represents a shared phenotype of mouse models of epilepsy and psychiatric disease. *Bipolar Disord* 2013; **15**: 405-421 [PMID: 23560889 DOI: 10.1111/bdi.12064]

51 **Takahashi S**, Glatt SJ, Uchiyama M, Faraone SV, Tsuang MT. Meta-analysis of data from the Psychiatric Genomics Consortium and additional samples supports association of CACNA1C with risk for schizophrenia. *Schizophr Res* 2015; **168**: 429-433 [PMID: 26276307 DOI: 10.1016/j.schres.2015.07.033]

52 **Hamshere ML**, Walters JT, Smith R, Richards AL, Green E, Grozeva D, Jones I, Forty L, Jones L, Gordon-Smith K, Riley B, O'Neill FA, Kendler KS, Sklar P, Purcell S, Kranz J; Schizophrenia Psychiatric Genome-wide Association Study Consortium; Wellcome Trust Case Control Consortium+; Wellcome Trust Case Control Consortium 2, Morris D, Gill M, Holmans P, Craddock N, Corvin A, Owen MJ, O'Donovan MC. Genome-wide significant associations in schizophrenia to ITIH3/4, CACNA1C and SDCCAG8, and extensive replication of associations reported by the Schizophrenia PGC. *Mol Psychiatry* 2013; **18**: 708-712 [PMID: 22614287 DOI: 10.1038/mp.2012.67]

53 **Zheng F**, Zhang Y, Xie W, Li W, Jin C, Mi W, Wang F, Ma W, Ma C, Yang Y, Du B, Li K, Liu C, Wang L, Lu T, Zhang H, Wang Y, Lu L, Lv L, Zhang D, Yue W. Further evidence for genetic association of CACNA1C and schizophrenia: new risk loci in a Han Chinese population and a meta-analysis. *Schizophr Res* 2014; **152**: 105-110 [PMID: 24355530 DOI: 10.1016/j.schres.2013.12.003]

54 **He K**, An Z, Wang Q, Li T, Li Z, Chen J, Li W, Wang T, Ji J, Feng G, Lin H, Yi Q, Shi Y. CACNA1C, schizophrenia and major depressive disorder in the Han Chinese population. *Br J Psychiatry* 2014; **204**: 36-39 [PMID: 24262814 DOI: 10.1192/bjp.bp.113.126979]

55 **Green EK**, Grozeva D, Jones I, Jones L, Kirov G, Caesar S, Gordon-Smith K, Fraser C, Forty L, Russell E, Hamshere ML, Moskvina V, Nikolov I, Farmer A, McGuffin P; Wellcome Trust Case Control Consortium, Holmans PA, Owen MJ, O'Donovan MC, Craddock N. The bipolar disorder risk allele at CACNA1C also confers risk of recurrent major depression and of schizophrenia. *Mol Psychiatry* 2010; **15**: 1016-1022 [PMID: 19621016 DOI: 10.1038/mp.2009.49]

56 **Purcell SM**, Moran JL, Fromer M, Ruderfer D, Solovieff N, Roussos P, O'Dushlaine C, Chambert K, Bergen SE, Kähler

A, Duncan L, Stahl E, Genovese G, Fernández E, Collins MO, Komiyama NH, Choudhary JS, Magnusson PK, Banks E, Shakir K, Garimella K, Fennell T, DePristo M, Grant SG, Haggarty SJ, Gabriel S, Scolnick EM, Lander ES, Hultman CM, Sullivan PF, McCarroll SA, Sklar P. A polygenic burden of rare disruptive mutations in schizophrenia. *Nature* 2014; **506**: 185-190 [PMID: 24463508 DOI: 10.1038/nature12975]

57 **Kabitzke PA**, Brunner D, He D, Fazio PA, Cox K, Sutphen J, Thiede L, Sabath E, Hanania T, Alexandrov V, Rasmusson R, Spooren W, Ghosh A, Feliciano P, Biemans B, Benedetti M, Clayton AL. Comprehensive analysis of two Shank3 and the Cacna1c mouse models of autism spectrum disorder. *Genes Brain Behav* 2018; **17**: 4-22 [PMID: 28753255 DOI: 10.1111/gbb.12405]

58 **Bader PL**, Faizi M, Kim LH, Owen SF, Tadross MR, Alfa RW, Bett GC, Tsien RW, Rasmusson RL, Shamloo M. Mouse model of Timothy syndrome recapitulates triad of autistic traits. *Proc Natl Acad Sci U S A* 2011; **108**: 15432-15437 [PMID: 21878566 DOI: 10.1073/pnas.1112667108]

59 **White JA**, McKinney BC, John MC, Powers PA, Kamp TJ, Murphy GG. Conditional forebrain deletion of the L-type calcium channel Ca V 1.2 disrupts remote spatial memories in mice. *Learn Mem* 2008; **15**: 1-5 [PMID: 18174367 DOI: 10.1101/lm.773208]

60 **Völkening B**, Schönig K, Kronenberg G, Bartsch D, Weber T. Deletion of psychiatric risk gene Cacna1c impairs hippocampal neurogenesis in cell-autonomous fashion. *Glia* 2017; **65**: 817-827 [PMID: 28230278 DOI: 10.1002/glia.23128]

61 **Temme SJ**, Bell RZ, Fisher GL, Murphy GG. Deletion of the Mouse Homolog of *CACNA1C* Disrupts Discrete Forms of Hippocampal-Dependent Memory and Neurogenesis within the Dentate Gyrus. *eNeuro* 2016; **3** [PMID: 27957527 DOI: 10.1523/ENEURO.0118-16.2016]

62 **D'Arcangelo G**, Miao GG, Chen SC, Soares HD, Morgan JI, Curran T. A protein related to extracellular matrix proteins deleted in the mouse mutant reeler. *Nature* 1995; **374**: 719-723 [PMID: 7715726 DOI: 10.1038/374719a0]

63 **Sekine K**, Kubo K, Nakajima K. How does Reelin control neuronal migration and layer formation in the developing mammalian neocortex? *Neurosci Res* 2014; **86**: 50-58 [PMID: 24969097 DOI: 10.1016/j.neures.2014.06.004]

64 **Kubo K**, Honda T, Tomita K, Sekine K, Ishii K, Uto A, Kobayashi K, Tabata H, Nakajima K. Ectopic Reelin induces neuronal aggregation with a normal birthdate-dependent "inside-out" alignment in the developing neocortex. *J Neurosci* 2010; **30**: 10953-10966 [PMID: 20720102 DOI: 10.1523/JNEUROSCI.0486-10.2010]

65 **Hirotsune S**, Takahara T, Sasaki N, Hirose K, Yoshiki A, Ohashi T, Kusakabe M, Murakami Y, Muramatsu M, Watanabe S. The reeler gene encodes a protein with an EGF-like motif expressed by pioneer neurons. *Nat Genet* 1995; **10**: 77-83 [PMID: 7647795 DOI: 10.1038/ng0595-77]

66 **Jossin Y**, Cooper JA. Reelin, Rap1 and N-cadherin orient the migration of multipolar neurons in the developing neocortex. *Nat Neurosci* 2011; **14**: 697-703 [PMID: 21516100 DOI: 10.1038/nn.2816]

67 **Howell BW**, Gertler FB, Cooper JA. Mouse disabled (mDab1): a Src binding protein implicated in neuronal development. *EMBO J* 1997; **16**: 121-132 [PMID: 9009273 DOI: 10.1093/emboj/16.1.121]

68 **Simó S**, Pujadas L, Segura MF, La Torre A, Del Río JA, Ureña JM, Comella JX, Soriano E. Reelin induces the detachment of postnatal subventricular zone cells and the expression of the Egr-1 through Erk1/2 activation. *Cereb Cortex* 2007; **17**: 294-303 [PMID: 16514107 DOI: 10.1093/cercor/bhj147]

69 **Impagnatiello F**, Guidotti AR, Pesold C, Dwivedi Y, Caruncho H, Pisu MG, Uzunov DP, Smalheiser NR, Davis JM, Pandey GN, Pappas GD, Tueting P, Sharma RP, Costa E. A decrease of reelin expression as a putative vulnerability factor in schizophrenia. *Proc Natl Acad Sci U S A* 1998; **95**: 15718-15723 [PMID: 9861036 DOI: 10.1073/pnas.95.26.15718]

70 **Fatemi SH**, Earle JA, McMenomy T. Reduction in Reelin immunoreactivity in hippocampus of subjects with schizophrenia, bipolar disorder and major depression. *Mol Psychiatry* 2000; **5**: 654-663, 571 [PMID: 11126396 DOI: 10.1038/sj.mp.4000783]

71 **Bai W**, Niu Y, Yu X, Yi J, Zhen Q, Kou C. Decreased serum levels of reelin in patients with schizophrenia. *Asian J Psychiatr* 2020; **49**: 101995 [PMID: 32143141 DOI: 10.1016/j.ajp.2020.101995]

72 **Guidotti A**, Auta J, Davis JM, Di-Giorgi-Gerevini V, Dwivedi Y, Grayson DR, Impagnatiello F, Pandey G, Pesold C, Sharma R, Uzunov D, Costa E. Decrease in reelin and glutamic acid decarboxylase67 (GAD67) expression in schizophrenia and bipolar disorder: a postmortem brain study. *Arch Gen Psychiatry* 2000; **57**: 1061-1069 [PMID: 11074872 DOI: 10.1001/archpsyc.57.11.1061]

73 **Costa E**, Davis J, Grayson DR, Guidotti A, Pappas GD, Pesold C. Dendritic spine hypoplasticity and downregulation of reelin and GABAergic tone in schizophrenia vulnerability. *Neurobiol Dis* 2001; **8**: 723-742 [PMID: 11592844 DOI: 10.1006/nbdi.2001.0436]

74 **Li M**, Luo XJ, Xiao X, Shi L, Liu XY, Yin LD, Ma XY, Yang SY, Pu XF, Yu J, Diao HB, Shi H, Su B. Analysis of common genetic variants identifies RELN as a risk gene for schizophrenia in Chinese population. *World J Biol Psychiatry* 2013; **14**: 91-99 [PMID: 21745129 DOI: 10.3109/15622975.2011.587891]

75 **Kuang WJ**, Sun RF, Zhu YS, Li SB. A new single-nucleotide mutation (rs362719) of the reelin (RELN) gene associated with schizophrenia in female Chinese Han. *Genet Mol Res* 2011; **10**: 1650-1658 [PMID: 21863557 DOI: 10.4238/vol10-3gmr1343]

76 **Li W**, Song X, Zhang H, Yang Y, Jiang C, Xiao B, Li W, Yang G, Zhao J, Guo W, Lv L. Association study of RELN polymorphisms with schizophrenia in Han Chinese population. *Prog Neuropsychopharmacol Biol Psychiatry* 2011; **35**: 1505-1511 [PMID: 21549172 DOI: 10.1016/j.pnpbp.2011.04.007]

77 **Marzan S**, Aziz MA, Islam MS. Association Between REELIN Gene Polymorphisms (rs7341475 and rs262355) and Risk of Schizophrenia: an Updated Meta-analysis. *J Mol Neurosci* 2021; **71**: 675-690 [PMID: 32889693 DOI: 10.1007/s12031-020-01696-4]

78 **Costa E**, Davis J, Pesold C, Tueting P, Guidotti A. The heterozygote reeler mouse as a model for the development of a new generation of antipsychotics. *Curr Opin Pharmacol* 2002; **2**: 56-62 [PMID: 11786309 DOI: 10.1016/s1471-4892(01)00121-7]

79 **Rogers JT**, Rusiana I, Trotter J, Zhao L, Donaldson E, Pak DT, Babus LW, Peters M, Banko JL, Chavis P, Rebeck GW, Hoe HS, Weeber EJ. Reelin supplementation enhances cognitive ability, synaptic plasticity, and dendritic spine density.

Learn Mem 2011; **18**: 558-564 [PMID: 21852430 DOI: 10.1101/lm.2153511]
80 **Glantz LA**, Lewis DA. Decreased dendritic spine density on prefrontal cortical pyramidal neurons in schizophrenia. *Arch Gen Psychiatry* 2000; **57**: 65-73 [PMID: 10632234 DOI: 10.1001/archpsyc.57.1.65]
81 **Katsuyama Y**, Terashima T. Developmental anatomy of reeler mutant mouse. *Dev Growth Differ* 2009; **51**: 271-286 [PMID: 19379278 DOI: 10.1111/j.1440-169X.2009.01102.x]
82 **Tueting P**, Costa E, Dwivedi Y, Guidotti A, Impagnatiello F, Manev R, Pesold C. The phenotypic characteristics of heterozygous reeler mouse. *Neuroreport* 1999; **10**: 1329-1334 [PMID: 10363948 DOI: 10.1097/00001756-199904260-00032]
83 **Qiu S**, Korwek KM, Pratt-Davis AR, Peters M, Bergman MY, Weeber EJ. Cognitive disruption and altered hippocampus synaptic function in Reelin haploinsufficient mice. *Neurobiol Learn Mem* 2006; **85**: 228-242 [PMID: 16376115 DOI: 10.1016/j.nlm.2005.11.001]
84 **Teixeira CM**, Kron MM, Masachs N, Zhang H, Lagace DC, Martinez A, Reillo I, Duan X, Bosch C, Pujadas L, Brunso L, Song H, Eisch AJ, Borrell V, Howell BW, Parent JM, Soriano E. Cell-autonomous inactivation of the reelin pathway impairs adult neurogenesis in the hippocampus. *J Neurosci* 2012; **32**: 12051-12065 [PMID: 22933789 DOI: 10.1523/JNEUROSCI.1857-12.2012]
85 **Kim HM**, Qu T, Kriho V, Lacor P, Smalheiser N, Pappas GD, Guidotti A, Costa E, Sugaya K. Reelin function in neural stem cell biology. *Proc Natl Acad Sci U S A* 2002; **99**: 4020-4025 [PMID: 11891343 DOI: 10.1073/pnas.062698299]
86 **Zhao S**, Chai X, Frotscher M. Balance between neurogenesis and gliogenesis in the adult hippocampus: role for reelin. *Dev Neurosci* 2007; **29**: 84-90 [PMID: 17148951 DOI: 10.1159/000096213]
87 **Han J**, Kim HJ, Schafer ST, Paquola A, Clemenson GD, Toda T, Oh J, Pankonin AR, Lee BS, Johnston ST, Sarkar A, Denli AM, Gage FH. Functional Implications of miR-19 in the Migration of Newborn Neurons in the Adult Brain. *Neuron* 2016; **91**: 79-89 [PMID: 27387650 DOI: 10.1016/j.neuron.2016.05.034]
88 **MacDonald BT**, Tamai K, He X. Wnt/beta-catenin signaling: components, mechanisms, and diseases. *Dev Cell* 2009; **17**: 9-26 [PMID: 19619488 DOI: 10.1016/j.devcel.2009.06.016]
89 **Steinhart Z**, Angers S. Wnt signaling in development and tissue homeostasis. *Development* 2018; **145** [PMID: 29884654 DOI: 10.1242/dev.146589]
90 **Arredondo SB**, Valenzuela-Bezanilla D, Mardones MD, Varela-Nallar L. Role of Wnt Signaling in Adult Hippocampal Neurogenesis in Health and Disease. *Front Cell Dev Biol* 2020; **8**: 860 [PMID: 33042988 DOI: 10.3389/fcell.2020.00860]
91 **Niehrs C**. The complex world of WNT receptor signalling. *Nat Rev Mol Cell Biol* 2012; **13**: 767-779 [PMID: 23151663 DOI: 10.1038/nrm3470]
92 **Clevers H**, Nusse R. Wnt/β-catenin signaling and disease. *Cell* 2012; **149**: 1192-1205 [PMID: 22682243 DOI: 10.1016/j.cell.2012.05.012]
93 **Nusse R**, Clevers H. Wnt/β-Catenin Signaling, Disease, and Emerging Therapeutic Modalities. *Cell* 2017; **169**: 985-999 [PMID: 28575679 DOI: 10.1016/j.cell.2017.05.016]
94 **Zhang L**, Yang X, Yang S, Zhang J. The Wnt /β-catenin signaling pathway in the adult neurogenesis. *Eur J Neurosci* 2011; **33**: 1-8 [PMID: 21073552 DOI: 10.1111/j.1460-9568.2010.7483.x]
95 **Zylka MJ**, Rice FL, Anderson DJ. Topographically distinct epidermal nociceptive circuits revealed by axonal tracers targeted to Mrgprd. *Neuron* 2005; **45**: 17-25 [PMID: 15629699 DOI: 10.1016/j.neuron.2004.12.015]
96 **Qu Q**, Sun G, Murai K, Ye P, Li W, Asuelime G, Cheung YT, Shi Y. Wnt7a regulates multiple steps of neurogenesis. *Mol Cell Biol* 2013; **33**: 2551-2559 [PMID: 23629626 DOI: 10.1128/MCB.00325-13]
97 **Arredondo SB**, Guerrero FG, Herrera-Soto A, Jensen-Flores J, Bustamante DB, Oñate-Ponce A, Henny P, Varas-Godoy M, Inestrosa NC, Varela-Nallar L. Wnt5a promotes differentiation and development of adult-born neurons in the hippocampus by noncanonical Wnt signaling. *Stem Cells* 2020; **38**: 422-436 [PMID: 31721364 DOI: 10.1002/stem.3121]
98 **Nadri C**, Dean B, Scarr E, Agam G. GSK-3 parameters in postmortem frontal cortex and hippocampus of schizophrenic patients. *Schizophr Res* 2004; **71**: 377-382 [PMID: 15474909 DOI: 10.1016/j.schres.2004.02.020]
99 **Kozlovsky N**, Regenold WT, Levine J, Rapoport A, Belmaker RH, Agam G. GSK-3beta in cerebrospinal fluid of schizophrenia patients. *J Neural Transm (Vienna)* 2004; **111**: 1093-1098 [PMID: 15254796 DOI: 10.1007/s00702-003-0127-0]
100 **Lovestone S**, Killick R, Di Forti M, Murray R. Schizophrenia as a GSK-3 dysregulation disorder. *Trends Neurosci* 2007; **30**: 142-149 [PMID: 17324475 DOI: 10.1016/j.tins.2007.02.002]
101 **Freyberg Z**, Ferrando SJ, Javitch JA. Roles of the Akt/GSK-3 and Wnt signaling pathways in schizophrenia and antipsychotic drug action. *Am J Psychiatry* 2010; **167**: 388-396 [PMID: 19917593 DOI: 10.1176/appi.ajp.2009.08121873]
102 **Alimohamad H**, Rajakumar N, Seah YH, Rushlow W. Antipsychotics alter the protein expression levels of beta-catenin and GSK-3 in the rat medial prefrontal cortex and striatum. *Biol Psychiatry* 2005; **57**: 533-542 [PMID: 15737669 DOI: 10.1016/j.biopsych.2004.11.036]
103 **Ftouh S**, Akbar MT, Hirsch SR, de Belleroche JS. Down-regulation of Dickkopf 3, a regulator of the Wnt signalling pathway, in elderly schizophrenic subjects. *J Neurochem* 2005; **94**: 520-530 [PMID: 15998302 DOI: 10.1111/j.1471-4159.2005.03239.x]
104 **Hoseth EZ**, Krull F, Dieset I, Mørch RH, Hope S, Gardsjord ES, Steen NE, Melle I, Brattbakk HR, Steen VM, Aukrust P, Djurovic S, Andreassen OA, Ueland T. Exploring the Wnt signaling pathway in schizophrenia and bipolar disorder. *Transl Psychiatry* 2018; **8**: 55 [PMID: 29507296 DOI: 10.1038/s41398-018-0102-1]
105 **Lijam N**, Paylor R, McDonald MP, Crawley JN, Deng CX, Herrup K, Stevens KE, Maccaferri G, McBain CJ, Sussman DJ, Wynshaw-Boris A. Social interaction and sensorimotor gating abnormalities in mice lacking Dvl1. *Cell* 1997; **90**: 895-905 [PMID: 9298901 DOI: 10.1016/s0092-8674(00)80354-2]
106 **Gould TD**, O'Donnell KC, Picchini AM, Dow ER, Chen G, Manji HK. Generation and behavioral characterization of beta-catenin forebrain-specific conditional knock-out mice. *Behav Brain Res* 2008; **189**: 117-125 [PMID: 18299155 DOI: 10.1016/j.bbr.2007.12.028]

107 **Koshimizu H**, Fukui Y, Takao K, Ohira K, Tanda K, Nakanishi K, Toyama K, Oshima M, Taketo MM, Miyakawa T. Adenomatous polyposis coli heterozygous knockout mice display hypoactivity and age-dependent working memory deficits. *Front Behav Neurosci* 2011; **5**: 85 [PMID: 22347851 DOI: 10.3389/fnbeh.2011.00085]

108 **Stefansson H**, Ophoff RA, Steinberg S, Andreassen OA, Cichon S, Rujescu D, Werge T, Pietiläinen OP, Mors O, Mortensen PB, Sigurdsson E, Gustafsson O, Nyegaard M, Tuulio-Henriksson A, Ingason A, Hansen T, Suvisaari J, Lonnqvist J, Paunio T, Børglum AD, Hartmann A, Fink-Jensen A, Nordentoft M, Hougaard D, Norgaard-Pedersen B, Böttcher Y, Olesen J, Breuer R, Möller HJ, Giegling I, Rasmussen HB, Timm S, Mattheisen M, Bitter I, Réthelyi JM, Magnusdottir BB, Sigmundsson T, Olason P, Masson G, Gulcher JR, Haraldsson M, Fossdal R, Thorgeirsson TE, Thorsteinsdottir U, Ruggeri M, Tosato S, Franke B, Strengman E, Kiemeney LA; Genetic Risk and Outcome in Psychosis (GROUP), Melle I, Djurovic S, Abramova L, Kaleda V, Sanjuan J, de Frutos R, Bramon E, Vassos E, Fraser G, Ettinger U, Picchioni M, Walker N, Toulopoulou T, Need AC, Ge D, Yoon JL, Shianna KV, Freimer NB, Cantor RM, Murray R, Kong A, Golimbet V, Carracedo A, Arango C, Costas J, Jönsson EG, Terenius L, Agartz I, Petursson H, Nöthen MM, Rietschel M, Matthews PM, Muglia P, Peltonen L, St Clair D, Goldstein DB, Stefansson K, Collier DA. Common variants conferring risk of schizophrenia. *Nature* 2009; **460**: 744-747 [PMID: 19571808 DOI: 10.1038/nature08186]

109 **Schizophrenia Psychiatric Genome-Wide Association Study (GWAS) Consortium**. Genome-wide association study identifies five new schizophrenia loci. *Nat Genet* 2011; **43**: 969-976 [PMID: 21926974 DOI: 10.1038/ng.940]

110 **De Rubeis S**, He X, Goldberg AP, Poultney CS, Samocha K, Cicek AE, Kou Y, Liu L, Fromer M, Walker S, Singh T, Klei L, Kosmicki J, Shih-Chen F, Aleksic B, Biscaldi M, Bolton PF, Brownfeld JM, Cai J, Campbell NG, Carracedo A, Chahrour MH, Chiocchetti AG, Coon H, Crawford EL, Curran SR, Dawson G, Duketis E, Fernandez BA, Gallagher L, Geller E, Guter SJ, Hill RS, Ionita-Laza J, Jimenz Gonzalez P, Kilpinen H, Klauck SM, Kolevzon A, Lee I, Lei I, Lei J, Lehtimäki T, Lin CF, Ma'ayan A, Marshall CR, McInnes AL, Neale B, Owen MJ, Ozaki N, Parellada M, Parr JR, Purcell S, Puura K, Rajagopalan D, Rehnström K, Reichenberg A, Sabo A, Sachse M, Sanders SJ, Schafer C, Schulte-Rüther M, Skuse D, Stevens C, Szatmari P, Tammimies K, Valladares O, Voran A, Li-San W, Weiss LA, Willsey AJ, Yu TW, Yuen RK; DDD Study; Homozygosity Mapping Collaborative for Autism; UK10K Consortium, Cook EH, Freitag CM, Gill M, Hultman CM, Lehner T, Palotie A, Schellenberg GD, Sklar P, State MW, Sutcliffe JS, Walsh CA, Scherer SW, Zwick ME, Barett JC, Cutler DJ, Roeder K, Devlin B, Daly MJ, Buxbaum JD. Synaptic, transcriptional and chromatin genes disrupted in autism. *Nature* 2014; **515**: 209-215 [PMID: 25363760 DOI: 10.1038/nature13772]

111 **Schizophrenia Working Group of the Psychiatric Genomics Consortium**. Biological insights from 108 schizophrenia-associated genetic loci. *Nature* 2014; **511**: 421-427 [PMID: 25056061 DOI: 10.1038/nature13595]

112 **Braun K**, Häberle BM, Wittmann MT, Lie DC. Enriched environment ameliorates adult hippocampal neurogenesis deficits in Tcf4 haploinsufficient mice. *BMC Neurosci* 2020; **21**: 50 [PMID: 33228529 DOI: 10.1186/s12868-020-00602-3]

113 **Kopan R**, Ilagan MX. The canonical Notch signaling pathway: unfolding the activation mechanism. *Cell* 2009; **137**: 216-233 [PMID: 19379690 DOI: 10.1016/j.cell.2009.03.045]

114 **Hatakeyama J**, Bessho Y, Katoh K, Ookawara S, Fujioka M, Guillemot F, Kageyama R. Hes genes regulate size, shape and histogenesis of the nervous system by control of the timing of neural stem cell differentiation. *Development* 2004; **131**: 5539-5550 [PMID: 15496443 DOI: 10.1242/dev.01436]

115 **Matsuno K**. Notch signaling. *Dev Growth Differ* 2020; **62**: 3 [PMID: 31995851 DOI: 10.1111/dgd.12642]

116 **Wei J**, Hemmings GP. The NOTCH4 Locus is associated with susceptibility to schizophrenia. *Nat Genet* 2000; **25**: 376-377 [PMID: 10932176 DOI: 10.1038/78044]

117 **Allen NC**, Bagade S, McQueen MB, Ioannidis JP, Kavvoura FK, Khoury MJ, Tanzi RE, Bertram L. Systematic meta-analyses and field synopsis of genetic association studies in schizophrenia: the SzGene database. *Nat Genet* 2008; **40**: 827-834 [PMID: 18583979 DOI: 10.1038/ng.171]

118 **Shayevitz C**, Cohen OS, Faraone SV, Glatt SJ. A re-review of the association between the NOTCH4 Locus and schizophrenia. *Am J Med Genet B Neuropsychiatr Genet* 2012; **159B**: 477-483 [PMID: 22488909 DOI: 10.1002/ajmg.b.32050]

119 **Hoseth EZ**, Krull F, Dieset I, Mørch RH, Hope S, Gardsjord ES, Steen NE, Melle I, Brattbakk HR, Steen VM, Aukrust P, Djurovic S, Andreassen OA, Ueland T. Attenuated Notch signaling in schizophrenia and bipolar disorder. *Sci Rep* 2018; **8**: 5349 [PMID: 29593239 DOI: 10.1038/s41598-018-23703-w]

120 **Xue F**, Chen YC, Zhou CH, Wang Y, Cai M, Yan WJ, Wu R, Wang HN, Peng ZW. Risperidone ameliorates cognitive deficits, promotes hippocampal proliferation, and enhances Notch signaling in a murine model of schizophrenia. *Pharmacol Biochem Behav* 2017; **163**: 101-109 [PMID: 29037878 DOI: 10.1016/j.pbb.2017.09.010]

121 **Marathe S**, Alberi L. Notch in memories: Points to remember. *Hippocampus* 2015; **25**: 1481-1488 [PMID: 25656274 DOI: 10.1002/hipo.22426]

122 **Costa RM**, Honjo T, Silva AJ. Learning and memory deficits in Notch mutant mice. *Curr Biol* 2003; **13**: 1348-1354 [PMID: 12906797 DOI: 10.1016/s0960-9822(03)00492-5]

123 **Lugert S**, Vogt M, Tchorz JS, Müller M, Giachino C, Taylor V. Homeostatic neurogenesis in the adult hippocampus does not involve amplification of Ascl1(high) intermediate progenitors. *Nat Commun* 2012; **3**: 670 [PMID: 22334073 DOI: 10.1038/ncomms1670]

124 **Breunig JJ**, Silbereis J, Vaccarino FM, Sestan N, Rakic P. Notch regulates cell fate and dendrite morphology of newborn neurons in the postnatal dentate gyrus. *Proc Natl Acad Sci U S A* 2007; **104**: 20558-20563 [PMID: 18077357 DOI: 10.1073/pnas.0710156104]

125 **Engler A**, Zhang R, Taylor V. Notch and Neurogenesis. *Adv Exp Med Biol* 2018; **1066**: 223-234 [PMID: 30030829 DOI: 10.1007/978-3-319-89512-3_11]

126 **Mason HA**, Rakowiecki SM, Gridley T, Fishell G. Loss of notch activity in the developing central nervous system leads to increased cell death. *Dev Neurosci* 2006; **28**: 49-57 [PMID: 16508303 DOI: 10.1159/000090752]

127 **Artavanis-Tsakonas S**, Rand MD, Lake RJ. Notch signaling: cell fate control and signal integration in development. *Science* 1999; **284**: 770-776 [PMID: 10221902 DOI: 10.1126/science.284.5415.770]

128 **Ables JL**, Decarolis NA, Johnson MA, Rivera PD, Gao Z, Cooper DC, Radtke F, Hsieh J, Eisch AJ. Notch1 is required

for maintenance of the reservoir of adult hippocampal stem cells. *J Neurosci* 2010; **30**: 10484-10492 [PMID: 20685991 DOI: 10.1523/JNEUROSCI.4721-09.2010]

129 **Imayoshi I**, Sakamoto M, Yamaguchi M, Mori K, Kageyama R. Essential roles of Notch signaling in maintenance of neural stem cells in developing and adult brains. *J Neurosci* 2010; **30**: 3489-3498 [PMID: 20203209 DOI: 10.1523/JNEUROSCI.4987-09.2010]

130 **Chubb JE**, Bradshaw NJ, Soares DC, Porteous DJ, Millar JK. The DISC locus in psychiatric illness. *Mol Psychiatry* 2008; **13**: 36-64 [PMID: 17912248 DOI: 10.1038/sj.mp.4002106]

131 **Facal F**, Costas J. Evidence of association of the DISC1 interactome gene set with schizophrenia from GWAS. *Prog Neuropsychopharmacol Biol Psychiatry* 2019; **95**: 109729 [PMID: 31398428 DOI: 10.1016/j.pnpbp.2019.109729]

132 **Wang HY**, Liu Y, Yan JW, Hu XL, Zhu DM, Xu XT, Li XS. Gene polymorphisms of DISC1 is associated with schizophrenia: Evidence from a meta-analysis. *Prog Neuropsychopharmacol Biol Psychiatry* 2018; **81**: 64-73 [PMID: 29031911 DOI: 10.1016/j.pnpbp.2017.10.008]

133 **Mahar I**, Tan S, Davoli MA, Dominguez-Lopez S, Qiang C, Rachalski A, Turecki G, Mechawar N. Subchronic peripheral neuregulin-1 increases ventral hippocampal neurogenesis and induces antidepressant-like effects. *PLoS One* 2011; **6**: e26610 [PMID: 22028923 DOI: 10.1371/journal.pone.0026610]

134 **Chenn A**, Walsh CA. Regulation of cerebral cortical size by control of cell cycle exit in neural precursors. *Science* 2002; **297**: 365-369 [PMID: 12130776 DOI: 10.1126/science.1074192]

135 **Qu Q**, Sun G, Li W, Yang S, Ye P, Zhao C, Yu RT, Gage FH, Evans RM, Shi Y. Orphan nuclear receptor TLX activates Wnt/beta-catenin signalling to stimulate neural stem cell proliferation and self-renewal. *Nat Cell Biol* 2010; **12**: 31-40; sup pp 1 [PMID: 20010817 DOI: 10.1038/ncb2001]

World Journal of Stem Cells

Submit a Manuscript: https://www.f6publishing.com

World J Stem Cells 2022 March 26; 14(3): 231-244

DOI: 10.4252/wjsc.v14.i3.231

ISSN 1948-0210 (online)

ORIGINAL ARTICLE

Basic Study

In vitro induced pluripotency from urine-derived cells in porcine

Kaiana Recchia, Lucas Simões Machado, Ramon Cesar Botigelli, Naira Caroline Godoy Pieri, Gabriela Barbosa, Raquel Vasconcelos Guimarães de Castro, Mariana Groke Marques, Laís Vicari de Figueiredo Pessôa, Paulo Fantinato Neto, Flávio Vieira Meirelles, Aline Fernanda de Souza, Simone Maria Massami Kitamura Martins, Fabiana Fernandes Bressan

Specialty type: Cell and tissue engineering

Provenance and peer review: Unsolicited article; Externally peer reviewed.

Peer-review model: Single blind

Peer-review report's scientific quality classification

Grade A (Excellent): 0
Grade B (Very good): B, B
Grade C (Good): C, C
Grade D (Fair): 0
Grade E (Poor): 0

P-Reviewer: Batool SN, Gao YT, Kumar D, Wahid M

Received: August 23, 2021
Peer-review started: August 23, 2021
First decision: October 3, 2021
Revised: October 11, 2021
Accepted: February 15, 2022
Article in press: February 15, 2022
Published online: March 26, 2022

Kaiana Recchia, Lucas Simões Machado, Flávio Vieira Meirelles, Fabiana Fernandes Bressan, Department of Surgery, Faculty of Veterinary Medicine and Animal Sciences, University of São Paulo, Pirassununga 13635-000, São Paulo, Brazil

Ramon Cesar Botigelli, Department of Pharmacology and Biotechnology, Institute of Bioscience, São Paulo State University, Botucatu 18618-689, São Paulo, Brazil

Naira Caroline Godoy Pieri, Gabriela Barbosa, Raquel Vasconcelos Guimarães de Castro, Laís Vicari de Figueiredo Pessôa, Paulo Fantinato Neto, Flávio Vieira Meirelles, Aline Fernanda de Souza, Fabiana Fernandes Bressan, Department of Veterinary Medicine, Faculty of Animal Sciences and Food Engineering, University of São Paulo, Pirassununga 13635-000, São Paulo, Brazil

Mariana Groke Marques, Embrapa Suínos e Aves, Empresa Brasileira de Pesquisa Agropecuária, Concordia 89715-899, Santa Catarina, Brazil

Simone Maria Massami Kitamura Martins, Department of Animal Sciences, Faculty of Animal Sciences and Food Engineering, University of São Paulo, Pirassununga 13635-000, São Paulo, Brazil

Corresponding author: Fabiana Fernandes Bressan, DVM, Professor, Department of Surgery, Faculty of Veterinary Medicine and Animal Sciences, University of São Paulo, Av Duque de Caxias Norte 225, Pirassununga 13635-000, São Paulo, Brazil. fabianabressan@usp.br

Abstract

BACKGROUND

The generation of induced pluripotent stem cells (iPSC) has been a game-changer in translational and regenerative medicine; however, their large-scale applicability is still hampered by the scarcity of accessible, safe, and reproducible protocols. The porcine model is a large biomedical model that enables translational applications, including gene editing, long term *in vivo* and offspring analysis; therefore, suitable for both medicine and animal production.

AIM

To reprogramme *in vitro* into pluripotency, and herein urine-derived cells (UDCs) were isolated from porcine urine.

METHODS
The UDCs were reprogrammed *in vitro* using human or murine octamer-binding transcription factor 4 (OCT4), SRY-box2 (SOX2), Kruppel-like factor 4 (KLF4), and C-MYC, and cultured with basic fibroblast growth factor (bFGF) supplementation. To characterize the putative porcine iPSCs three clonal lineages were submitted to immunocytochemistry for alkaline phosphatase (AP), OCT4, SOX2, NANOG, TRA1 81 and SSEA 1 detection. Endogenous transcripts related to the pluripotency (OCT4, SOX2 and NANOG) were analyzed *via* reverse transcription quantitative real-time polymerase chain reaction in different time points during the culture, and all three lineages formed embryoid bodies (EBs) when cultured in suspension without bFGF supplementation.

RESULTS
The UDCs were isolated from swine urine samples and when at passage 2 submitted to *in vitro* reprogramming. Colonies of putative iPSCs were obtained only from UDCs transduced with the murine factors (mOSKM), but not from human factors (hOSKM). Three clonal lineages were isolated and further cultured for at least 28 passages, all the lineages were positive for AP detection, the OCT4, SOX2, NANOG markers, albeit the immunocytochemical analysis also revealed heterogeneous phenotypic profiles among lineages and passages for NANOG and SSEA1, similar results were observed in the abundance of the endogenous transcripts related to pluripotent state. All the clonal lineages when cultured in suspension without bFGF were able to form EBs expressing ectoderm and mesoderm layers transcripts.

CONCLUSION
For the first time UDCs were isolated in the swine model and reprogrammed into a pluripotent-like state, enabling new numerous applications in both human or veterinary regenerative medicine.

Key Words: Induced pluripotent stem cells; Noninvasive; Pluripotency; Reprogramming; Urine; Porcine

Core Tip: The porcine induced pluripotent stem cells (piPSCs) derived from urine derived cells (UDCs) may facilitate their routine and large-scale use by avoiding injury or stress during collection for autologous purposes. However, the precise reprogramming process and characterization is not fully elucidated in other species than murine or human. The generation of piPSCs from UDCs can contribute as a biomedical model for regenerative and translational medicine, as well as for animal production and to elucidate the reprogramming process in porcine, a large animal model.

Citation: Recchia K, Machado LS, Botigelli RC, Pieri NCG, Barbosa G, de Castro RVG, Marques MG, Pessôa LVF, Fantinato Neto P, Meirelles FV, Souza AF, Martins SMMK, Bressan FF. *In vitro* induced pluripotency from urine-derived cells in porcine. *World J Stem Cells* 2022; 14(3): 231-244
URL: https://www.wjgnet.com/1948-0210/full/v14/i3/231.htm
DOI: https://dx.doi.org/10.4252/wjsc.v14.i3.231

INTRODUCTION

The generation of pluripotent cells *in vitro* has been reported in numerous studies; however, pluripotent cell generation protocols and their characterization are not as robust in animal models as they are in humans and mice. The generation of induced pluripotent stem cells (iPSCs), unlike embryonic stem cells, creates the possibility of autologous therapies and circumvents ethical barriers. iPSCs applications range from basic to applied research, for example, from regenerative medicine to the enhancement of animal production to generate functional gametes or even iPSCs-derived embryos[1-3]. For wild and domestic animal models, the establishment of pluripotent cells and their maintenance *in vitro* may enable diverse translational, clinical and reproductive applications. A robust approach, along with a well-known understanding of the pluripotency pathways for each species, is still to be reported, as previously discussed and reviewed[4-6].

The reprogramming of porcine cells into a pluripotent state can significantly contribute not only to applications in veterinary medicine and animal production, but also, the porcine as a large biomedical model is greatly acknowledged for their physiological and immunological similarities to humans, being suitable to preclinical and translational studies, in special when compared to the murine model[3,5,7-

11]. Cells used for the *in vitro* reprogramming into iPSCs are mostly from invasive collection procedures, such as from embryos and interrupted gestations (embryonic and foetal cells), or biopsies (adult fibroblasts and mesenchymal cells)[1,12,13]. The derivation of cultured cells from embryos or foetuses impedes their development, and consequently is considered an unethical practice in humans. The isolation of adult fibroblasts and other tissue-derived cells through biopsies is usual, especially when autologous therapies or *in vitro* modelling of specific genomes is needed. Biopsies, however, usually demand minimally invasive procedures performed by health professionals. Post procedure care may lead to complications such as scars, inflammation, and infection. In particular, the ability of iPSCs to model *in vitro* syndromes or diseases from patients with affected cognitive, neurological, and muscular-skeletal functions may be impaired by such procedures, often requiring special attention and ethics approval. Therefore, using cells from a noninvasive source for the generation of iPSCs would facilitate their use in regenerative and translational human or veterinary medicine, aiming for its large scale use without resulting in injuries or stress[14,15].

Urine-derived cells (UDCs) have been recently reported in humans, and the *in vitro* modelling of diseases using these cells or iPSCs derived from them is increasingly being explored[16,17]. Studies on the *in vitro* differentiation of human UDCs into cardiomyocytes[16] and hepatocyte-like cells[18], the generation of patient-specific iPSC lineages for multiple sclerosis[19], X-linked retinoschisis[20], heart failure[21], phenylketonuria[22], glaucoma[23], and retinitis pigmentosa[24], and recently, the derivation of iPSCs from UDCs in nonhuman primates[25] reinforce the importance of this recent *in vitro* modelling tool.

Noninvasive cell isolation in domestic animals has also been recently reported from milk[26], an exclusive female possibility, and from urine in the rabbit and canine models[27,28]; however, no pluripotent cells have been derived from these models aiming at its use in regenerative medicine so far. In this context, porcine are nonprimate large animals widely known to present physiological and immunological similarities with humans, as well as they are considered an important species for animal production, with standardized management with pathogen-free conditions[29,30], and consequently, their use as a biomedical model is advantageous compared to nonhuman primates. The fully reprogramming, consistent and robust characterization of porcine iPSCs (piPSCs) are not frequently reported; however, *in vitro* differentiation of these cells into other cell types, and importantly, the generation of chimeras has been presented and discussed, endorsing their use for *in vitro* disease modeling or even for cell therapy[14,18,19,31,32].

Herein, we describe urine collection, cellular isolation, and *in vitro* reprogramming of a noninvasive cell source used for iPSC generation in a large domestic animal, the porcine model. Three clonal lineages were evaluated throughout the passages. Porcine iPSCs derived from UDCs are important not only for agricultural traits, for example, for enabling the *in vitro* generation of gametes and embryos and contributing to future genetic improvement, but also as an excellent platform for the *in vitro* and *in vivo* modelling of several diseases.

MATERIALS AND METHODS

All procedures were performed following the National Council for Control of Animal Experimentation (CONCEA) rules and were approved by the Ethics Committee on Animal Experimentation of the Faculty of Animal Science and Food Engineering and Faculty of Veterinary Medicine and Animal Sciences, University of São Paulo (protocols 6372070119 and 7051150717).

Urine collection, UDC isolation, and culture

Swine urine samples (approximately 250 mL) were collected from three females at reproductive age (2 year) after spontaneous urination. The samples were identified as UDC1, UDC2, and UDC3, and processed following the protocol previously described for human samples[33]. Briefly, the urine was aliquoted into conical tubes and centrifuged at 400 × g and 25 °C for 10 min; the supernatant was removed, leaving approximately 1 mL in each tube, washed with 45 mL of D-polybutylene succinate (PBS) (Life Technologies) containing 1% penicillin/streptomycin (Life Technologies), and centrifuged at 200 × g and 25 °C for 10 min. The supernatant was discarded, and the pellet was resuspended in 12 mL of previously prepared medium containing 22.5 mL DMEM high glucose (Life Technologies), 2.5 mL FBS (HyClone), 0.25 mL penicillin/streptomycin (Life Technologies), 0.25 mL 100 × GlutaMAX supplement (Life Technologies), 0.25 mL 100 × nonessential amino acid solution (Life Technologies), 25 mL REBM medium (Renal Epithelial Basal Medium, Lonza) and REGM supplements: 5 µL/mL FBS, hEGF, insulin, hydrocortisone, GA-1000, transferrin, triiodothyronine, epinephrine (all 0.5 µL/mL, Lonza), and basic fibroblast growth factor (bFGF) (2.5 ng/mL, PeproTech).

Cells were plated onto 0.1% gelatine (Sigma-Aldrich)-coated 24-well plates. The medium was replaced at D3 (3rd day after plating) and then partially refreshed every day. The UDC1 cell lineage was further used in the cellular reprogramming protocol, and clonal iPSC lineages were used for statistical analyses.

In vitro induced reprogramming of porcine UDCs

In vitro reprogramming was performed by transducing UDCs with polycistronic lentiviral vectors harboring either murine or human transcription factors OCT4, SOX2, KLF-4 and C-MYC (mOSKM or hOSKM, STEMCCA, Millipore), as previously reported[34,35]. Briefly, for the production of lentiviral particles, the lipofection protocol (Lipofectamine 3000, Life Technologies) was performed using OSKM and auxiliary vectors TAT, REV, Hgpm2, VSVG, in 293 FT cells (Life Technologies) as previously described. UDCs, at a concentration of 2 × 10^4 per well, were transduced with viral particles and incubated overnight at 38.5 °C, 5% CO_2, and maximum humidity for 12-16 h, when media were refreshed.

After 5-6 d, the transduced cells were replaced onto a 6-well plate coated with a monolayer of mitomycin C (M4287 Sigma-Aldrich)-inactivated MEFs and cultured in iPSC medium composed of DMEM/F12 knockout medium supplemented with 20% KSR, 1% glutamine, 3.85 μM β-mercapto-ethanol, 1% nonessential amino acids, 1% penicillin/streptomycin (all from Life Technologies), and 10 ng/mL bFGF (PeproTech) and incubated at 38.5 °C, 5% CO_2 and maximum humidity. After approximately 1 wk, colonies were manually picked at the first passage, and further on, clonal lineages (putative iPSCs, or iPSC-like cells) were dissociated for passaging (TrypLe Express, Life Technologies). Three clonal lineages (C1, C2, and C3) were further analysed throughout passaging. Cryopreservation (10% DMSO), and therefore a freeze-and-thaw cycle, was performed at approximately passage 18 and again at approximately passage 30.

Reprogramming efficiency and alkaline phosphatase detection

The reprogramming efficiency was assessed by analysing the ratio of morphologically typical and alkaline phosphatase (AP)-positive iPSCs colonies per the number of transduced cells initially plated (2 × 10^4 cells per well of a 6-well plate). The AP detection protocol was performed using the Alkaline Phosphatase Detection Kit (86R, Sigma-Aldrich) according to the manufacturer's instructions.

Immunocytochemistry

Immunocytochemistry was used to detect OCT4, SOX2, NANOG, SSEA1, and TRA1 81 in two different passage windows for the three lineages: p16, p15, and p9 for C1, C2, and C3, respectively, and again after p20 (p23, p22, and p22, respectively). The cultured putative piPSCs were fixed in paraformaldehyde for 10 min and washed in PBS. The pluripotency-related markers test was performed as previously described[36]. Briefly, the antibodies were used to detect OCT4 (1:100, cat# SC8628, Santa Cruz), SOX2 (1:500, cat# ab97959; Abcam), NANOG (1:100, cat# ab77095, Abcam), SSEA1 (1:50, cat# MAB4301, Millipore) and TRA1 81 (1:50, cat# MAB4381, Millipore), and the respective secondary antibodies were used (donkey anti-goat 594, cat# A11058, donkey anti-rabbit 488, A21206, 1:500, donkey anti-goat 488, cat# A11055, Invitrogen, 1:500 goat anti-mouse 594, cat# A21044, Invitrogen). When necessary, the cells underwent permeabilization and blocking following previously described methods [37]. At the end of each protocol, the cell nuclei were labelled with Hoechst 33342 (1:1000) and analysed using the EVOS™ photodocumentation system.

Analysis of endogenous OCT4, SOX2, and NANOG transcripts

RNA extraction and reverse transcription: The specific expression of endogenous factors OCT4, SOX2, NANOG, and exogenous reprogramming factors (mOSKM) was evaluated in UDCs and reprogrammed cells. Additionally, porcine embryos were collected on day 5 after insemination and cultured *in vitro* for 24 h to obtain blastocysts[38]. A pool of 20 porcine blastocysts was used as a positive technical control for pluripotency-related gene expression.

UDCs and iPSCs were recovered from culture plates and centrifuged in microtubes. The pellets were resuspended in linear acrylamide (0.05 mg/mL, Ambion) and UltraPure™ DNase/RNase-Free Distilled Water (Invitrogen), and RNA was extracted using TRIzol Reagent (Invitrogen) following the manufacturer's instructions. The RNA samples were analyzed regarding quantity and quality using a spectrophotometer (Nanodrop 2000). Reverse transcription of the extracted RNA was performed using the commercial High-Capacity cDNA Reverse Transcription Kit (QIAGEN) according to the manufacturer's instructions.

Gene expression quantification: The three reprogrammed clonal lineages (C1, C2, and C3) were analysed for the expression of the endogenous factors OCT4, SOX2, and NANOG as well as exogenous reprogramming factors (mOSKM) at different time points of *in vitro* culture: Early passages (EP: 15 to 18), intermediate passages (IP: 20 to 24), and late passages (LP: 29 to 32). To quantitatively evaluate expression, primers were designed using Primer-BLAST software (NCBI) with GenBank sequences (Supplementary Table 1). Polymerase chain reaction (PCR) products were sequenced for specificity analysis. The reference genes were glyceraldehyde-3-phosphate dehydrogenase (GAPDH) and beta-actin 3 (β-ACTIN-3) and normalization was performed based on their geometric means. The primers for endogenous pluripotency gene expression were designed to detect porcine and not murine transcripts, whereas exogenous expression was detected using the mOSKM primers.

Relative expression of candidate genes was quantified by SYBR Green PCR Master Mix (Life Technologies) using the QuantStudio 5 PCR System (Thermo Fisher). Cycling conditions for amplification were 95 °C for 15 min; 40 cycles of 95 °C for 15 s, 60 °C for 5 s, and 72 °C for 30 s; and 72 °C for 2 min; the melting curve was analysed up to 90 cycles starting at 50 °C with a 0.5 °C increase. The three clonal lineages were considered biological triplicates when compared to UDCs, whereas different passages from the same lineage were considered biological triplicates when these were compared, and all reactions were performed in technical duplicates. The relative gene abundance was performed by $2^{\Delta CT}$ [39].

Embryoid body assay

The piPSCs from the three lineages at passages 15-16 and also at passages 24-25 were replated into a 6-well plate previously treated with 0.6% agarose and cultured in bFGF-free iPSC medium for 48 to 60 h. The embryoid bodies (EBs) were collected and centrifuged at 900 × g for 5 min, and RNA extraction was performed as described before. Reverse transcription was performed using the commercial High-Capacity cDNA Reverse Transcription Kit (Qiagen) according to the manufacturer's instructions to evaluate the expression of endodermal (AFP), mesodermal (VIMENTIN and BMP4), and ectodermal (β-TUBULIN III) genes by reverse transcription quantitative real-time PCR (RT-qPCR), as described before (Supplementary Table 1).

Statistical analysis

Data obtained from the experimental procedures were analyzed using the statistical program Statistical Analysis System (SAS University Edition), with previous verification of the normality of the residues by the Shapiro-Wilk test (PROC UNIVARIATE). The variables that did not meet the statistical assumptions were submitted to a logarithmic transformation [Log (X + 1)]. The original or transformed data, when necessary, were submitted to analysis of variance. When significant with the variance analysis, the data related to the different cell lineages were submitted to the Bonferroni test. A significance level of 5% was considered for all statistical analyses.

RESULTS

UDC isolation and culture

Cells isolated from urine first appeared resembling epithelial-like colonies at 3 to 5 d post isolation and then acquired fibroblastic morphology after passaging (Figure 1).

In vitro induced reprogramming of porcine UDCs

Cellular reprogramming was performed using murine (mOSKM) or human (hOSKM) polycistronic lentiviral vectors. The transduced cells were evaluated for morphological alterations, and twelve days after transduction, typical colonies were observed and tested for AP presence.

Reprogramming efficiency was assessed by analysing the ratio of typical AP-positive iPSC colonies per number of cells initially plated for transduction (Figure 2 and Supplementary Table 2). Reprogramming with the hOSKM vector presented an initial efficiency of 2.46%; however, the cells did not maintain typical colonies after passage 5 under our culture conditions (cells underwent spontaneous differentiation). Hence, experimentation with hOSKM-derived iPSCs was discontinued. mOSKM presented 3.37% initial reprogramming efficiency, and colonies isolated and further characterized herein maintained a typical morphology and AP expression pattern (Figure 2).

Eight colonies were chosen, manually picked, and replated onto new MEFs to obtain clonal lineages. Three clonal lineages designated as C1, C2, and C3 were remained in the culture at least 28 passages and were positive for AP, however, C2 colonies spontaneously differentiated after 28 passages, and the colonies C1 and C3 were further remained in culture for at least 30 passages.

Immunocytochemistry

The clonal lineages were tested in two distinct passaging windows: Between p9 and p16 (p16, p15, and p9, respectively, for C1, C2 and C3) and after p20 (p23, p22, and p22, respectively), enabling analysis among colonies and between culture periods. Cell lineages at p9-16 were positive for OCT4, SOX2, and NANOG and generally negative for SSEA1 and TRA1 81. The C3 (p9) clonal lineage presented some cells positive for SSEA1 and TRA1 81 (Figure 3 and Supplementary Table 3).

In passages > p20, detection of OCT4 and SOX2 was observed, and some cells were also positive for SSEA1. C1 and C2 were negative for NANOG and TRA1 81; however, C3 cells presented mild positivity for both NANOG and TRA1 81 (Figure 3). The results are summarized in Supplementary Table 3.

RT-qPCR analysis

As expected, mOSKM was not amplified in UDCs or blastocysts; and endogenous genes were expressed in blastocysts (Figure 4). Then, reprogrammed lineages were compared to each other and the analysis of

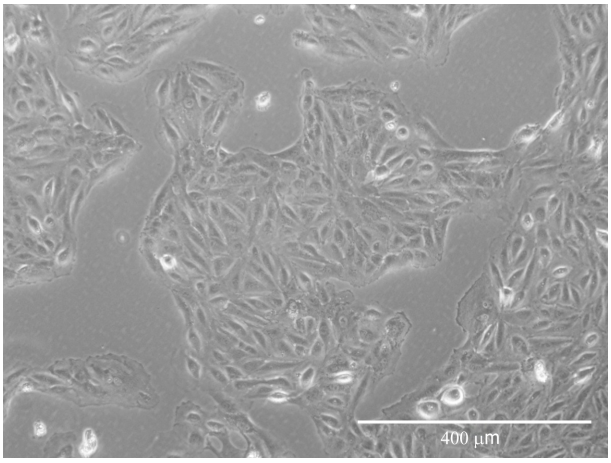

Figure 1 Porcine urine-derived cells at passage 4. After single-cell dissociation, the cells present a fibroblastic morphology but compact cell culture. Scale bar = 400 μM.

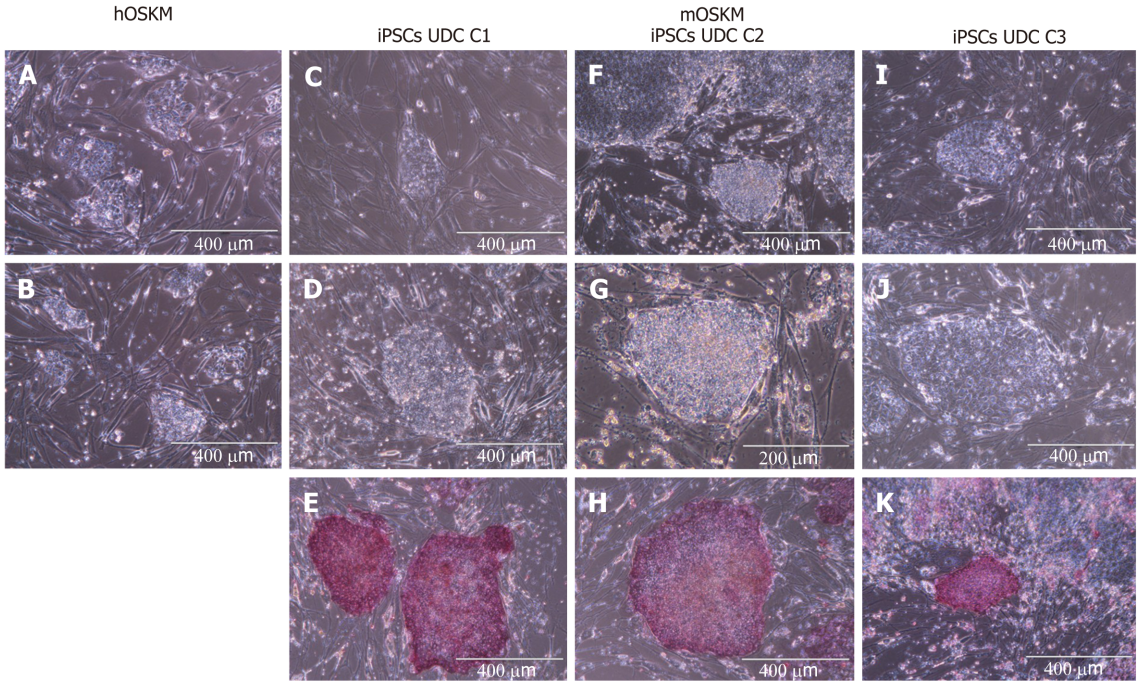

Figure 2 Urine-derived cells reprogrammed with hOSKM and mOSKM. A and B: Urine-derived cells (UDCs) reprogrammed with hOSKM, scale bar: 400 μM; C, D, and E: UDCs reprogrammed with mOSKM: C1, scale bar: 400 μM; F: UDCs reprogrammed with mOSKM: C2, scale bar: 400 μM; G: UDCs reprogrammed with mOSKM: C2, scale bar: 200 μM; H: UDCs reprogrammed with mOSKM: C2, scale bar: 400 μM; I, J and K: UDCs reprogrammed with mOSKM: C3, scale bar: 400 μM. Colonies are flat, with well-defined edges and tightly packed cells in the centre. UDC: Urine-derived cell; iPSCs: Induced pluripotent stem cells.

the expression of endogenous OCT4, SOX2, NANOG, and mOSKM in the different lineages (C1, C2, and C3) revealed that exogenous reprogramming factors were still detected in later passages of iPSCLCs. C3 showed higher expression of the exogenous vector ($P < 0.0001$) and lower expression of SOX2 than lineage C1 ($P = 0.0099$). OCT4 and NANOG expression did not differ among lineages (Figure 5 and Supplementary Table 4).

The analysis of the effect of time in culture (passaging) of the endogenous gene expression in UDCs and the iPSCLCs different groups (EP: 15 to 18; IP: 20 to 24; and LP: 29 to 32) revealed that IP and LP presented higher expression of SOX2, augmenting during culture period; and OCT4 levels were detected in all periods, differing from UDCs. The expression of the exogenous vector did not differ among passages. NANOG expression, however, decreased in intermediate passages, possibly due to a freeze-thaw cycle between EP and IP *in vitro*. At LP, NANOG was again slightly increased. The LP group of the C2 Lineage was not shown once these cells underwent spontaneous differentiation at passage 28 (Supplementary Table 5 and Figure 6).

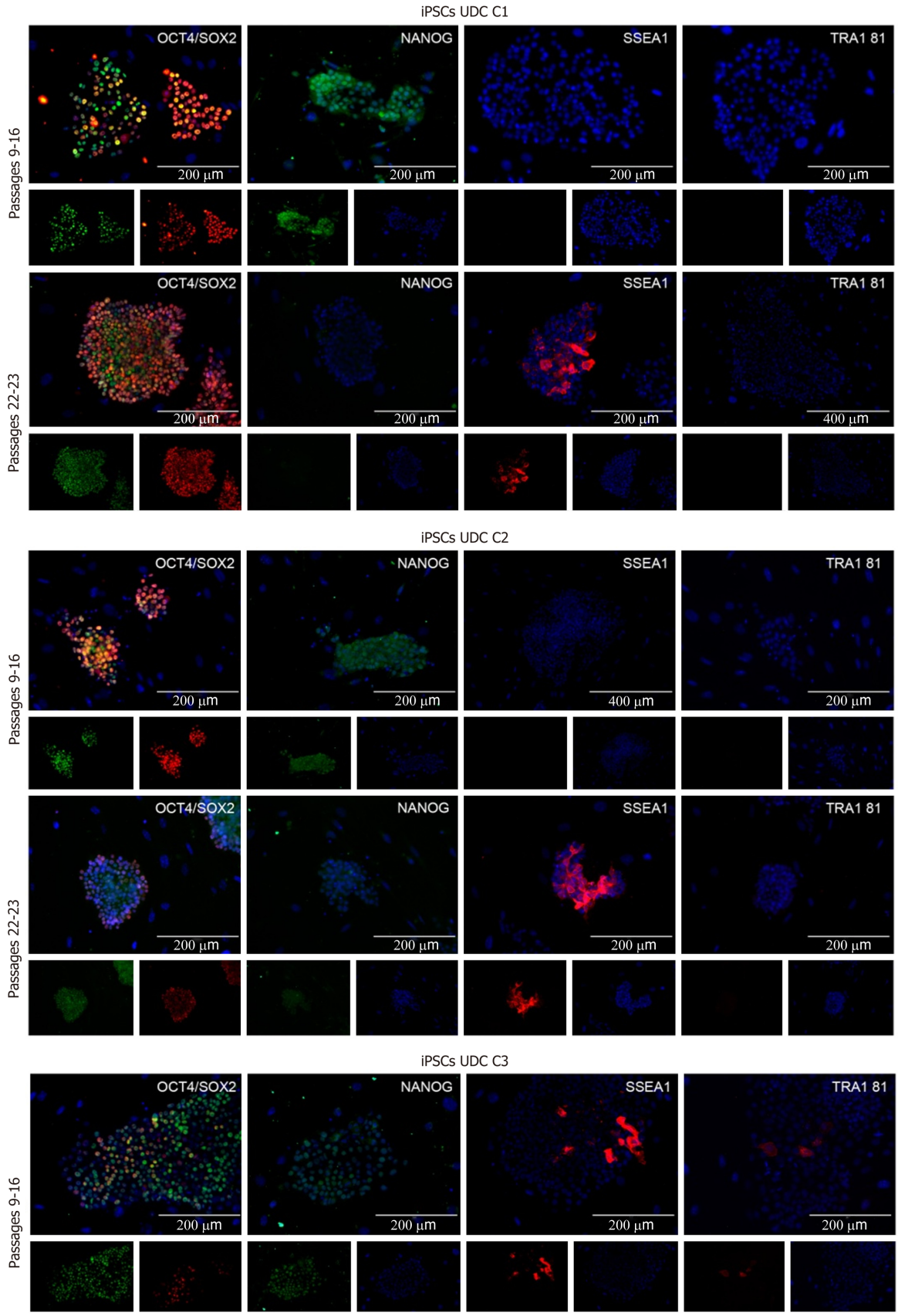
iPSCs UDC C1
Passages 9-16
Passages 22-23
OCT4/SOX2
NANOG
SSEA1
TRA1 81
200 µm
400 µm
iPSCs UDC C2
iPSCs UDC C3

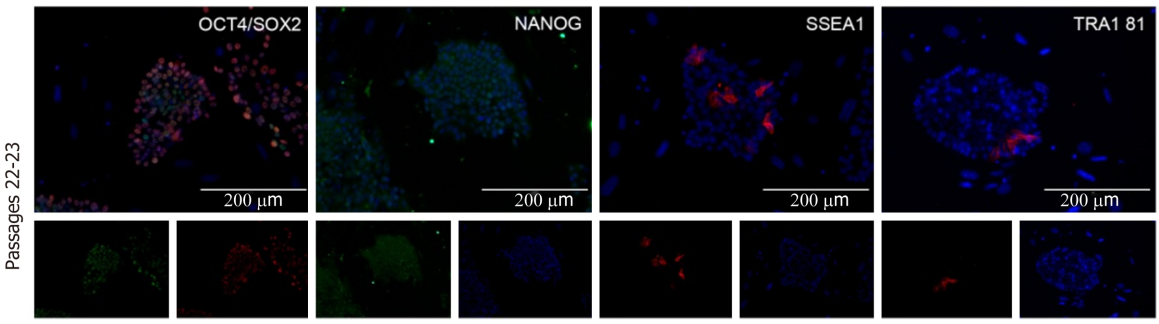

Figure 3 Immunofluorescence for SOX2, octamer-binding transcription factor 4 (OCT4), NANOG, SSEA1, and TRA1 81 detection in C1, C2, and C3 at different passages. Cell lines at p9-16 were positive for OCT4, SOX2, and NANOG and negative for SSEA1 and TRA1 81. C3 presented some cells positive for SSEA1 and TRA1 81. At later passages, OCT4 and SOX2 were observed, and some cells also presented SSEA1. C1 and C2 were negative for NANOG and TRA1 81, while C3 presented a mildly positive detection for both. UDC: Urine-derived cell; iPSCs: Induced pluripotent stem cells.

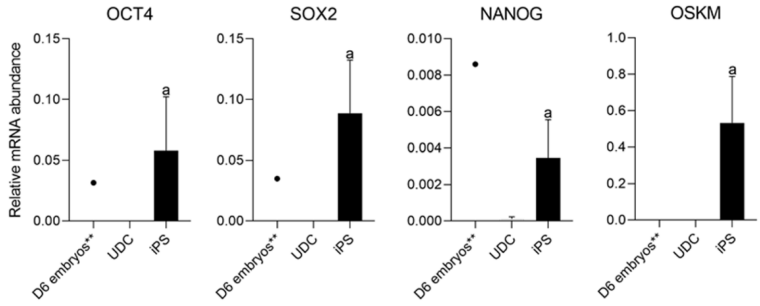

Figure 4 Analysis of the expression of endogenous factors octamer-binding transcription factor 4 (OCT4), SOX2, NANOG, and exogenous OSKM between urine-derived cell and induced pluripotent stem cells. [a]*P* < 0.05 between urine-derived cells (UDCs) and induced pluripotent stem cells (iPSCs). **Represents gene expression analysis of a pool of D6 porcine blastocysts, which did not integrate statistical analyses. Both endogenous and exogenous reprogramming factors were detected on iPSCs but not on UDCs, and porcine blastocysts presented endogenous pluripotency-related gene expression only. UDC: Urine-derived cell; iPSCs: Induced pluripotent stem cells.

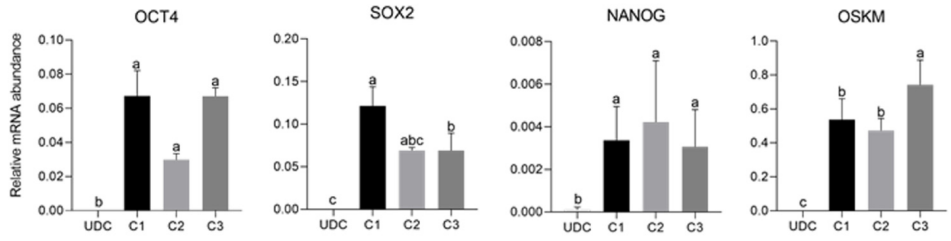

Figure 5 Analysis of the expression of endogenous factors octamer-binding transcription factor 4 (OCT4), SOX2, NANOG, and exogenous OSKM in the different lineages (C1, C2, and C3) of induced pluripotent stem cells. Exogenous reprogramming factors were still detected in later passages. Superscript letters represent differences (*P* < 0.05) between groups. [a]Represents higher relative mRNA abundance, [b]represents lower relative mRNA abundance when compared to a, and [c]represents lower relative mRNA abundance when compared to b. UDC: Urine-derived cell.

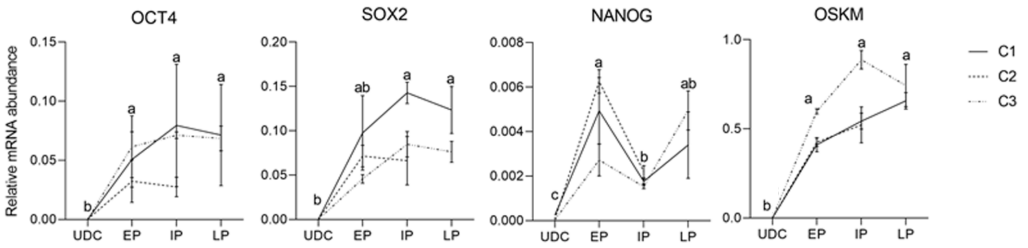

Figure 6 Analysis of endogenous gene expression in urine-derived cell s and the different groups (early passages, intermediate passages, and late passages) of induced pluripotent stem cells. Exogenous reprogramming factors were still detected in later passages. Superscript letters represent differences ($P < 0.05$) between groups. [a]Represents higher relative mRNA abundance, [b]represents lower relative mRNA abundance when compared to a, and [c]represents lower relative mRNA abundance when compared to b. EP: Early passages; IP: Intermediate passages; LP: Late passages; UDC: Urine-derived cell.

Embryoid body assay

All clonal lineages were replated as single cells onto a nonadherent plate without bFGF supplementation, and these cells formed EBs with typical morphology at different passages (Figure 7). The expression of VIMENTIN, BMP4 and β-TUBULIN-III was detected in the EBs (Figure 8), and AFP was not detected in our conditions (data not shown).

DISCUSSION

Herein, cells derived from urine sample (UDCs) were *in vitro* reprogrammed in a large domestic animal model, the swine. Previous studies on porcine have mostly derived iPSCs from foetal or adult fibroblasts, and fewer with multipotent adult cells[1]. UDC-derived piPSCs are highly advantageous for veterinary and regenerative medicine due to the simple collection procedure, avoiding stress or injuries, and in addition, is an inexpensive procedure unlike surgeries aiming biopsies, also important for the feasibility of large-scale sample collection[14,15,17,27,40].

Raab *et al*[40] reported a higher reprogramming efficiency of human UDCs when compared with other somatic cell types. Indeed, several studies have reported cell heterogeneity from urine-derive cells in human, including renal tubular cells[41], urine-stem cells (renal progenitor cells)[42], and urine-derived epithelial cells[16]. It is already known the cells' origin can influence the reprogramming process, and a more complete characterization and sorting for each cell type prior to reprogramming may be essential to understand the contribution of each cell population to the generation of iPSCs[35, 43].

In recent years, it has been showed by several reports the establishment of pluripotency, or at least a state similar to embryonic pluripotency, in several species other than human and mice, and although the main molecular mechanisms involved in pluripotency acquisition *in vitro* are considered rather conserved between species, there are notable differences between species turning the generation of bonafide iPSCs challenging, however still extremely promising.

Indeed, the same human/mouse protocols for iPSCs generation are not extendable to other species[1, 3]. Herein we used a previous strategy already reported for large animals reprogramming[34-36,43-45], and widely used to reprogram porcine somatic cells[1]. In the conditions described, the results showed that UDCs transduced with human factors failed to be maintained in culture for more than 5 passages due to early differentiation of the cells cultured *in vitro*, and similar results was described by Pieri *et al* [36] when reprogramming of porcine foetal fibroblasts. Conversely, cells transduced with murine factors were maintained in culture for at least 28 passages, showing typical morphology, positive AP detection and endogenous pluripotency-related gene expression through the different passages. Next steps to improve *in vitro* reprogramming must consider possible epigenetic modulation or even the identification of species-specific pluripotency pathways to improve the nonintegrative reprogramming.

Lineages at p9-16 were positive for SSEA1 and weakly positive for NANOG. These results correlate with a decrease in NANOG expression at IPs, and it might be an effect associated with the freeze-and-thaw process, which was performed in the lineages between EP and IP in this study. Interestingly, the abundance of NANOG transcription increased between the IP and LP. Li *et al*[12] reported that the staining for NANOG, SOX2 and OCT4, increased at passage 20 when compared to p10, indicating a stabilization of the pluripotency phenotype of intermediate type piPSCs. In addition, an elegant discussion was provided by Yamanaka[46] on the heterogeneous profile of each iPSCs lineage, leading to different phenotypes. Furthermore, in our conditions, we infer that a longer time in culture without the freeze-and-thaw process may lead to better reprogramming, as observed by the late acquisition of the SSEA1+ phenotype, a reported marker for human naïve stem cells[47].

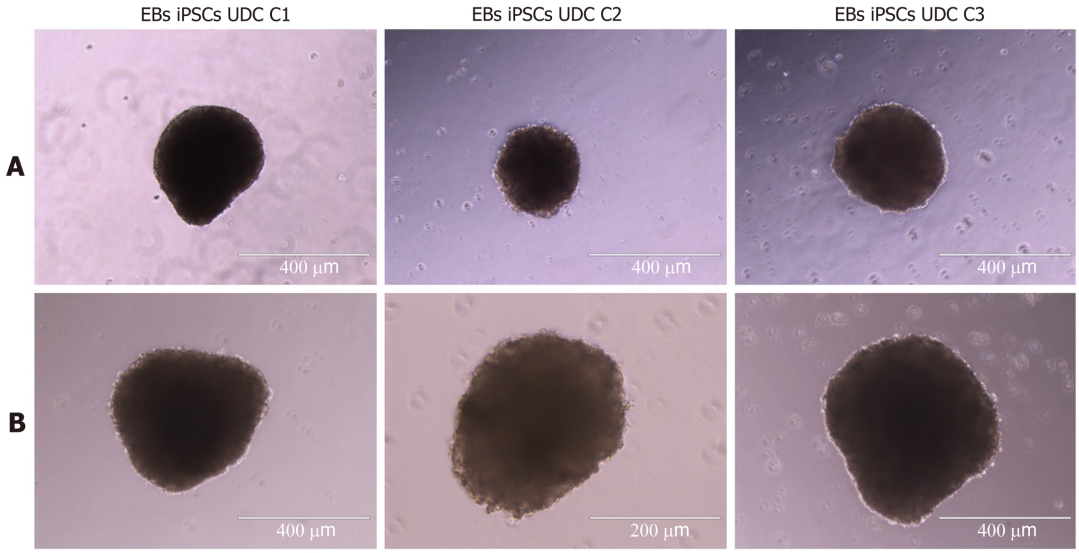

Figure 7 All three clonal induced pluripotent stem cell lineages formed embryoid bodies with typical 3D morphology. A: Embryoid bodies (EBs) from induced pluripotent stem cells (iPSCs) at passages 15-16 (scale bar = 400 μM); B: EBs from iPSCs at passages 24-15 (scale bar = 400 μM-200 μM). EBs: Embryoid bodies; UDC: Urine-derived cell; iPSCs: Induced pluripotent stem cells.

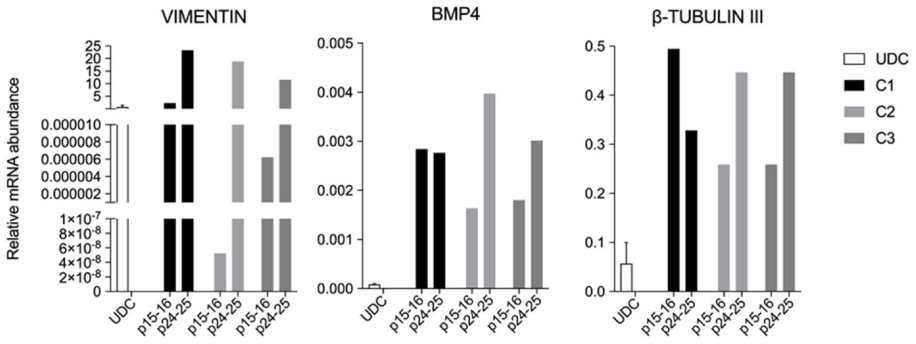

Figure 8 Relative mRNA abundance of urine-derived cells and embryoid bodies derived from the three porcine induced pluripotent stem cells lines showing VIMENTIN, BMP4 and β-TUBULIN-III detection. Embryoid bodies were analysed when porcine induced pluripotent stem cells were at p15-16 and again at p24-25. UDC: Urine-derived cell.

All lineages formed EBs that expressed VIMENTIN, BMP4 and b-TUBULIN-III, known markers of mesodermal and ectodermal lineages, respectively. However, none of the EBs presented AFP transcripts, a marker of the endodermal lineage. Rodríguez *et al*[41] has shown that EBs differentiated from piPSCs cultured in different conditions have shown mesoderm, endoderm and ectoderm markers after 15 d of undirected differentiation, and moreover, some markers not or mildly found at D15, were shown after D30 of differentiation[41]. Hence, further markers and other periods during spontaneous differentiation should be tested for complete characterization and discussion.

Overall, the results presented describe novel ways to derive *in vitro* reprogrammed cells in an important biomedical model, the porcine model. The isolation of UDCs is also relevant for other reproductive technologies, for example, for the conservation of many mammal species through nuclear reprogramming, or even to produce *in vitro* viable gametes, which could decrease the interval between generations for the acquisition of a genetically superior herd. Although the scenario of complete and robust *in vitro* cellular reprogramming is still under discussion in the porcine model; the advances described herein, in our conditions, are valuable for both translational studies and animal production, hence these putative piPSCs can be used to enable future autologous therapies, to the creation of gene-edited or not *in vitro* and *in vivo* biomedical models, to the study of the mechanism of cell differentiation, and also to future generation of gamete- or embryos-derived from iPSCs, contributing to the conservation and propagation of genetic material.

CONCLUSION

The results presented herein report, for the first time, the isolation and reprogramming of cells derived through the noninvasive collection of urine in a porcine model. Under our conditions, three putative iPSC lineages generated with murine OSKM presented typical morphology, AP and endogenous pluripotency-related gene expression, which was analyzed in three different passaging periods of the *in vitro* culture, and two lineages were maintained *in vitro* for more than 28 passages. Further studies on pluripotency induction in domestic animals are still needed to thoroughly understand and achieve full reprogramming, including more complete molecular profiles during *in vitro* and *in vivo* reprogramming processes, representing a novel tool for biomedical models of regenerative and translational medicine and animal production improvement.

ARTICLE HIGHLIGHTS

Research background

Induced pluripotent stem cells (iPSCs) derived from large animal models can greatly contribute to translational medicine and also to animal production, although robust and safe protocols are still uncommon. Cellular reprogramming of urine derived cells presents great advantages for iPSCs use in regenerative medicine due to the easy collection, injury and stress free, and is herein described for the first time in large animals.

Research motivation

The porcine iPSCs generation is promising for both translational medicine and animal production; and iPSCs derived from a noninvasive cell source would greatly contribute to its large-scale use, especially for *in vivo* autologous purposes using large animal models.

Research objectives

Isolate cells from porcine urine and generate iPSCs through their transduction with Yamanaka's human or murine factors.

Research methods

We isolated urine-derived cells (UDCs), which were reprogrammed *in vitro* into pluripotent cells. The porcine induced pluripotent cells generated were investigated regarding morphology, markers and endogenous transcripts related to the pluripotency.

Research results

From the porcine urine samples we isolated the UDCs, and colonies were formed when murine factors were used in the reprogramming. Endogenous pluripotent markers were detected in all three isolated lineages, in different time points during *in vitro* culture, and were able to differentiate into embryoid bodies (EBs) with mesoderm and ectoderm transcripts.

Research conclusions

In an unprecedented way, UDCs were isolated from noninvasive collection and reprogrammed into a pluripotent state using murine factors, the cells formed colonies presenting the expected characteristics, such as colonies with limited borders, transcripts and markers related to the pluripotency, and ability to differentiate into EBs.

Research perspectives

As we reported here, iPSCs can be derived from an easy collection and noninvasive source in the porcine model, and with our methodology represents a novel tool for iPSCs production in large animals and biomedical models of regenerative or translational medicine.

ACKNOWLEDGEMENTS

The authors would like to acknowledge Professors José Eduardo Krieger, Clara Steichen, and Carlos Eduardo Ambrosio for scientific discussion.

FOOTNOTES

Author contributions: Recchia K and Bressan FF conceptualized the experiments and wrote the manuscript; Recchia K, Machado LS, Barbosa G, Marques MG and Martins SMMK collected and processed samples; Recchia K, Botigelli RC, Pieri NCG, de Castro RVG, Meirelles FV, de Souza AF, Pessôa LVF, Fantinato Neto P and Bressan FF collected data and interpreted the collected data; all authors revised the manuscript.

Supported by the São Paulo Research Foundation (FAPESP) - Brazil (financial support grants #2015/26818-5, #2013/08135-2, #2019/02811-2); Coordination of Superior Level Staff Improvement (CAPES 23038.006964/2014-43 and financial code 001) and National Council for Scientific and Technological Development (CNPq 433133/2018-0).

Institutional review board statement: The study was reviewed and approved by the Institutional Review Board at Faculty of Veterinary Medicine and Animal Sciences, University of São Paulo.

Institutional animal care and use committee statement: All procedures were performed following the National Council for Control of Animal Experimentation (CONCEA) rules and were approved by the Ethics Committee on Animal Experimentation of the Faculty of Animal Science and Food Engineering and Faculty of Veterinary Medicine and Animal Sciences, University of São Paulo (protocols 6372070119 and 7051150717).

Conflict-of-interest statement: The authors declare that there are no conflicts of interest.

Data sharing statement: No additional data are available.

ARRIVE guidelines statement: The authors have read the ARRIVE guidelines, and the manuscript was prepared and revised according to the ARRIVE guidelines.

Country/Territory of origin: Brazil

ORCID number: Kaiana Recchia 0000-0002-4697-4201; Lucas Simões Machado 0000-0003-2946-1129; Ramon Cesar Botigelli 0000-0002-2796-6062; Naira Caroline Godoy Pieri 0000-0002-6800-6025; Gabriela Barbosa 0000-0003-4705-7808; Raquel Vasconcelos Guimarães de Castro 0000-0001-9672-027X; Mariana Groke Marques 0000-0002-3110-1280; Laís Vicari de Figueiredo Pessôa 0000-0002-3780-6046; Paulo Fantinato Neto 0000-0002-3243-8248; Flávio Vieira Meirelles 0000-0003-0372-4920; Aline Fernanda de Souza 0000-0002-5702-1166; Simone Maria Massami Kitamura Martins 0000-0002-5895-3678; Fabiana Fernandes Bressan 0000-0001-9862-5874.

Corresponding Author's Membership in Professional Societies: Brazilian Society of Embryo Technologies; International Embryo Technology Society; Colégio Brasileiro de Reprodução Animal; Associação Brasileira de Terapia Celular e Gênica (ABTCel-Gen); International Society for Stem Cell Research; Sociedade Brasileira de Biologia Celular (SBBC).

S-Editor: Wang JJ
L-Editor: A
P-Editor: Zhang YL

REFERENCES

1 **Pessôa LVF**, Bressan FF, Freude KK. Induced pluripotent stem cells throughout the animal kingdom: Availability and applications. *World J Stem Cells* 2019; **11**: 491-505 [PMID: 31523369 DOI: 10.4252/wjsc.v11.i8.491]
2 **Sierra H**, Cordova M, Chen CJ, Rajadhyaksha M. Confocal imaging-guided laser ablation of basal cell carcinomas: an ex vivo study. *J Invest Dermatol* 2015; **135**: 612-615 [PMID: 25178106 DOI: 10.1038/jid.2014.371]
3 **Pieri NCG**, de Souza AF, Botigelli RC, Machado LS, Ambrosio CE, Dos Santos Martins D, de Andrade AFC, Meirelles FV, Hyttel P, Bressan FF. Stem cells on regenerative and reproductive science in domestic animals. *Vet Res Commun* 2019; **43**: 7-16 [PMID: 30656543 DOI: 10.1007/s11259-019-9744-6]
4 **Kitala D**, Maurício AC. Novel Perspectives of Stem Cell Manufacturing and Therapies. In: Vicari de Figueiredo Pessôa L, Caroline Godoy Pieri N, Recchia K, Fernandes Bressan F. Induced Pluripotent Stem Cells from Animal Models: Applications on Translational Research. 2020
5 **Nowak-Imialek M**, Kues W, Carnwath JW, Niemann H. Pluripotent stem cells and reprogrammed cells in farm animals. *Microsc Microanal* 2011; **17**: 474-497 [PMID: 21682936 DOI: 10.1017/S1431927611000080]
6 **Bogliotti YS**, Wu J, Vilarino M, Okamura D, Soto DA, Zhong C, Sakurai M, Sampaio RV, Suzuki K, Izpisua Belmonte JC, Ross PJ. Efficient derivation of stable primed pluripotent embryonic stem cells from bovine blastocysts. *Proc Natl Acad Sci U S A* 2018; **115**: 2090-2095 [PMID: 29440377 DOI: 10.1073/pnas.1716161115]

7 **Perin EC**, Miller LW, Taylor DA, Willerson JT. Stem Cell and Gene Therapy for Cardiovascular Disease. In: Migliati E. Large Animal Models for Cardiac Cell Therapy. New York: Elsevier, 2015: 25-36

8 **Cong X**, Zhang SM, Ellis MW, Luo J. Large Animal Models for the Clinical Application of Human Induced Pluripotent Stem Cells. *Stem Cells Dev* 2019; **28**: 1288-1298 [PMID: 31359827 DOI: 10.1089/scd.2019.0136]

9 **Su Y**, Zhu J, Salman S, Tang Y. Induced pluripotent stem cells from farm animals. *J Anim Sci* 2020; **98** [PMID: 33098420 DOI: 10.1093/jas/skaa343]

10 **Cooper DKC**, Hara H, Iwase H, Yamamoto T, Jagdale A, Kumar V, Mannon RB, Hanaway MJ, Anderson DJ, Eckhoff DE. Clinical Pig Kidney Xenotransplantation: How Close Are We? *J Am Soc Nephrol* 2020; **31**: 12-21 [PMID: 31792154 DOI: 10.1681/ASN.2019070651]

11 **Ellis CE**, Korbutt GS. Justifying clinical trials for porcine islet xenotransplantation. *Xenotransplantation* 2015; **22**: 336-344 [PMID: 26381492 DOI: 10.1111/xen.12196]

12 **Li D**, Secher J, Hyttel P, Ivask M, Kolko M, Hall VJ, Freude KK. Generation of transgene-free porcine intermediate type induced pluripotent stem cells. *Cell Cycle* 2018; **17**: 2547-2563 [PMID: 30457474 DOI: 10.1080/15384101.2018.1548790]

13 **Esteban MA**, Xu J, Yang J, Peng M, Qin D, Li W, Jiang Z, Chen J, Deng K, Zhong M, Cai J, Lai L, Pei D. Generation of induced pluripotent stem cell lines from Tibetan miniature pig. *J Biol Chem* 2009; **284**: 17634-17640 [PMID: 19376775 DOI: 10.1074/jbc.M109.008938]

14 **Gao P**, Jiang D, Liu W, Li H, Li Z. Urine-derived Stem Cells, A New Source of Seed Cells for Tissue Engineering. *Curr Stem Cell Res Ther* 2016; **11**: 547-553 [PMID: 25697496 DOI: 10.2174/1574888X10666150220161506]

15 **Ji X**, Wang M, Chen F, Zhou J. Urine-Derived Stem Cells: The Present and the Future. *Stem Cells Int* 2017; **2017**: 4378947 [PMID: 29250119 DOI: 10.1155/2017/4378947]

16 **Jiang YF**, Chen M, Zhang NN, Yang HJ, Rui Q, Zhou YF. *In vitro* and *in vivo* differentiation of induced pluripotent stem cells generated from urine-derived cells into cardiomyocytes. *Biol Open* 2018; **7** [PMID: 29212797 DOI: 10.1242/bio.029157]

17 **Bento G**, Shafigullina AK, Rizvanov AA, Sardão VA, Macedo MP, Oliveira PJ. Urine-Derived Stem Cells: Applications in Regenerative and Predictive Medicine. *Cells* 2020; **9** [PMID: 32121221 DOI: 10.3390/cells9030573]

18 **Zhou M**, Shen L, Qiao Y, Sun Z. Inducing differentiation of human urine-derived stem cells into hepatocyte-like cells by coculturing with human hepatocyte L02 cells. *J Cell Biochem* 2020; **121**: 566-573 [PMID: 31407401 DOI: 10.1002/jcb.29301]

19 **Massa MG**, Gisevius B, Hirschberg S, Hinz L, Schmidt M, Gold R, Prochnow N, Haghikia A. Multiple Sclerosis Patient-Specific Primary Neurons Differentiated from Urinary Renal Epithelial Cells *via* Induced Pluripotent Stem Cells. *PLoS One* 2016; **11**: e0155274 [PMID: 27158987 DOI: 10.1371/journal.pone.0155274]

20 **Yan X**, Guo Y, Chen J, Cui Z, Gu J, Wang Y, Mao S, Ding C, Tang S. Establishment of CSUASOi001-A, a non-integrated induced pluripotent stem cell line from urine-derived cells of a Chinese patient carrying RS1 gene mutation. *Stem Cell Res* 2019; **38**: 101466 [PMID: 31141763 DOI: 10.1016/j.scr.2019.101466]

21 **Cao Y**, Xu J, Wen J, Ma X, Liu F, Li Y, Chen W, Sun L, Wu Y, Li S, Li J, Huang G. Generation of a Urine-Derived Ips Cell Line from a Patient with a Ventricular Septal Defect and Heart Failure and the Robust Differentiation of These Cells to Cardiomyocytes *via* Small Molecules. *Cell Physiol Biochem* 2018; **50**: 538-551 [PMID: 30308486 DOI: 10.1159/000494167]

22 **Qi Z**, Cui Y, Shi L, Luan J, Zhou X, Han J. Generation of urine-derived induced pluripotent stem cells from a patient with phenylketonuria. *Intractable Rare Dis Res* 2018; **7**: 87-93 [PMID: 29862149 DOI: 10.5582/irdr.2018.01032]

23 **Zhang J**, Wu S, Hu M, Liu Q. Generation of a human induced pluripotent stem cell line from urinary cells of a patient with primary congenital glaucoma using integration free Sendai technology. *Stem Cell Res* 2018; **29**: 162-165 [PMID: 29677590 DOI: 10.1016/j.scr.2018.04.004]

24 **Guo Y**, Zeng Q, Liu S, Yu Q, Wang P, Ma H, Shi S, Yan X, Cui Z, Xie M, Xue Y, Zha Q, Li Z, Zhang J, Tang S, Chen J. Generation of an iPS cell line *via* a non-integrative method using urine-derived cells from a patient with USH2A-associated retinitis pigmentosa. *Stem Cell Res* 2018; **29**: 139-142 [PMID: 29660607 DOI: 10.1016/j.scr.2018.03.022]

25 **Geuder J**, Wange LE, Janjic A, Radmer J, Janssen P, Bagnoli JW, Müller S, Kaul A, Ohnuki M, Enard W. A non-invasive method to generate induced pluripotent stem cells from primate urine. *Sci Rep* 2021; **11**: 3516 [PMID: 33568724 DOI: 10.1038/s41598-021-82883-0]

26 **Pipino C**, Mandatori D, Buccella F, Lanuti P, Preziuso A, Castellani F, Grotta L, Di Tomo P, Marchetti S, Di Pietro N, Cichelli A, Pandolfi A, Martino G. Identification and Characterization of a Stem Cell-Like Population in Bovine Milk: A Potential New Source for Regenerative Medicine in Veterinary. *Stem Cells Dev* 2018; **27**: 1587-1597 [PMID: 30142991 DOI: 10.1089/scd.2018.0114]

27 **Yang H**, Chen B, Deng J, Zhuang G, Wu S, Liu G, Deng C, Yang G, Qiu X, Wei P, Wang X, Zhang Y. Characterization of rabbit urine-derived stem cells for potential application in lower urinary tract tissue regeneration. *Cell Tissue Res* 2018; **374**: 303-315 [PMID: 30066105 DOI: 10.1007/s00441-018-2885-z]

28 **Xu Y**, Zhang T, Chen Y, Shi Q, Li M, Qin T, Hu J, Lu H, Liu J, Chen C. Isolation and Characterization of Multipotent Canine Urine-Derived Stem Cells. *Stem Cells Int* 2020; **2020**: 8894449 [PMID: 33061993 DOI: 10.1155/2020/8894449]

29 **Du X**, Feng T, Yu D, Wu Y, Zou H, Ma S, Feng C, Huang Y, Ouyang H, Hu X, Pan D, Li N, Wu S. Barriers for Deriving Transgene-Free Pig iPS Cells with Episomal Vectors. *Stem Cells* 2015; **33**: 3228-3238 [PMID: 26138940 DOI: 10.1002/stem.2089]

30 **Perleberg C**, Kind A, Schnieke A. Genetically engineered pigs as models for human disease. *Dis Model Mech* 2018; **11** [PMID: 29419487 DOI: 10.1242/dmm.030783]

31 **Wang H**, Xiang J, Zhang W, Li J, Wei Q, Zhong L, Ouyang H, Han J. Induction of Germ Cell-like Cells from Porcine Induced Pluripotent Stem Cells. *Sci Rep* 2016; **6**: 27256 [PMID: 27264660 DOI: 10.1038/srep27256]

32 **West FD**, Terlouw SL, Kwon DJ, Mumaw JL, Dhara SK, Hasneen K, Dobrinsky JR, Stice SL. Porcine induced pluripotent stem cells produce chimeric offspring. *Stem Cells Dev* 2010; **19**: 1211-1220 [PMID: 20380514 DOI: 10.1089/scd.2009.0458]

33 **Steichen C**, Si-Tayeb K, Wulkan F, Crestani T, Rosas G, Dariolli R, Pereira AC, Krieger JE. Human Induced Pluripotent

Stem (hiPS) Cells from Urine Samples: A Non-Integrative and Feeder-Free Reprogramming Strategy. *Curr Protoc Hum Genet* 2017; **92**: 21.7.1-21.7.22 [PMID: 28075482 DOI: 10.1002/cphg.26]

34 **Machado LS**, Pieri NCG, Botigelli RC, de Castro RVG, de Souza AF, Bridi A, Lima MA, Fantinato Neto P, Pessôa LVF, Martins SMMK, De Andrade AFC, Freude KK, Bressan FF. Generation of neural progenitor cells from porcine-induced pluripotent stem cells. *J Tissue Eng Regen Med* 2020; **14**: 1880-1891 [PMID: 33049106 DOI: 10.1002/term.3143]

35 **Bressan FF**, Bassanezze V, de Figueiredo Pessôa LV, Sacramento CB, Malta TM, Kashima S, Fantinato Neto P, Strefezzi RF, Pieri NCG, Krieger JE, Covas DT, Meirelles FV. Generation of induced pluripotent stem cells from large domestic animals. *Stem Cell Res Ther* 2020; **11**: 247 [PMID: 32586372 DOI: 10.1186/s13287-020-01716-5]

36 **Pieri NCG**, de Souza AF, Botigelli RC, Pessôa LVF, Recchia K, Machado LS, Glória MH, de Castro RVG, Leal DF, Fantinato Neto P, Martins SMMK, Dos Santos Martins D, Bressan FF, de Andrade AFC. Porcine Primordial Germ Cell-Like Cells Generated from Induced Pluripotent Stem Cells Under Different Culture Conditions. *Stem Cell Rev Rep* 2021 [PMID: 34115317 DOI: 10.1007/s12015-021-10198-8]

37 **de Souza AF**, Pieri NCG, Roballo KCS, Bressan FF, Casals JB, Ambrósio CE, Perecin F, Martins DS. Dynamics of male canine germ cell development. *PLoS One* 2018; **13**: e0193026 [PMID: 29489867 DOI: 10.1371/journal.pone.0193026]

38 **Marques MG**, de Souza AP, Pandolfi JRC. Metodologia para coleta in vitro de embriões em suínos. 2019

39 **Livak KJ**, Schmittgen TD. Analysis of relative gene expression data using real-time quantitative PCR and the 2(-Delta Delta C(T)) Method. *Methods* 2001; **25**: 402-408 [PMID: 11846609 DOI: 10.1006/meth.2001.1262]

40 **Raab S**, Klingenstein M, Liebau S, Linta L. A Comparative View on Human Somatic Cell Sources for iPSC Generation. *Stem Cells Int* 2014; **2014**: 768391 [PMID: 25431601 DOI: 10.1155/2014/768391]

41 **Zhou T**, Benda C, Duzinger S, Huang Y, Li X, Li Y, Guo X, Cao G, Chen S, Hao L, Chan YC, Ng KM, Ho JC, Wieser M, Wu J, Redl H, Tse HF, Grillari J, Grillari-Voglauer R, Pei D, Esteban MA. Generation of induced pluripotent stem cells from urine. *J Am Soc Nephrol* 2011; **22**: 1221-1228 [PMID: 21636641 DOI: 10.1681/ASN.2011010106]

42 **Burdeyron P**, Giraud S, Hauet T, Steichen C. Urine-derived stem/progenitor cells: A focus on their characterization and potential. *World J Stem Cells* 2020; **12**: 1080-1096 [PMID: 33178393 DOI: 10.4252/wjsc.v12.i10.1080]

43 **Pessôa LVF**, Pires PRL, Del Collado M, Pieri NCG, Recchia K, Souza AF, Perecin F, da Silveira JC, de Andrade AFC, Ambrosio CE, Bressan FF, Meirelles FV. Generation and miRNA Characterization of Equine Induced Pluripotent Stem Cells Derived from Fetal and Adult Multipotent Tissues. *Stem Cells Int* 2019; **2019**: 1393791 [PMID: 31191664 DOI: 10.1155/2019/1393791]

44 **Bessi BW**, Botigelli RC, Pieri NCG, Machado LS, Cruz JB, de Moraes P, de Souza AF, Recchia K, Barbosa G, de Castro RVG, Nogueira MFG, Bressan FF. Cattle In Vitro Induced Pluripotent Stem Cells Generated and Maintained in 5 or 20% Oxygen and Different Supplementation. *Cells* 2021; **10** [PMID: 34204517 DOI: 10.3390/cells10061531]

45 **de Castro RVG**, Pieri NCG, Fantinato Neto P, Grizendi BM, Dória RGS, Meirelles FV, Smith LC, Garcia JM, Bressan FF. In Vitro Induction of Pluripotency from Equine Fibroblasts in 20% or 5% Oxygen. *Stem Cells Int* 2020; **2020**: 8814989 [PMID: 33456472 DOI: 10.1155/2020/8814989]

46 **Yamanaka S**. Pluripotent Stem Cell-Based Cell Therapy-Promise and Challenges. *Cell Stem Cell* 2020; **27**: 523-531 [PMID: 33007237 DOI: 10.1016/j.stem.2020.09.014]

47 **Inada E**, Saitoh I, Kubota N, Iwase Y, Murakami T, Sawami T, Yamasaki Y, Sato M. Increased Expression of Cell Surface SSEA-1 is Closely Associated with Naïve-Like Conversion from Human Deciduous Teeth Dental Pulp Cells-Derived iPS Cells. *Int J Mol Sci* 2019; **20** [PMID: 30987116 DOI: 10.3390/ijms20071651]

World Journal of Stem Cells

Submit a Manuscript: https://www.f6publishing.com

World J Stem Cells 2022 March 26; 14(3): 245-263

DOI: 10.4252/wjsc.v14.i3.245

ISSN 1948-0210 (online)

ORIGINAL ARTICLE

Basic Study

Optimization of adipose tissue-derived mesenchymal stromal cells transplantation for bone marrow repopulation following irradiation

Min-Jung Kim, Won Moon, Jeonghoon Heo, Sangwook Lim, Seung-Hyun Lee, Jee-Yeong Jeong, Sang Joon Lee

Specialty type: Cell and tissue engineering

Provenance and peer review: Unsolicited article; Externally peer reviewed.

Peer-review model: Single blind

Peer-review report's scientific quality classification

Grade A (Excellent): A
Grade B (Very good): B
Grade C (Good): 0
Grade D (Fair): 0
Grade E (Poor): 0

P-Reviewer: Lo Furno D, Italy; Prasetyo EP, Indonesia

Received: November 19, 2021
Peer-review started: November 19, 2021
First decision: December 12, 2021
Revised: January 12, 2022
Accepted: February 27, 2022
Article in press: February 27, 2022
Published online: March 26, 2022

Min-Jung Kim, Jee-Yeong Jeong, Department of Biochemistry, Cancer Research Institute Kosin University College of Medicine, Seo-gu 49267, Busan, South Korea

Won Moon, Department of Internal Medicine, Kosin University College of Medicine, Seo-gu 49267, Busan, South Korea

Jeonghoon Heo, Department of Molecular Biology and Immunology, Kosin University College of Medicine, Seo-gu 49267, Busan, South Korea

Sangwook Lim, Department of Radiation Oncology, Kosin University College of Medicine, Seo-gu 49267, Busan, South Korea

Seung-Hyun Lee, Department of General Surgery, Kosin University College of Medicine, Seo-gu 49267, Busan, South Korea

Sang Joon Lee, Department of Ophthalmology, Gospel Hospital, Kosin University College of Medicine, Seo-gu 49267, Busan, South Korea

Corresponding author: Sang Joon Lee, MD, PhD, Doctor, Professor, Department of Ophthalmology, Gospel Hospital, Kosin University College of Medicine, 262 Gamcheon-ro, Seo-gu 49267, Busan, South Korea. hhiatus@gmail.com

Abstract

BACKGROUND

Bone marrow (BM) suppression is one of the most common side effects of radiotherapy and the primary cause of death following exposure to irradiation. Despite concerted efforts, there is no definitive treatment method available. Recent studies have reported using mesenchymal stromal cells (MSCs), but their therapeutic effects are contested.

AIM

We administered and examined the effects of various amounts of adipose-derived MSCs (ADSCs) in mice with radiation-induced BM suppression.

METHODS

Mice were divided into three groups: Normal control group, irradiated (RT) group, and stem cell-treated group following whole-body irradiation (WBI).

Mouse ADSCs (mADSCs) were transplanted into the peritoneal cavity either once or three times at 5×10^5 cells/200 μL. The white blood cell count and the levels of, plasma cytokines, BM mRNA, and BM surface markers were compared between the three groups. Human BM-derived $CD34^+$ hematopoietic progenitor cells were co-cultured with human ADSCs (hADSCs) or incubated in the presence of hADSCs conditioned media to investigate the effect on human cells *in vitro*.

RESULTS

The survival rate of mice that received one transplant of mADSCs was higher than that of mice that received three transplants. Multiple transplantations of ADSCs delayed the repopulation of BM hematopoietic stem cells. Anti-inflammatory effects and M2 polarization by intraperitoneal ADSCs might suppress erythropoiesis and induce myelopoiesis in sub-lethally RT mice.

CONCLUSION

The results suggested that an optimal amount of MSCs could improve survival rates post-WBI.

Key Words: Adipose tissue-derived stem cells; Bone marrow suppression; Mesenchymal stromal cells; Radiation; Cell therapy

Core Tip: Bone marrow (BM) suppression is one of the most common side effects of radiotherapy and the primary cause of death following exposure to irradiation. Although adipose tissue-derived stromal cell transplantation has emerged as a new treatment for BM suppression, the therapeutic effects are not proven conclusively. Our study showed that multiple transplantations of the adipose-derived mesenchymal stromal cells (ADSCs) delayed repopulation of BM hematopoietic stem cells. The administration of an optimal amount of ADSCs can improve survival rates following whole-body irradiation.

Citation: Kim MJ, Moon W, Heo J, Lim S, Lee SH, Jeong JY, Lee SJ. Optimization of adipose tissue-derived mesenchymal stromal cells transplantation for bone marrow repopulation following irradiation. *World J Stem Cells* 2022; 14(3): 245-263

URL: https://www.wjgnet.com/1948-0210/full/v14/i3/245.htm

DOI: https://dx.doi.org/10.4252/wjsc.v14.i3.245

INTRODUCTION

Acute exposure to high doses of ionizing radiation (IR) can lead to acute radiation syndrome (ARS), which affects the hematopoietic, gastrointestinal, and neurovascular systems[1,2]. Hematopoietic symptoms, particularly those induced by ARS, develop into severe neutropenia and thrombocytopenia, which eventually lead to bleeding, infection, and death[3]. The same clinical results are obtained when myeloablative therapy is performed in patients with conditions such as leukemia, lymphoma, and myeloma[4]. Although significant advances have been made in the development of safe, non-toxic, and effective radiation over the past six decades, no ARS drug has yet been approved by the United States Food and Drug Administration[5].

Bone marrow (BM) suppression is one of the most common side effects of radiotherapy and the primary cause of death post-exposure to a moderate or high dose of whole-body irradiation (WBI)[6]. The main therapeutic treatment is the administration of cytokines, such as granulocyte-colony stimulating factor (G-CSF), granulocyte-macrophage CSF (GM-CSF), and transplantation of hematopoietic stem cells (HSCs). Among these, G-CSF is a well-established and effective drug for the treatment of IR-induced acute BM suppression[7]. However, recent data have demonstrated that G-CSF could exhaust BM capacity during radiotherapy[8-10]. Currently, the modulation of the BM microenvironment post-irradiation has emerged as a novel target for hematopoiesis reconstruction in patients with ARS[11,12].

Novel cytokine-based treatments have been proposed for accidentally irradiated (RT) victims, particularly to prevent the apoptosis of hematopoietic stem and progenitor cells (HSPCs)[13-16]. The concept of "emergency anti-apoptotic cytokine therapy" is based on the administration of a four-cytokine cocktail: Stem cell factor (SCF), FLT3-ligand, thrombopoietin (TPO), and interleukin (IL)-3, to mitigate the apoptosis of HSPCs and promote balanced differentiation[14]. MSCs can secrete a number of cytokines required for hematopoietic re-proliferation post-irradiation, including IL-6, IL-11, leukemia inhibitor factor, SCF, FLT3 ligand, and stromal cell-derived factor (SDF), and can potentially be used as therapeutic agents[17].

BM-derived mesenchymal stem cells (BM-MSCs) are the major components of the hematopoietic microenvironment and play key roles in hematopoiesis. In pre-clinical studies, BM-MSCs have been shown to protect against radiation-induced liver injury[18], promote healing in RT murine skin wounds [19], improve survival in RT mice[20], mitigate gastrointestinal syndrome in mice[21], and restore the intestinal mucosal barrier in RT mice[22]. Superoxide dismutase gene-transfected MSCs improved survival in RT mice[23]; however, several other reports using similar models showed that MSCs alone did not affect survival[19,20,24]. Thus, the effectiveness of MSCs in promoting the proliferation of the RT BM remains controversial and requires investigation of the exact mechanisms to achieve consistent results in the MSC-based treatment of radiation-induced damage.

Adipose-derived mesenchymal stromal cells (ADSCs) were first identified in 2001 by Zuk *et al*[25], as cells with multilineage differentiation characteristics. ADSCs are characterized as a type of adult stem cells, *i.e.*, pluripotent cells with limited differentiation capacity. The International Fat Applied Technology Society defines any fat-derived pluripotent cell population capable of adherent, proliferative, and differentiating capacity as an ADSC[26]. These ADSCs are able to differentiate into adipogenic, osteogenic, chondrogenic, myogenic, cardiac, and neuronal cells *in vitro*[27-29]. The plasticity and pluripotency of these ADSCs, as well as their clinically abundant and non-invasive harvestability, have enabled researchers to regenerate dead or damaged cells or organs.

ADSCs have been used in several studies to alleviate the side effects of radiation, particularly cicatricial changes in the salivary glands, liver, and skin[30-33]. A few studies have demonstrated that ADSCs can support hematopoiesis both *in vitro* and *in vivo*[34-36]. ADSCs injected into the BM cavity of RT mice promoted BM reconstitution by supporting the homing, proliferation, and differentiation of BM progenitors, especially those for megakaryocytes[35], granulocytes, and monocytes[34,36]. Unfortunately, none of these studies examined the effect of ADSC transplantation on erythropoiesis, which is one of the most important aspects of hematopoiesis.

In the present study, we demonstrated that during BM repopulation post-WBI, mouse ADSC (mADSC) transplantation into the abdominal cavity delayed differentiation into red blood cells (RBCs) and accelerated the granulocyte/macrophage (GM) lineage differentiation and M2 macrophage polarization. Compared to low-dose, high-dose mADSC transplantation reduced survival rates. Therefore, the number of ADSCs for transplantation needs to be optimized to improve post-irradiation survival.

MATERIALS AND METHODS

Animal model

Male C57BL/6 mice (7-8-wk-old, weighing 21-23 g) were purchased from Central Laboratory Animals (Seoul, South Korea). The mice were kept under controlled conditions at a constant temperature (23.6 °C) and a 12 h light/dark cycle. The mice were provided with regular chow and water ad libitum. All animal experiments were approved by the Institutional Animal Care and Use Committee of Kosin University College of Medicine, and the animals were maintained and treated according to the regulations of the Association for Research in Vision and Ophthalmology.

The mice were randomly divided into three groups (n = 10/group): Normal control (NC), RT, and stem cell-treated (ST). The mice were RT with a single dose of 900 cGy using therapeutic 6 MV photon beams from a linear accelerator (Clinac iX, Varian Medical Systems, Palo Alto, CA, United States). The irradiation dose was calculated using a treatment planning system (Eclipse v13.0, Varian Medical Systems). During irradiation, the mice were anesthetized for immobilization to ensure homogeneous delivery of the photon beams. After WBI, mice in the ST group were intraperitoneally injected with mADSCs [5×10^5 cells/200 μL phosphate buffer solution (PBS)] once (#1) on day 1 or three times (#3) on days 1, 5, and 12. The mice in the RT group were intraperitoneally injected with 200 μL PBS; those in the NC group were not RT. The animals were placed in sterile cages immediately after the experiments. All experiments were repeated three times. To assess survival, animals were monitored for four weeks post-irradiation and subsequently euthanized using CO_2.

Preparation of ADSCs

ADSCs were isolated as previously described, with some modifications[37]. Briefly, mouse adipose tissues were obtained from epididymal and dorsal subcutaneous fat layers; human adipose tissues were obtained from fat discarded during elective breast surgeries. All procedures using human adipose tissue were conducted with informed consent under the Kosin University Gospel Hospital IRB approval protocol (protocol number 09-36).

Raw adipose tissue was processed to obtain the stromal vascular fraction (SVF). To isolate SVF, adipose tissues were washed extensively with equal volumes of PBS (Lonza, Basel, Switzerland). The extracellular matrix was digested at 37 °C for 30 min with 0.075% type I collagenase (Worthington Biochemical Corporation, Lakewood, NJ, United States). Enzyme activity was neutralized with Dulbecco's modified Eagle's medium/nutrient mixture F-12 (DMEM/F-12; GibcoBRL, Grand Island, NY, United States) containing 10% fetal bovine serum (FBS; GE Healthcare, Little Chalfont, United

Kingdom) and centrifuged at 1200 × g for 10 min to obtain a high-density SVF pellet. The cell pellet was resuspended in DMEM/F-12 supplemented with 10% FBS; filtered through a 100 mm mesh to remove cellular debris; seeded in culture plates; and incubated overnight at 37 °C with 5% CO_2 in DMEM/F-12 medium containing 10% FBS, 1% penicillin/streptomycin solution (Gibco, MD, United States), 10 ng/mL epidermal growth factor (Sigma-Aldrich, St. Louis, MO, United States), and 2 ng/mL basic fibroblast growth factor (bFGF) (Sigma-Aldrich). Following incubation, the plates were washed extensively with PBS to remove residual non-adherent RBCs. To prevent spontaneous differentiation, ADSCs were maintained at sub-confluent levels. Cells were subcultured with 0.05% trypsin and 1 mmol/L ethylenediaminetetraacetic acid (EDTA); and passaged at a ratio of 1:4.

Multilineage differentiation assay of ADSCs

In vitro differentiation of ADSCs was performed as previously described[37]. Briefly, P3 ADSCs were trypsinized and seeded in 6-well plates at a density of 5 × 10^4 cells/well. The cells were divided into four groups, *i.e.*, control, adipogenic, chondrogenic, and osteogenic, and were incubated for three weeks in control, adipogenic (A10070-01, Gibco), chondrogenic (A10071-01, Gibco), and osteogenic (A10072-01, Gibco) differentiation media, respectively. The hanging drop method was used for chondrogenic differentiation[38]. In the adipogenic, chondrogenic, and osteogenic groups, the culture medium was replaced every 2 d and the cells were stained with Oil Red O (Sigma-Aldrich), Alcian Blue (Sigma-Aldrich), and Alizarin Red S (Sigma-Aldrich), respectively, to confirm differentiation.

Peripheral blood cell evaluation

Peripheral blood was drawn from the tail vein, streaked as thin smears across a sterile slide, and air-dried. Peripheral blood was stained with Wright stain (Muto, Tokyo, Japan) for 2 min, rinsed with PBS, and dried before examination. The number of WBCs was counted in three random fields at 200 × magnification. Wright staining was performed once on the day before and twice per week post-WBI, until euthanasia.

For complete blood cell counting, blood was drawn from cardiac puncture using a 26-gauge needle syringe and collected in an EDTA-coated bottle (BD Biosciences, Franklin Lakes, NJ, United States). Total differential blood cell counts (WBCs, RBCs, and platelets) were obtained using a veterinary hematology analyzer (Hemavet 950; CDC Technologies, Oxford, CT, United States) at three weeks post-irradiation.

Histology

Femurs were fixed in 10% formalin and decalcified in 5% nitric acid (Ducksan, Gwangju, Korea) for 2 h. The femurs were then embedded in paraffin wax and sectioned. The blocks were cut into 5-μm sections using a rotary microtome (Leica RM2235, Leica Biosystems, Germany). The slides were either stained with hematoxylin and eosin or processed for immunohistochemistry (IHC).

For IHC staining, paraffin-embedded sections were deparaffinized in xylene (Duksan, Ansan, Korea) and rehydrated using ethanol (Duksan) gradients and PBS. Paraffin slides were immersed in 1 × citrate buffer (pH 6.0; Sigma-Aldrich), heated for 2 min in a microwave oven, and rinsed three times with PBS. Next, the sections were blocked for 1 h with blocking buffer containing 0.5% goat serum (Sigma-Aldrich) and 0.5% Tween-20 in PBS, and incubated overnight with primary antibodies (mouse anti-PCNA [BD Biosciences, San Jose, CA, United States], rabbit anti-Iba-1 (Wako, Tokyo, Japan), and rabbit anti-CD34 (GeneTex, Irvine, CA, United States). After incubation, the sections were washed three times with PBS and incubated for 1 h at room temperature with secondary antibodies [goat anti-mouse Alexa Fluor™ 568 and 488 (Invitrogen, Carlsbad, CA, United States), goat anti-rabbit Alexa Fluor™ 568 and 488 (Invitrogen)]. Next, the sections were stained with 4',6-diamidino-2-phenylindole (DAPI, Sigma-Aldrich), washed three times with PBS, mounted using 2-3 drops of a water-soluble mounting medium (Biomeda Crystal mount, Foster City, CA, United States), and then stored at 4 °C for immediate use or at -70 °C. Images were acquired using a fluorescence microscope (Nikon, Tokyo, Japan). Slides processed without the primary antibody were used as negative controls.

For cryosections, samples were fixed in 4% paraformaldehyde in 0.1 M phosphate buffer for 20 min, followed by three washes with 0.1 M phosphate buffer. The tissues were sequentially cryoprotected with 5%, 10%, and 15% sucrose for 1 h and 20% sucrose overnight. Next, the tissues were embedded using polyvinyl alcohol and a 2:1 ratio of polyethylene glycol-based optimal cutting temperature reagent (OCT; Tissue-Tek, Tokyo, Japan) and 20% sucrose. Serial sections of 10 μm were made using a cryostat and mounted on slides. Frozen sections were prepared by dissolving the OCT compound in a slide warmer (Chang Shin Science, Seoul, Korea). Immunostaining was performed after incubating the slides with cold 100% acetone for 10 min.

The numbers of CD34-, PCNA-, and Iba-1-positive cells were calculated as follows: For each group, three or more tissues stained with primary/secondary antibodies and DAPI were randomly selected, and their images captured at 400 × magnification. The number of positive cells in the merged images was counted using a preset area (190 μm × 170 μm). Immunostaining was considered positive if > 50% of the cells fluoresced, regardless of cell size. The percentage of positive cells was calculated as a proportion of the total DAPI-positive cells, multiplied by 100.

Polymerase chain reaction

The mRNA expression levels in mouse BM or human BM CD34$^+$ cells were evaluated using reverse transcription polymerase chain reaction (PCR). Total RNA was extracted with a TRIzol™ reagent (Invitrogen) or an RNAqueous™-4PCR kit (Ambion, Austin, TX, United States). Total RNA (1-3 μg) in a 20 μL reaction volume was reverse-transcribed into cDNA using a TOPscript™ cDNA synthesis kit (Enzynomics, Daejeon, Korea). Reactions were performed in a 20 μL volume using SYBR® Premix Ex Taq™ II (Takara, Dalian, China) with 2 μL cDNA. The sequences of human PCR primers for IL-4, IL-10, IL-1β, tumor necrosis factor-α (TNF-α), CD68, CD80, CD206, and β-actin as well as mouse PCR primers for IL-1β, TNF-α, CD14, CD68, CD163, CD206, IL-10, M-CSF, GM-CSF, SDF-1, TPO, IL-7, and glyceraldehyde 3-phosphate dehydrogenase (GAPDH), are listed in Supplementary Table 1. Quantitative real-time PCR was performed using an ABI PRISM 7300 sequence detection system (Applied Biosystems, Foster City, CA, United States) with thermal cycling consisting of denaturation for 10 s at 95 °C, followed by 40 cycles of 5 s at 95 °C, and 31 s at 60 °C. All values were normalized to GAPDH or β-actin and are presented as the average of three independent experiments.

For mouse BM samples, standard reverse transcription PCR was used for IL-1β, TNF-α, CD14, CD68, CD163, and CD206 primers. PCR was performed with TB Green™ Premix Ex Taq™ II (Takara) in a 20 μL volume containing 2 μL of cDNA, 0.25 μM of primer, and 10 μL of 2 × PCR Master Mix, using the following conditions: 35 cycles of 15 s at 95 °C for denaturation and 30 s at 60 °C for primer annealing and extension. The PCR products were analyzed using agarose gel electrophoresis.

Flow cytometry

To characterize ADSCs, trypsinized cells were incubated with monoclonal antibodies conjugated to either fluorescein isothiocyanate (FITC) or phycoerythrin (PE) for 30 min at room temperature. The following antibodies were used for mouse cells: CD31 (Abcam, Cambridge, United Kingdom), CD34, CD105, CD73 (Bioss Antibodies, Woburn, MA, United States), CD45, and CD90 (BD Biosciences). The antibodies used for human cells were CD34, CD45, CD90, CD105 (Beckman Coulter, Brea, CA, United States), and CD73 (BD Pharmingen, San Diego, CA, United States). The cells were assessed using flow cytometry (BD Accuri C6 Plus Flow Cytometer) and the data were analyzed using the BD Accuri C6 software (BD Biosciences).

The RT mice were euthanized with CO_2. The BM was removed from the femurs and tibiae by flushing with 1 mL DMEM/F-12 media using a 27-gauge needle and resuspended in PBS containing 1% bovine serum albumin (Sigma-Aldrich). The BM cells were filtered using a 30 μm polyamide filter (Myltenyi Biotec, Auburn, CA, United States), and labeled with Sca-1-PE (BD Biosciences), c-Kit-FITC (CD117; MACS, Cambridge, United Kingdom), CD34-FITC (Bioss Antibodies), IL-3R-PE (Miltenyi Biotec, Bergisch Gladbach, Germany), IL-7R-PE (Miltenyi Biotec), CD45RA-PE (Miltenyi Biotec), CD80-PE (eBioscience, San Diego, CA, United States), and CD206-FITC (R&D Systems, Minneapolis, MN, United States) antibodies.

Human BM CD34$^+$ stem cells were washed with PBS and labeled with CD34-PE, CD45-APC, CD15-PE, CD71-FITC, and CD235a (Gly-A)-PE (Miltenyi Biotec) antibodies at 4 °C for 30 min after 7 d of culturing.

Cytokine microarray

To determine the plasma cytokine profiles of the mice in each treatment group, blood samples were collected in heparin tubes and centrifuged at 2000 × g for 20 min at 4 °C. The plasma was separated, kept on ice, and stored at -80 °C. Next, the plasma samples were incubated on a pre-coated Proteome Profiler array membrane (ARY006, Mouse Cytokine Antibody Array kit; R&D Systems) and processed according to the manufacturer's instructions. Briefly, the array membranes were treated with blocking buffer for 1 h at room temperature on a rocking platform shaker. The blocking buffer was removed, and a mixture of plasma and antibody cocktail was added and incubated overnight at 2-8 °C. The incubated membranes were washed and incubated with streptavidin-horseradish peroxidase for 30 min at room temperature. After washing, the membranes were incubated with Chemi Reagent Mix and exposed to an X-ray film for 4-7 min. Densitometry analysis of dot blots was performed using the FluorChemHD2 software (ProteinSimple, Santa Clara, CA, United States). The density of each sample was normalized to that of a reference spot. The cytokine levels in each sample were determined relative to the cytokine levels expressed in the plasma samples of the NC group. A hierarchical clustering algorithm was applied to measure the Euclidean distance for the similarity metric and average linkage clustering method using the Cluster 3.0 open-source software.

Co-culture of human CD34$^+$ HSCs with human ADSCs

Frozen human BM CD34$^+$ HSPCs were purchased from Lonza (Walkersville, MD, United States). According to flow cytometry analysis with anti-CD34-PE conjugates (Miltenyi Biotec), the purity of the CD34$^+$ cells was consistently > 95%. To produce conditioned media (CM), human ADSCs (hADSCs) at P4 were cultured in DMEM/F-12 (Corning, Corning, NY, United States) containing 10% FBS (Hyclone, Logan, UT, United States) and arrested with 20 μg/mL mitomycin C (Sigma-Aldrich) for 2.5 h at 37 °C in 5% CO_2 atmosphere. After cell growth inhibition, the cells were washed twice with PBS and

incubated for 72 h in serum-free StemSpan™ medium (STEMCELL Technologies, Vancouver, Canada) supplemented with recombinant human SCF (50 ng/mL, Peprotech, Rocky Hill, NJ, United States), IL-3 (10 ng/mL, Peprotech), and low-density lipoprotein (LDL, 25 μg/mL, STEMCELL Technologies). The CM was collected, centrifuged at 500 × g for 20 min to remove cellular debris, and then concentrated 10-fold by means of centrifugation using a Centriprep® Centrifugal Filter Unit (Millipore, Bedford, MA, United States) with a 10 kDa cutoff membrane.

For co-culturing with $CD34^+$ cells, the hADSCs (1×10^5 cells/well) were seeded in 12-well plates (Corning) and incubated until about 80% confluence. hADSC growth was arrested by treating the cells with 20 μg/mL mitomycin C for 2.5 h, followed by two washes with PBS and incubation for an additional 24 h prior to co-culturing with $CD34^+$ cells. BM $CD34^+$ cells (1×10^4/well) were cultured in StemSpan™ medium supplemented with SCF (50 ng/mL), IL-3 (10 ng/mL), LDL (25 μg/mL), and TPO (100 ng/mL, Peprotech) in three different conditions: (1) In a control medium (control group); (2) In 1 × CM (CM group); or (3) In direct contact by co-culturing on a layer of hADSC (contact group). The fresh medium and cytokines were replaced on days 3 and 5 of the culture. On day 7, the cells were counted to determine the total cell number, and the proportion of $CD34^+$ cells was analyzed using flow cytometry and colony-forming cell (CFC) assays.

hADSC layers for co-culture were prepared as described above. BM $CD34^+$ cells (1×10^4 cells/well) were cultured in StemSpan™ medium supplemented with SCF (50 ng/mL), IL-3 (10 ng/mL), LDL (25 mg/mL), GM-CSF (10 ng/mL), and erythropoietin (EPO, 1 U/mL) in three different culture conditions: (1) In a control medium (control group); (2) In 1 × CM (CM group); or (3) In direct contact by co-culturing on a layer of hADSC (contact group). The fresh medium and cytokines were added on days 3 and 5 of the culture. On day 7, the cells were counted to determine the total cell number, and the expression of surface markers was analyzed using flow cytometry, as described above.

CFC assay

CFC assays were performed in triplicate for the control, CM, and contact groups. $CD34^+$ cells (1×10^3 cells/dish) were plated in methylcellulose medium (MethoCult™ H4100, STEMCELL Technologies) supplemented with SCF (50 ng/mL), IL-3 (10 ng/mL), GM-CSF (10 ng/mL, Peprotech), and EPO (1 U/mL) in 35 mm culture dishes and incubated at 37 °C in 5% CO_2 atmosphere for 14 d. Colonies were counted and analyzed using a scoring grid and an inverted microscope (Olympus, Tokyo, Japan). Colonies were classified based on their morphology as colony-forming unit erythroid (CFU-E), burst-forming unit erythroid (BFU-E), CFU-GM, and granulocyte/erythroid/macrophage/megakaryocytes.

Statistics

Data are expressed as mean ± SD. Statistical significance was set at $P < 0.05$. Five sections were evaluated per sample, and cell counts were used for immunohistochemical analysis. Each analysis was repeated three times. The Kaplan-Meier method was used to estimate the distribution of survival rates over time. A repeated measures two-way repeated measures ANOVA with Sidak's or Tukey's multiple comparison test was used to compare groups over time. A Kruskal-Wallis test and Dunn's multiple comparison test were used to compare the three mouse and human experimental groups, respectively. The GraphPad Prism 7 software for windows (San Diego, CA, United States) was used for statistical analysis.

RESULTS

Characterization of mouse and hADSCs

Mouse ADSCs (mADSCs) and hADSCs appeared as flat cubic cells in the initial culture and changed to spindle-shaped cells similar to fibroblasts with successive subcultures (Supplementary Figures1A and 1F). ADSCs were differentiated into adipose, cartilage, and bone, as evidenced by staining with Oil Red O, toluidine blue, and von Kossa, respectively (Supplementary Figures 1B-D and 2G-I). Surface markers of cultured hADSCs, passaged 3-5 times, were > 95% positive for CD73 and CD105, but negative for CD45 and CD34 (Supplementary Figure 1E). The surface markers of mADSCs were positive for CD29, CD73, and CD90, and negative for CD34, CD45, and CD31 (Supplementary Figure 1J).

Survival rates

Kaplan-Meier plots showed that WBI induced a mortality rate of 49.2% in the RT group by day 30 (Figure 1). The survival rates of the ST group transplanted with mADSCs once (ST#1) and three times (ST#3) were 92.3% and 55.6%, respectively. The survival rate of the ST#1 group was significantly higher than that of the ST#3 ($P = 0.043$) and RT groups ($P = 0.021$). The reduced survival rates of the ST#3 group are similar to the results reported by Hu *et al*[20], which showed that the mortality rates of RT BALB/c mice increased post-transplantation with BM-MSCs. Due to the relatively high survival rates, the ST#1 group was used in subsequent analyses.

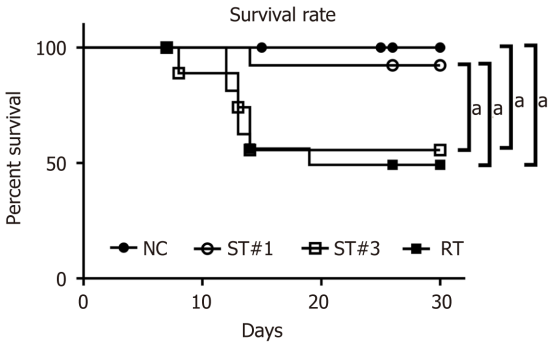

Figure 1 Survival curves of normal control, stem cell-treated, and irradiated mice. Mice were irradiated with a single dose of 900 cGy. After irradiation, mouse adipose tissue-derived stem cells (mADSCs) were transplanted intraperitoneally once (#1) or three times (#3) on days 1, 5, and 12. The irradiated (RT) group was injected intraperitoneally with the same volume of saline. The survival rates are presented as Kaplan-Meier plots. The stem cell-treated (ST) group that received one transplant (ST#1) showed higher survival than the RT group. There was no difference in survival between the ST#3 and RT groups. $^{a}P < 0.05$. NC: Normal control; ST: Stem cell-treated; RT: Irradiated.

Peripheral blood analysis

WBI significantly reduced the number of WBCs, as determined using Wright staining (Figure 2). Compared to the NC group on day 2 post-WBI, the number of WBCs was reduced to 25.7% and 23.8% in the ST#1 and RT groups, respectively. Moreover, the number of WBCs in the ST#1 group was significantly higher ($P < 0.01$) than in the RT group on days 14-21 post-WBI (Figure 2). However, by day 28, the number of WBCs in the ST and RT groups was partially restored to 70.8% and 57.8%, respectively, compared to that in the NC group. These results indicated that 9 Gy WBI induced a significant reduction in peripheral leukocyte counts, whereas peritoneal transplantation of mADSCs partially restored the number of peripheral leukocytes.

Hematocrit (Hct) and hemoglobin (Hb) levels and RBC and platelet counts were significantly lower in the ST#1 group than in the other groups on day 21 post-WBI (Figure 3A, 3B and 3C). However, there were no differences in the mean corpuscular volume, mean corpuscular Hb, and mean corpuscular Hb concentration between the groups (Figure 3D, 3E and 3F). These results suggested that mADSCs injected into the abdominal cavity secreted factors that affected the repopulation of BM post-WBI, thus changing the peripheral blood parameters.

Delayed repopulation of CD34⁺ HSCs in the BM post-WBI

CD34-expressing BM cells were assessed in the ST and RT groups on day 21 post-WBI. Our results indicated that administration of stem cells delayed the emergence of $CD34^+$ HSCs (Figure 3G-M). Next, we compared the percentage of proliferating cell nuclear antigen $(PCNA)^+$ cells in the $CD34^+$ HSCs of all three groups. At week 3 post-WBI, the percentage of $PCNA^+$ cells in $CD34^+$ HSCs was significantly higher ($P \leq 0.0001$) in the ST#1 group than in the RT group (Figure 4A, 4B and 4C). These findings suggest that the secretome from mADSCs delays the repopulation of $CD34^+$ BM progenitor cells and promotes the proliferation of $CD34^+$ progenitor cells in the third week post-WBI. Furthermore, the number of ionized calcium-binding adaptor molecule-1 $(Iba\text{-}1)^+$ cells was similar between the RT and ST#1 groups; however, the number of cells expressing both PCNA and Iba-1 was significantly higher in the ST group ($P \leq 0.01$, Figure 4D, 4E and 4F). It has previously been reported that Iba-1 is expressed in the BM of rat monoblastic cells[39]. Upon mADSC administration, $CD34^+$ HSCs were still observed a week later than in the RT group and the number of proliferating $Iba\text{-}1^+$ monoblastic cells was significantly higher in the ST#1 group than in the RT group. To identify the cell lineages that were proliferating during repopulation post-WBI, we performed a fluorescence-activated cell sorting analysis.

Characterization of repopulated BM cells post-mADSC transplantation

To compare the differentiation of HSCs during repopulation, Sca-1, c-Kit, and CD34 for HSCs; IL-3R for common myeloid progenitor cells; IL-7R for common lymphoid progenitor cells; CD45RA for common granulocyte-macrophage progenitor cells; and CD80 and CD206 for macrophage polarization were evaluated in BM cells harvested 3 wk post-WBI (Figure 5A-I). Sca-1 levels were significantly reduced in the RT and ST#1 groups compared to those in the NC group. Interestingly, $CD34^+$ HSCs were more abundant in the ST#1 group than in the RT group. These findings were consistent with our IHC results where the analyzed samples were also harvested 3 wk post-WBI. There was no difference in the number of BM cells expressing IL-3R between the RT and ST#1 groups. At the same time, IL-7R levels were significantly lower and CD45RA levels were significantly higher in the ST#1 group than those in the RT group. These results suggested that intraperitoneal mADSCs induced an increase in the number of $CD34^+$ HSCs and differentiation toward the common granulocyte-macrophage lineage during repopulation post-WBI. The polarization of the granulocyte-macrophage lineage toward the M2 phenotype was

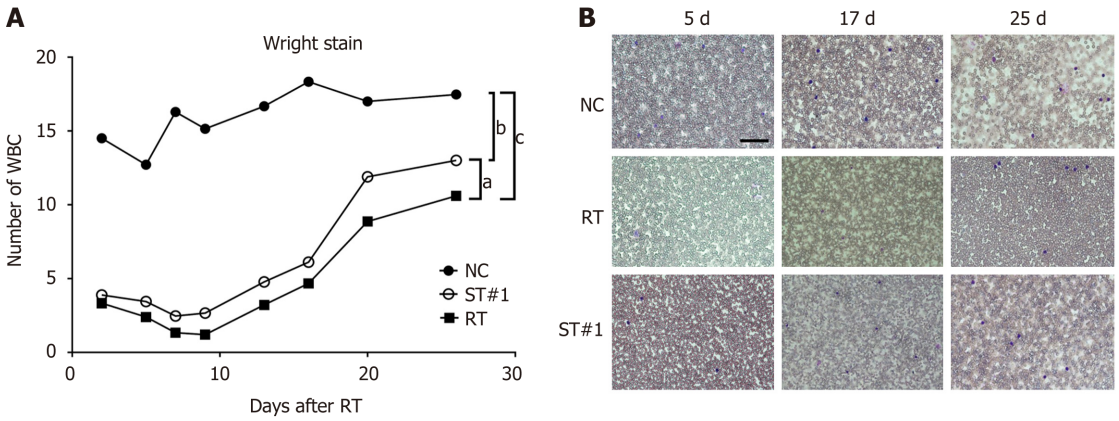

Figure 2 Evaluation of white blood cell count in peripheral blood using Wright staining. A: The number of white blood cells were compared between the normal control NC, stem cell-treated, and irradiated groups; B: Representative images of the cells harvested on days 5, 17, and 25 after 9 Gy whole-body irradiation. Magnification 200 ×; scale bar: 20 μm; $^{a}P < 0.01$, $^{b}P < 0.001$, and $^{c}P < 0.0001$ *vs* controls, as indicated. NC: Normal control; ST: Stem cell-treated; RT: Irradiated; WBC: White blood cell.

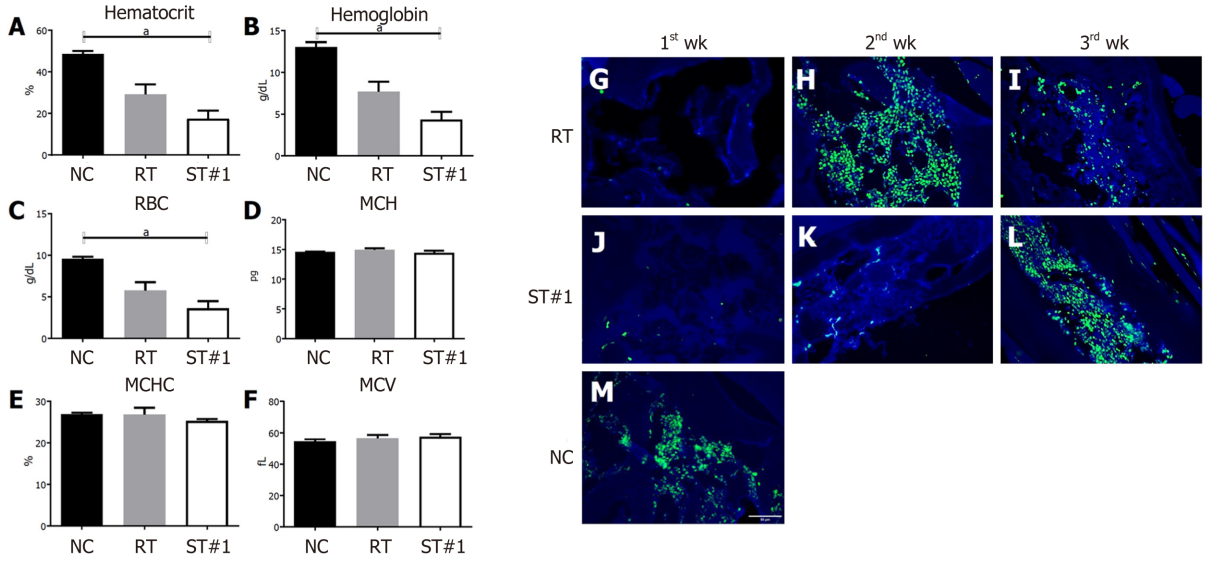

Figure 3 Characterization of red blood cell parameters in peripheral blood and CD34⁺ hematopoietic stem cells in the bone marrow. A-C: Hematocrit level, hemoglobin level, and red blood cells count in the control, irradiated (RT), and stem cell-treated (ST)#1 groups at three weeks post-whole-body irradiation (WBI); D-F: Mean corpuscular hemoglobin, mean corpuscular hemoglobin concentration, and mean corpuscular volume for the control, RT, and ST#1 groups at three weeks post-WBI; G-M: Immunohistochemistry for CD34⁺ hematopoietic cells (green) in bone marrow; nuclei were counterstained with 4',6-diamidino-2-phenylindole (blue). Magnification 400 ×; scale bar 50 μm; $^{a}P < 0.01$ *vs* controls. RBC: Red blood cell; MCH: Mean corpuscular hemoglobin; MCHC: Mean corpuscular hemoglobin concentration; MCV: Mean corpuscular volume; NC: Normal control; ST: Stem cell-treated; RT: Irradiated.

also observed using flow cytometry. In particular, the CD80:CD206 ratio was reversed in the ST#1 group compared to that in the RT group, indicating M2 polarization during repopulation post-WBI in mice transplanted with mADSCs (Figure 5H and 5I)[40].

The mRNA expression levels of CD163, CD206, and IL-10 were higher in the BM of the ST#1 group than in the other groups. At the same time, IL-1β and TNF-α mRNA levels were lower in the ST#1 group than in the other groups during the first and second week post-WBI (Figure 5J and Supplementary Figure 2). These results indicated that intraperitoneal ADSCs induced M2 polarization during repopulation post-WBI. The mRNA levels of GM-CSF, SCF, SDF-1, and IL-7 in the ST#1 group increased mainly in the first and second weeks post-WBI compared to those in the NC and RT groups (Supplementary Figure 2).

Assessment of plasma cytokine levels

To evaluate the effect of stem cell transplantation on plasma cytokine levels in RT mice, cytokine array analysis was performed using a mouse cytokine antibody kit and plasma collected from mice in the NC group, RT group at week 2, and ST group at week 2 (ST2w) and 3 (ST3w) post-WBI. The protein levels in the plasma of the RT, ST2w, and ST3w groups were normalized to those of the NC group. According

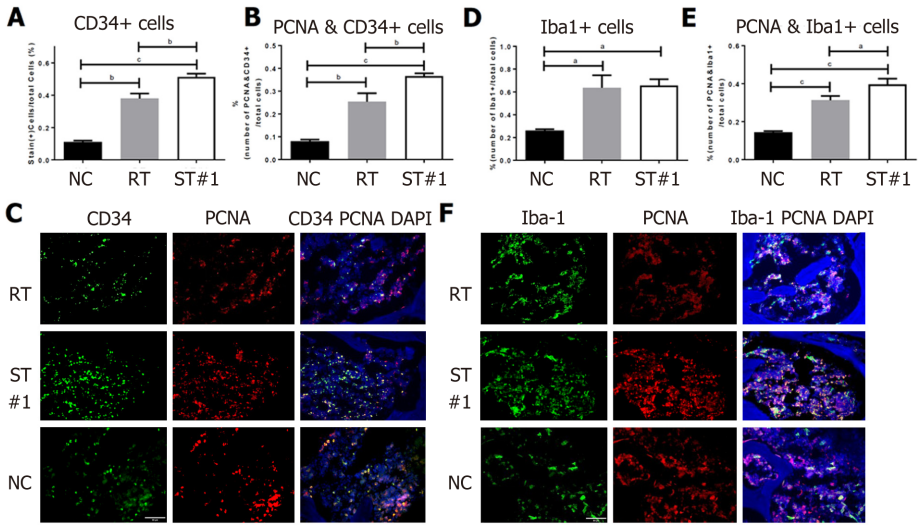

Figure 4 Immunohistochemical assessment of CD34, proliferating cell nuclear antigen, and ionized calcium-binding adaptor molecule-1 expression in bone marrow. Three weeks following whole-body irradiation, mouse femurs were fixed, decalcified, and embedded in paraffin wax. The sections were deparaffinized, stained with antibodies, and imaged under 400 × magnification. A-C: The number of CD34$^+$ cells in the stem cell-treated (ST)#1 group was higher than that in the irradiated (RT) group. The number of proliferating cell nuclear antigen (PCNA)$^+$ cells in CD34$^+$ hematopoietic stem cells was significantly higher in the ST#1 group than in the RT group; D-F: The number of ionized calcium-binding adaptor molecule-1 (Iba-1$^+$) cells, a marker of monoblastic cells, was similar between the ST and RT groups; however, the number of cells expressing both PCNA and Iba-1 was significantly higher in the ST group. Magnification 400 ×; scale bar: 50 μm; $^aP < 0.001$, $^bP < 0.001$, and $^cP < 0.0001$ *vs* controls. NC: Normal control; ST: Stem cell-treated; RT: Irradiated; CD: Cluster of differentiation; PCNA: Proliferating cell nuclear antigen; Iba-1: Ionized calcium-binding adaptor molecule-1; DAPI: 4',6-diamidino-2-phenylindole.

to the clustering analysis of all 39 proteins detected in the RT, ST2, and ST3 groups, expression patterns in the RT group were more similar to that of the ST3w group than those in the ST2w group (Figure 6A). The expression patterns of significant proteins (those showing more than 1.5-fold difference in expression level) in the ST3w group varied from those in the RT and ST2w groups (Figure 6B). Interestingly, G-CSF, C-X-C Motif Chemokine Ligand 13, and IL-2 levels increased in the ST2w group at week 2 post-WBI, which, with the exception of IL-2, was not observed in the ST3w group.

In vitro co-culture of human CD34$^+$ HSCs with hADSCs

BM CD34$^+$ cells were cultured in StemSpan™ medium supplemented with SCF, IL-3, LDL, and TPO in the absence (control group) or presence of the hADSC CM group or directly on a hADSC layer (contact group). After 7 d of incubation, the total cell numbers in the control, CM, and contact groups were (32.6 ± 3.75) × 10^4, (62.3 ± 2.95) × 10^4, and (81.7 ± 1.65) × 10^4, respectively (Figure 7A), indicating that cell proliferation was the highest in the contact group. The proportions of CD34$^+$ cells are illustrated in Figure 7B. The number of CD34$^+$ cells was (7.9 ± 1.38) × 10^4 in the control group, (13.4 ± 0.89) × 10^4 in the CM group, and (24.9 ± 2.21) × 10^4 in the contact group (Figure 7C). Therefore, the number of CD34$^+$ cells was highest in the contact group.

Next, we evaluated colony-forming ability by incubating CD34$^+$ cells in three different culture conditions for 7 d. As shown in Figure 7D, the differentiation of CD34$^+$ cells cultured in the presence of hADSC CM (CM group) or on an hADSC layer (contact group) into CFU-E and BFU-E was lower than that in the control group; however, differentiation into CFU-GM was higher in the CM and contact groups than in the control group. These results suggest that secretory factors from hADSCs suppress erythroid differentiation and promote GM differentiation.

We also investigated the effects of culture conditions (control, CM, and contact groups) on the differentiation of fresh BM CD34$^+$ cells in a suspension culture. After 7 d of differentiation, the total cell numbers in the control, CM, and contact groups were (26.4 ± 1.32) × 10^5, (32.5 ± 3.15) × 10^5, and (25.6 ± 0.90) × 10^5, respectively. Each surface marker was evaluated as a percentage of positive cells and total cell number. Both the percentage and number of CD15$^+$ and CD45$^+$ cells (granulocyte markers) were significantly higher in the CM and contact groups than in the control group (Figure 7E-J). While the percentage of CD71$^+$ and Gly A$^+$ cells (erythroid markers) were lower in the CM and contact groups than in the control group, the number of CD71$^+$ and Gly A$^+$ cells were lower only in the contact group compared to the control group (Figure 7K-P). These results suggest that the secretory factors of hADSCs may be sufficient to promote GM differentiation, but not enough to suppress erythroid differentiation under liquid differentiation conditions.

Macrophage polarity of BM CD34$^+$ cells differentiated in liquid culture

We examined the gene expression of several cytokines and surface markers in BM CD34$^+$ cells differen-

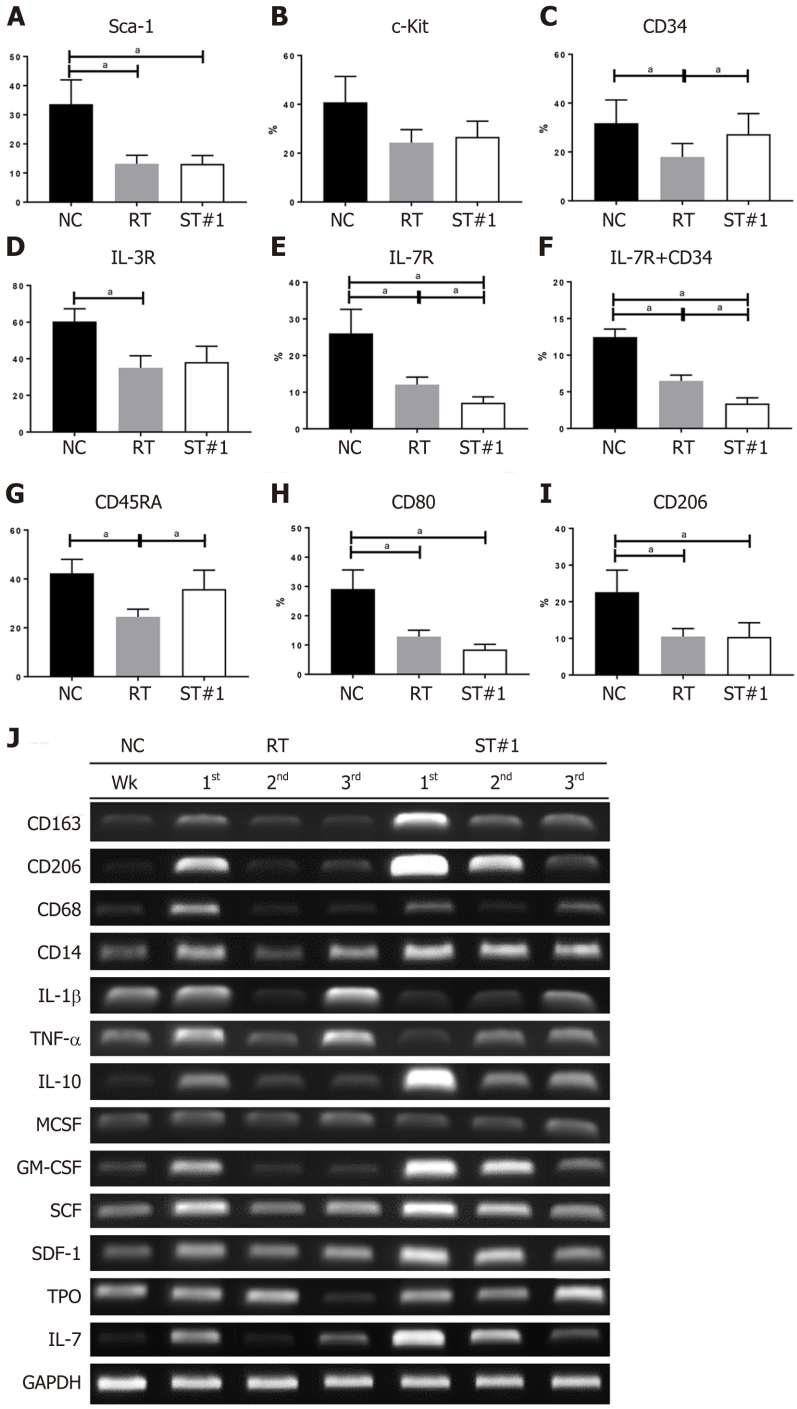

Figure 5 Characterization of repopulated bone marrow post-whole-body irradiation in the normal control, irradiated, and stem cell-treated groups. A-I: The expression levels of Sca-1, c-Kit, CD34, interleukin (IL)-3R, IL-7R, CD45RA, CD80, and CD206 in the bone marrow (BM) at 3 wk after post-whole-body irradiation (WBI) was examined using flow cytometry; J: mRNA expression in the BM at weeks 1, 2, and 3 post-WBI was evaluated using reverse transcription PCR. $^{a}P < 0.05$ *vs* controls, as indicated. NC: Normal control; ST: Stem cell-treated; RT: Irradiated; Sca-1: Stem cells antigen-1; c-KIT: Tyrosine-protein kinase KIT; CD: Cluster of differentiation; IL: Interleukin; TNF-α: Tumor necrotic factor-a; M-CSF: Macrophage colony-stimulating factor; GM-CSF: Granulocyte-macrophage colony-stimulating factor; SCF: Stem cell factor; SDF-1: Stromal cell-derived factor 1; TPO: Thrombopoietic growth factor; GAPDH: Glyceraldehyde 3-phosphate dehydrogenase.

tiated in liquid culture for 7 d. As shown in Figure 8, the gene expression levels of IL-4 and CD68 were not affected by the CM or contact conditions; however, the gene expression levels of IL-10, IL-1β, TNF-α, CD80, and CD206 were higher in the contact group than in the control group. Interestingly, CM alone was sufficient to increase the gene expression of IL-10 and CD206, markers that are highly expressed in M2 polarized macrophages, suggesting that secretory factors from hADSCs may promote macrophage polarization into the M2 phenotype.

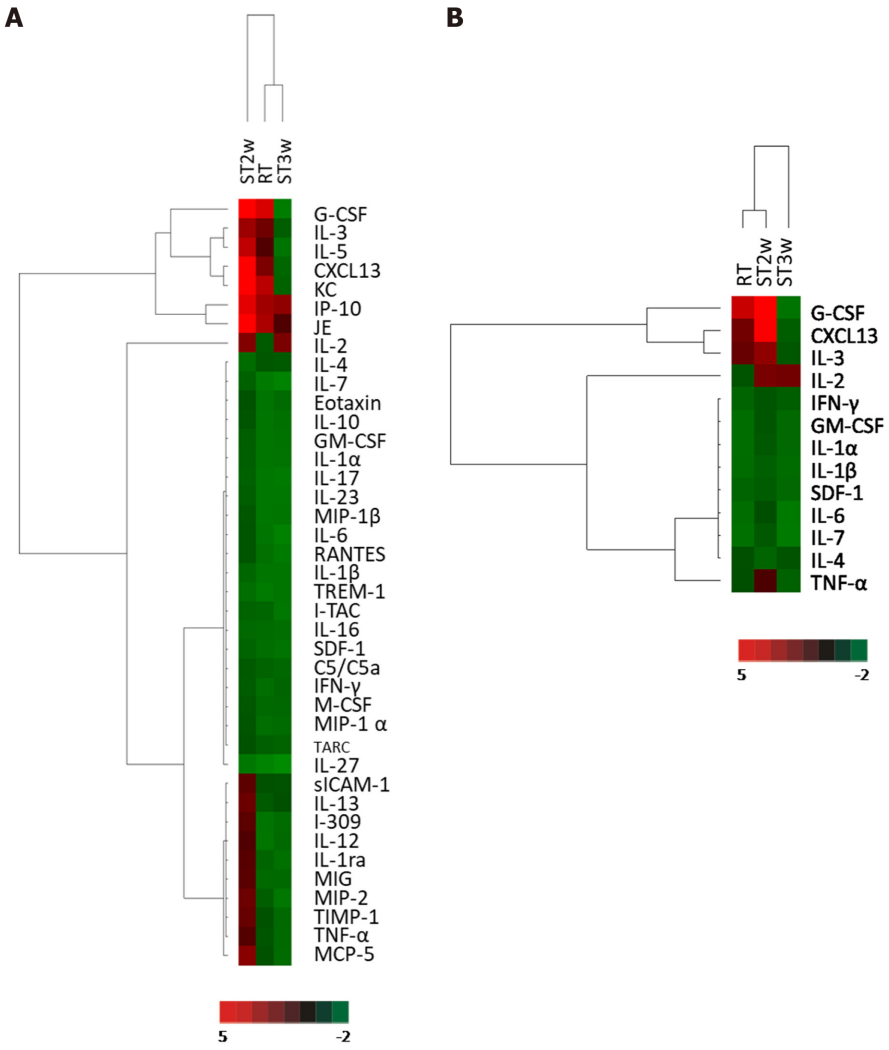

Figure 6 Clustering analysis of cytokine array from plasma samples. A: Thirty-nine proteins in the plasma were investigated in normal control (NC) and irradiated (RT) groups at week 2 and the stem cell-treated (ST) group at weeks 2 and 3 (ST2w and ST3w, respectively). Proteins in the plasma of RT and ST groups were normalized to the NC group before comparison; B: The proteins with 1.5-fold higher expression in the three groups than in the NC group were selected and compared. NC: Normal control; ST: Stem cell-treated; RT: Irradiated; IL: Interleukin; TNF-α: Tumor necrotic factor-α; GM-CSF: Granulocyte-macrophage colony-stimulating factor; SDF-1: Stromal cell-derived factor 1; IFN: Interferon.

DISCUSSION

In the present study, we present evidence that transplantation of ADSCs into the abdominal cavity of RT mice delayed the repopulation of $CD34^+$ HSCs and simultaneously promoted the proliferation of the granulocyte/monocyte lineage, particularly toward M2 polarization. Similar results were observed in the *in vitro* co-culture of hADSCs and human $CD34^+$ HPSCs. However, RT mice with multiple transplantations of mADSCs showed a lower survival rate than those with a single transplantation. Therefore, the dosage of MSCs could be an important determinant of survival rates.

Different survival rates have been reported for post-irradiation MSC treatment[20,23,35,41]. Shim *et al* [41] suggested that treatment with human umbilical cord blood-derived MSCs (2×10^6) was more effective than that with G-CSF for hematopoietic reconstitution, following sublethal dose (7 Gy) radiation exposure. Abdel-Mageed *et al*[23] proposed that extracellular superoxide dismutase-transduced mouse BM-MSCs could improve survival rate post-WBI. However, the control BM-MSC group did not display an enhanced survival rate compared to the WBI group[23]. Compared to RT and untreated animals, Kovalenko *et al*[24] found considerably increased survival rates in animals that received 2×10^8 human umbilical cord blood mononucleated cells with antibiotics. However, Hu *et al* [20] showed that transplantation of more than 1.5×10^8 cells/kg BM-MSCs increased mortality rates compared to those at lower BM-MSC concentrations, though the exact mechanism underlying these contradictory results is unclear. Similarly, our results indicated that survival rates after three MSC transplantations were lower than that after a single transplantation. After WBI, mice with multiple transplantations of mADSCs showed delayed $CD34^+$ hematopoietic repopulation and recovery of Hct and Hb levels in peripheral blood, which could be associated with increased mortality. We hypothesize

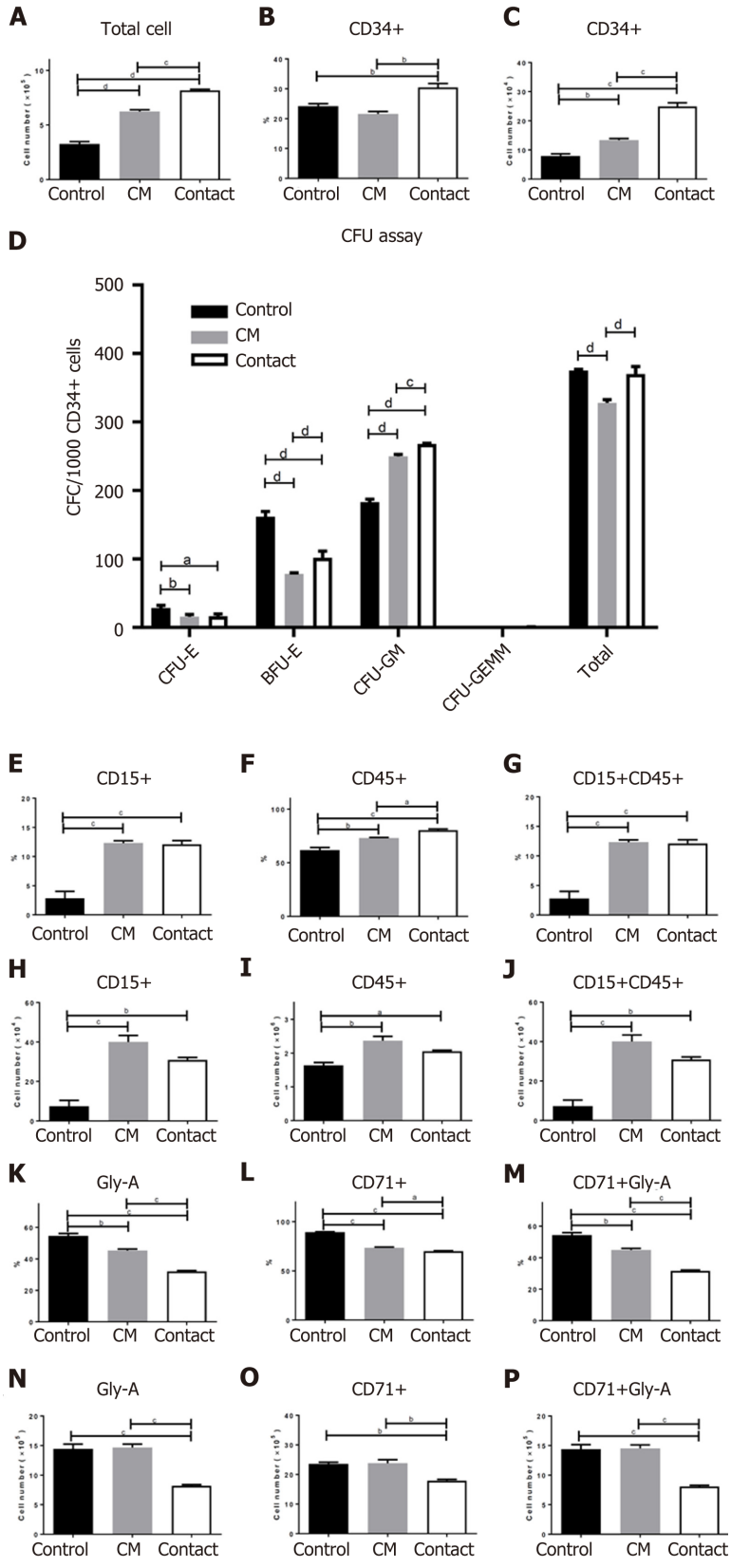

Figure 7 Effect of co-culture on CD34⁺ cell fate. CD34⁺ cells were incubated in the absence (control group) or presence of human adipose tissue-derived stem cells (hADSCs) conditioned medium (CM group) or directly on a hADSC layer (contact group). A: Total cell number; B: Percentage of CD34⁺ cells; C: The number of CD34⁺ cells were determined after 7 d of incubation; D: Colony-forming unit assays were performed using MethoCult™ by plating an equal number of CD34⁺ cells. The number of colonies was counted after 14 d of incubation; E-P: Differentiation assays of bone marrow CD34⁺ cells in liquid cultures, in the absence (control group) or presence of hADSC CM group or directly on a hADSC layer (contact group). The percentage of each surface marker was analyzed using flow cytometry (upper panel) and the marker-positive cell numbers were calculated (lower panel). $^{a}P < 0.05$, $^{b}P < 0.01$, $^{c}P < 0.001$, and $^{d}P < 0.0001$ *vs* controls. CFU: Colony-forming unit; CM: Conditioned media; CFU-E: Colony-forming unit erythroid; BFU-E: Burst-forming unit erythroid.

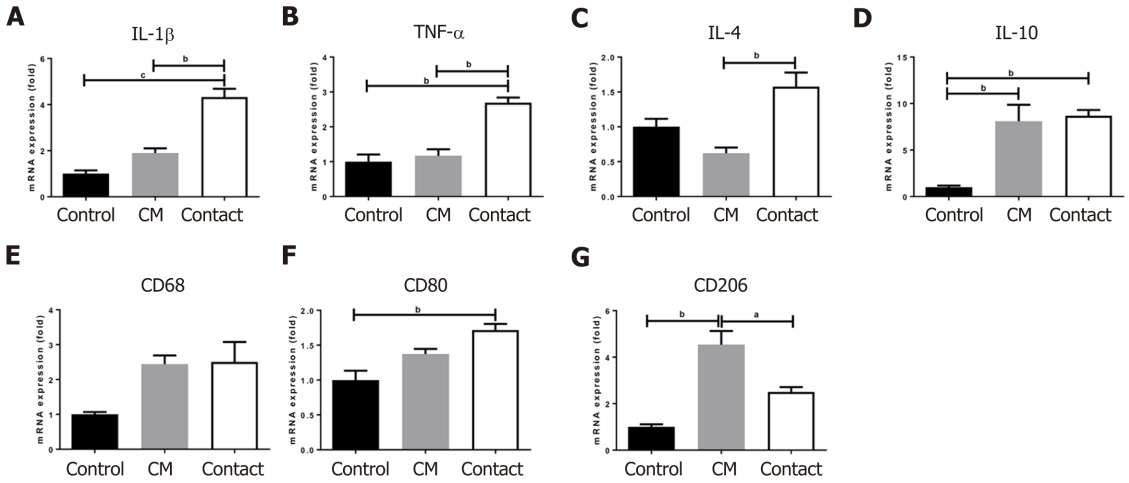

Figure 8 Gene expression analysis of bone marrow CD34⁺ cells cultured in the absence (control) or presence of human adipose tissue-derived stem cell conditioned medium or directly on a human adipose tissue-derived stem cell layer (contact). Relative expression levels of the indicated genes were determined using qRT-PCR. $^{a}P < 0.05$, $^{b}P < 0.01$, and $^{c}P < 0.001$ *vs* controls. CM: Conditioned media; IL: Interleukin; TNF-α: Tumor necrotic factor-α.

that the anti-inflammatory effects of MSCs on BM could mediate this delay.

Previous studies have shown that MSCs exert their immunosuppressive effects through the release of IL-6, IL-10, transforming growth factor β (TGF-β), tumor necrosis factor-inducible gene-6 (TSG-6), and indoleamine 2,3-dioxygenase[42,43]. MSC spheroids displayed anti-inflammatory activity mediated by prostaglandin E2 (PGE2), thus altering the phenotype of lipopolysaccharide - or zymosan-stimulated macrophages[44]. MSCs can also alleviate inflammation in macrophages by secreting TSG-6 and stanniocalcin-1[45]. Furthermore, MSCs decrease TNF-α secretion by mature DC type 1 (DC1), increase IL-10 secretion by mature DC2 cells, reduce interferon-γ (IFN-γ) production by Th1 cells, increase the secretion of IL-4 by Th2 cells, expand the proportion of regulatory T cells, and decrease IFN-γ secretion by natural killer cells[46]. The anti-inflammatory effects of MSCs have also demonstrated a beneficial effect on organ damage caused by irradiation. Dong *et al*[47] confirmed that the systemic infusion of human ADSCs ameliorated lung fibrosis in rats that received semi-thoracic irradiation (15 Gy) by upregulating hepatocyte growth factor (HGF) and PGE2, and downregulating TNF-α and TGF-β1. Saha *et al*[21] found that, in male C57BL/6 mice that received 10 Gy WBI or 16–20 Gy of abdominal irradiation, a bone mesenchymal stem cell (BMSC) transplant increased the levels of R-spondin1, keratinocyte growth factor, platelet-derived growth factor, bFGF, and anti-inflammatory cytokines in the serum, with reduced levels of pro-inflammatory cytokines. The anti-inflammatory effects of MSCs were also examined in our experiments. IL-1β and TNF-α mRNA levels were lower in the ST#1 group than in the RT group. At the same time, the mRNA level of the anti-inflammatory cytokine IL-10 was higher in the ST#1 group than in the RT group.

Although the reduction of pro-inflammatory cytokines can relieve sequelae caused by radiation irradiation, these inflammatory factors are essential for the proliferation of HSCs during repopulation. Interferons act as major regulators of HSC[48,49]. TNF-α and its receptors play a critical role in facilitating HSC engraftment and function[50,51]. TNF-α signaling is also necessary for the maintenance of HSCs, suggesting that baseline inflammatory signaling is crucial for the maintenance of proper HSC division and, subsequently, function[52]. In our study, mRNA levels of TNF-α and IL-1β were suppressed shortly after WBI in the ST#1 group compared to those in the other groups. Therefore, the anti-inflammatory effects derived from the secretome of mADSCs might delay reconstitution. It is also plausible that multiple doses (or an overdose) of MSCs lead to a severe delay in BM repopulation and, eventually, poor survival rates.

In the present study, the number of WBCs in the peripheral blood was higher in the ST#1 group than in the RT group at three weeks post-WBI; the number of proliferating myeloblasts (Iba1⁺ and PCNA⁺) in the BM was higher in the ST#1 group than in the RT and NC groups; and the number of CD45RA⁺ cells (GM progenitors) was higher in the ST#1 group than in the RT group. mADSCs indirectly affected myeloid differentiation in the BM. In previous studies, intraosseous or retrobulbar transplants of ADSCs with BMSCs promoted the differentiation of the myeloid lineage in the BM[34,36,53,54]. In the present study, the mRNA levels of GM-CSF and SDF-1 in the BM and G-CSF in the plasma were higher in the ST#1 group than in the RT group. G-CSF and GM-CSF are well-known hematopoietic factors that induce HSC differentiation into the myeloid lineage[55]. SDF-1 also promotes myeloid differentiation [56], and is expressed by stromal cells in several tissues and organs, including the skin, thymus, lymph nodes, lung, liver, and BM. Nakao *et al*[34] reported that SDF-1 secreted from ADSCs can induce the differentiation of CD34⁺ HSCs into myeloid cells. De Toni *et al*[36] showed that the co-culture of ADSCs

and CD34$^+$ HSCs *in vitro* without any cytokine supplement promoted CD34$^+$ HSC differentiation into granulocyte/monocyte lineages. In the present study, *in vitro* experiments demonstrated that hADSC CM or direct contact with the hADSC layer increased differentiation in CD34$^+$ HSCs toward the granulocyte-macrophage lineage.

ADSCs have been reported to have an effect on M2 polarization[43,57,58]. M1 macrophages are known to stimulate umbilical cord-MSCs and increase the expression of IL-6: A cytokine that upregulates IL-4R, promotes phosphorylation of STAT6 in macrophages, and eventually polarizes macrophages toward the M2 phenotype[43]. In mice with mutations in the gene encoding for IL-6Ra, IL-6 was found to be an important determinant of M2 macrophage activation[57]. These results suggest that the secretion of IL-6 by MSCs plays a key role in mediating macrophage polarization[43,57]. MSCs can also promote M2 macrophage polarization *via* IL-10[58]. In our study, M2 macrophage markers, such as CD206, CD164, and IL-10, were upregulated in the BM of the ST#1 group. IL-6, M-CSF, and IL-10, which can be secreted by mADSCs, can also induce M2 polarization in the BM. Therefore, M2 polarization could act as an anti-inflammatory suppressor in BM during the first week following radiation.

MSCs are multipotent cells that were originally isolated from BM and subsequently from other tissues, including fat[59], cardiac tissue[60], umbilical cord[61], and oral tissue[62]. BM-MSCs, which have been widely used for treating various diseases, traditionally required invasive harvesting procedures with low yields. On the other hand, ADSCs are abundant in the human body and have multiple differentiation potentials, making them a promising source for wound healing and tissue engineering, with low-risk cell harvesting and easy processing[63]. MSCs derived from the BM or adipose tissue share many similar biological characteristics, such as immunophenotype, multipotent differentiation, profiles of cytokine secretion, and immunomodulatory effects[64,65]. However, depending on tissue sources, donors, and isolation and culture protocols, the properties of MSCs may vary slightly[65-67]. Given the convenience of harvesting and multitude of sources, ADSCs appear to have numerous clinical advantages over cells derived from BM or other sources.

Umbilical cord derived MSCs (UC-MSCs) from fetal tissue have better proliferation capacity than ADSCs, which are MSCs from adult tissue[68]. However, compared to ADSC, UC-MSC is difficult to collect and secure, and the culture success rate is low[68,69]. It is not yet known whether MSCs derived from various tissues will have the same effect on BM repopulation. However, according to previous studies, UC-MSC, BM-MSC, and ADSC showed similar immunomodulatory effects[43,46,70]. In this regard, future research should evaluate variation in treatment efficacy according to the origin, age, and passage of MSCs. In treating BM repopulation with MSCs in humans, future clinical trials should specifically consider the dose to be administered. In the present study, mADSCs and hADSCs were used in the *in vivo* and *in vitro* experiments, respectively. In mice, P3-5 of mADSC were used, and P5-7 of hADSC were used; we recognize this to be a limitation in the interpretation of our results.

CONCLUSION

We present evidence that multiple intraperitoneal transplantations of mADSCs increased mortality post-WBI. The anti-inflammatory effects and M2 polarization promoted by the intraperitoneal administration of mADSCs might suppress erythropoiesis and induce myelopoiesis in sub-lethally RT mice. To improve survival rates post-WBI, the amount of MSCs should be optimized for administration.

ARTICLE HIGHLIGHTS

Research background

Bone marrow (BM) suppression is one of the most common side effects of radiotherapy and the primary cause of death following exposure to irradiation. Despite concerted efforts, no definitive treatment method is available. Transplantation of adipose tissue-derived stromal cells has been proposed as a promising therapy for BM suppression.

Research motivation

Although adipose tissue-derived stromal cell transplantation has shown reasonable efficacy in studies of BM suppression, the therapeutic effects are controversial.

Research objectives

We administered and examined the effects of various amounts of adipose-derived mesenchymal stromal cells (ADSCs) in mice with radiation-induced BM suppression.

Research methods

Mice were divided into three groups: Normal control group, irradiated (RT) group, and stem cell-treated group after whole-body irradiation (WBI). Mouse ADSCs were intraperitoneally transplanted either once or three times at 5 × 10^5 cells/200 μL. The white blood cell count and levels of plasma cytokines, BM mRNA, and BM surface markers were compared between the three groups. Human BM-derived $CD34^+$ hematopoietic progenitor cells were co-cultured with human ADSCs (hADSCs) or incubated in the presence of hADSC conditioned media (CM) to investigate the effect on human cells *in vitro*.

Research results

The survival rate of mice that received one ADSC transplant was higher than that in the three-transplant group. Multiple transplants of ADSCs delayed the repopulation of BM hematopoietic stem cells. Anti-inflammatory effects and M2 polarization by intraperitoneal ADSCs might suppress erythropoiesis and induce myelopoiesis in sub-lethally RT mice.

Research conclusions

To improve survival rates post-whole-body (WBI) irradiation, the amount of mesenchymal stromal cells should be optimized for transplantation.

Research perspectives

We demonstrated the effects of ADSC doses on BM suppression and suggest that the mechanisms involved can determine the success of future experiments and clinical applications.

ACKNOWLEDGEMENTS

The authors would like to thank Myung-Joo Lee and Eun-Sook Kim for their assistance with immunostaining, genetic analysis, and animal breeding.

FOOTNOTES

Author contributions: Lee SJ and Jeong JY contributed to the conception and design of the study, data interpretation, and funding acquisition; Lee SH, Lim S, Moon W, and Kim MJ contributed to the methodology, data acquisition, and analysis; Lee SJ wrote the original draft of the article; Lee SJ, Jeong JY, and Heo J drafted, reviewed and edited the manuscript, and contributed to project administration and supervision; all authors read and approved the final version of the manuscript.

Supported by The Basic Science Research Program Through The National Research Foundation of Korea (NRF) Grant Funded By The Korean Government To Lee S.J., No. 2021R1F1A1052084.

Institutional review board statement: The animal study was reviewed and approved by the Institutional Animal Care and Use Committee of Kosin University College of Medicine (KMAP-16-18) and all procedures for human adipose tissue were conducted with informed consent under the Kosin University Gospel Hospital IRB approval protocol (protocol number 09–36).

Institutional animal care and use committee statement: All animal experiments were approved by the Institutional Animal Care and Use Committee of Kosin University College of Medicine, and the animals were maintained and treated according to the regulations of the Association for Research in Vision and Ophthalmology.

Conflict-of-interest statement: The authors declare no conflicts of interest.

Data sharing statement: No additional data are available.

ARRIVE guidelines statement: The authors have read the ARRIVE guidelines, and the manuscript was prepared and revised according to the ARRIVE guidelines.

Country/Territory of origin: South Korea

ORCID number: Min-Jung Kim 0000-0002-3283-5737; Won Moon 0000-0002-3963-8680; Jeonghoon Heo 0000-0002-7176-2411; Sangwook Lim 0000-0003-3788-5108; Seung-Hyun Lee 0000-0002-5610-5237; Jee-Yeong Jeong 000-0001-9482-4526; Sang Joon Lee 0000-0001-6673-569X.

S-Editor: Wang JJ
L-Editor: A
P-Editor: Zhang YL

REFERENCES

1 **Waselenko JK**, MacVittie TJ, Blakely WF, Pesik N, Wiley AL, Dickerson WE, Tsu H, Confer DL, Coleman CN, Seed T, Lowry P, Armitage JO, Dainiak N; Strategic National Stockpile Radiation Working Group. Medical management of the acute radiation syndrome: recommendations of the Strategic National Stockpile Radiation Working Group. *Ann Intern Med* 2004; **140**: 1037-1051 [PMID: 15197022 DOI: 10.7326/0003-4819-140-12-200406150-00015]

2 **Zhang Y**, Guo C, Zhang H, Dong S. Synergistic protecting effect of cord blood CD34+ cells over-expressing both interleukin-3 and Flt3 ligand on lethally irradiated mice. *Int J Hematol* 2009; **90**: 64-73 [PMID: 19529981 DOI: 10.1007/s12185-009-0348-8]

3 **López M**, Martín M. Medical management of the acute radiation syndrome. *Rep Pract Oncol Radiother* 2011; **16**: 138-146 [PMID: 24376971 DOI: 10.1016/j.rpor.2011.05.001]

4 **Kroemeke A**, Sobczyk-Kruszelnicka M, Kwissa-Gajewska Z. Everyday life following hematopoietic stem cell transplantation: decline in physical symptoms within the first month and change-related predictors. *Qual Life Res* 2018; **27**: 125-135 [PMID: 28900828 DOI: 10.1007/s11136-017-1705-3]

5 **Singh VK**, Newman VL, Berg AN, MacVittie TJ. Animal models for acute radiation syndrome drug discovery. *Expert Opin Drug Discov* 2015; **10**: 497-517 [PMID: 25819367 DOI: 10.1517/17460441.2015.1023290]

6 **Mason KA**, Withers HR, McBride WH, Davis CA, Smathers JB. Comparison of the gastrointestinal syndrome after total-body or total-abdominal irradiation. *Radiat Res* 1989; **117**: 480-488 [PMID: 2648450 DOI: 10.2307/3577353]

7 **Dainiak N**. Rationale and recommendations for treatment of radiation injury with cytokines. *Health Phys* 2010; **98**: 838-842 [PMID: 20445391 DOI: 10.1097/HP.0b013e3181b3fce5]

8 **Li C**, Lu L, Zhang J, Huang S, Xing Y, Zhao M, Zhou D, Li D, Meng A. Granulocyte colony-stimulating factor exacerbates hematopoietic stem cell injury after irradiation. *Cell Biosci* 2015; **5**: 65 [PMID: 26609358 DOI: 10.1186/s13578-015-0057-3]

9 **van Os R**, Robinson S, Sheridan T, Mauch PM. Granulocyte-colony stimulating factor impedes recovery from damage caused by cytotoxic agents through increased differentiation at the expense of self-renewal. *Stem Cells* 2000; **18**: 120-127 [PMID: 10742384 DOI: 10.1634/stemcells.18-2-120]

10 **van Os R**, Robinson S, Sheridan T, Mislow JM, Dawes D, Mauch PM. Granulocyte colony-stimulating factor enhances bone marrow stem cell damage caused by repeated administration of cytotoxic agents. *Blood* 1998; **92**: 1950-1956 [PMID: 9731052 DOI: 10.1182/blood.v92.6.1950]

11 **Greenberger JS**, Epperly M. Bone marrow-derived stem cells and radiation response. *Semin Radiat Oncol* 2009; **19**: 133-139 [PMID: 19249651 DOI: 10.1016/j.semradonc.2008.11.006]

12 **Colombo ES**, Menicucci G, McGuire PG, Das A. Hepatocyte growth factor/scatter factor promotes retinal angiogenesis through increased urokinase expression. *Invest Ophthalmol Vis Sci* 2007; **48**: 1793-1800 [PMID: 17389513 DOI: 10.1167/iovs.06-0923]

13 **Borge OJ**, Ramsfjell V, Cui L, Jacobsen SE. Ability of early acting cytokines to directly promote survival and suppress apoptosis of human primitive CD34+CD38- bone marrow cells with multilineage potential at the single-cell level: key role of thrombopoietin. *Blood* 1997; **90**: 2282-2292 [PMID: 9310479 DOI: 10.1182/blood.v90.6.2282]

14 **Drouet M**, Mathieu J, Grenier N, Multon E, Sotto JJ, Herodin F. The reduction of in vitro radiation-induced Fas-related apoptosis in CD34+ progenitor cells by SCF, FLT-3 ligand, TPO, and IL-3 in combination resulted in CD34+ cell proliferation and differentiation. *Stem Cells* 1999; **17**: 273-285 [PMID: 10527462 DOI: 10.1002/stem.170273]

15 **Hérodin F**, Bourin P, Mayol JF, Lataillade JJ, Drouet M. Short-term injection of antiapoptotic cytokine combinations soon after lethal gamma -irradiation promotes survival. *Blood* 2003; **101**: 2609-2616 [PMID: 12468435 DOI: 10.1182/blood-2002-06-1634]

16 **Kashiwakura I**, Inanami O, Murakami M, Takahashi TA, Kuwabara M, Takagi Y. Effects of the combination of thrombopoietin with cytokines on the survival of X-irradiated CD34(+) megakaryocytic progenitor cells from normal human peripheral blood. *Radiat Res* 2002; **158;** 202-209 [PMID: 12105991 DOI: 10.1667/0033-7587(2002)158]

17 **Aqmasheh S**, Shamsasanjan K, Akbarzadehlaleh P, Pashoutan Sarvar D, Timari H. Effects of Mesenchymal Stem Cell Derivatives on Hematopoiesis and Hematopoietic Stem Cells. *Adv Pharm Bull* 2017; **7**: 165-177 [PMID: 28761818 DOI: 10.15171/apb.2017.021]

18 **Francois S**, Mouiseddine M, Allenet-Lepage B, Voswinkel J, Douay L, Benderitter M, Chapel A. Human mesenchymal stem cells provide protection against radiation-induced liver injury by antioxidative process, vasculature protection, hepatocyte differentiation, and trophic effects. *Biomed Res Int* 2013; **2013**: 151679 [PMID: 24369528 DOI: 10.1155/2013/151679]

19 **Kiang JG**. Adult Mesenchymal Stem Cells and Radiation Injury. *Health Phys* 2016; **111**: 198-203 [PMID: 27356065 DOI: 10.1097/HP.0000000000000459]

20 **Hu KX**, Sun QY, Guo M, Ai HS. The radiation protection and therapy effects of mesenchymal stem cells in mice with acute radiation injury. *Br J Radiol* 2010; **83**: 52-58 [PMID: 20139249 DOI: 10.1259/bjr/61042310]

21 **Saha S**, Bhanja P, Kabarriti R, Liu L, Alfieri AA, Guha C. Bone marrow stromal cell transplantation mitigates radiation-

induced gastrointestinal syndrome in mice. *PLoS One* 2011; **6**: e24072 [PMID: 21935373 DOI: 10.1371/journal.pone.0024072]

22 **Garg S**, Wang W, Prabath BG, Boerma M, Wang J, Zhou D, Hauer-Jensen M. Bone marrow transplantation helps restore the intestinal mucosal barrier after total body irradiation in mice. *Radiat Res* 2014; **181**: 229-239 [PMID: 24568131 DOI: 10.1667/RR13548.1]

23 **Abdel-Mageed AS**, Senagore AJ, Pietryga DW, Connors RH, Giambernardi TA, Hay RV, Deng W. Intravenous administration of mesenchymal stem cells genetically modified with extracellular superoxide dismutase improves survival in irradiated mice. *Blood* 2009; **113**: 1201-1203 [PMID: 19179476 DOI: 10.1182/blood-2008-07-170936]

24 **Kovalenko OA**, Azzam EI, Ende N. Human umbilical-cord-blood mononucleated cells enhance the survival of lethally irradiated mice: dosage and the window of time. *J Radiat Res* 2013; **54**: 1010-1014 [PMID: 23792493 DOI: 10.1093/jrr/rrt062]

25 **Zuk PA**, Zhu M, Mizuno H, Huang J, Futrell JW, Katz AJ, Benhaim P, Lorenz HP, Hedrick MH. Multilineage cells from human adipose tissue: implications for cell-based therapies. *Tissue Eng* 2001; **7**: 211-228 [PMID: 11304456 DOI: 10.1089/107632701300062859]

26 **Bourin P**, Bunnell BA, Casteilla L, Dominici M, Katz AJ, March KL, Redl H, Rubin JP, Yoshimura K, Gimble JM. Stromal cells from the adipose tissue-derived stromal vascular fraction and culture expanded adipose tissue-derived stromal/stem cells: a joint statement of the International Federation for Adipose Therapeutics and Science (IFATS) and the International Society for Cellular Therapy (ISCT). *Cytotherapy* 2013; **15**: 641-648 [PMID: 23570660 DOI: 10.1016/j.jcyt.2013.02.006]

27 **Halvorsen YD**, Bond A, Sen A, Franklin DM, Lea-Currie YR, Sujkowski D, Ellis PN, Wilkison WO, Gimble JM. Thiazolidinediones and glucocorticoids synergistically induce differentiation of human adipose tissue stromal cells: biochemical, cellular, and molecular analysis. *Metabolism* 2001; **50**: 407-413 [PMID: 11288034 DOI: 10.1053/meta.2001.21690]

28 **Yamada Y**, Wang XD, Yokoyama S, Fukuda N, Takakura N. Cardiac progenitor cells in brown adipose tissue repaired damaged myocardium. *Biochem Biophys Res Commun* 2006; **342**: 662-670 [PMID: 16488397 DOI: 10.1016/j.bbrc.2006.01.181]

29 **Casteilla L**, Dani C. Adipose tissue-derived cells: from physiology to regenerative medicine. *Diabetes Metab* 2006; **32**: 393-401 [PMID: 17110894 DOI: 10.1016/s1262-3636(07)70297-5]

30 **Qiu X**, Zhang S, Zhao X, Fu K, Guo H. The Therapeutic Effect of Adipose-Derived Mesenchymal Stem Cells for Radiation-Induced Bladder Injury. *Stem Cells Int* 2016; **2016**: 3679047 [PMID: 27051426 DOI: 10.1155/2016/3679047]

31 **Huang SP**, Huang CH, Shyu JF, Lee HS, Chen SG, Chan JY, Huang SM. Promotion of wound healing using adipose-derived stem cells in radiation ulcer of a rat model. *J Biomed Sci* 2013; **20**: 51 [PMID: 23876213 DOI: 10.1186/1423-0127-20-51]

32 **Choi JS**, An HY, Shin HS, Kim YM, Lim JY. Enhanced tissue remodelling efficacy of adipose-derived mesenchymal stem cells using injectable matrices in radiation-damaged salivary gland model. *J Tissue Eng Regen Med* 2018; **12**: e695-e706 [PMID: 27860388 DOI: 10.1002/term.2352]

33 **Chang P**, Qu Y, Liu Y, Cui S, Zhu D, Wang H, Jin X. Multi-therapeutic effects of human adipose-derived mesenchymal stem cells on radiation-induced intestinal injury. *Cell Death Dis* 2013; **4**: e685 [PMID: 23788042 DOI: 10.1038/cddis.2013.178]

34 **Nakao N**, Nakayama T, Yahata T, Muguruma Y, Saito S, Miyata Y, Yamamoto K, Naoe T. Adipose tissue-derived mesenchymal stem cells facilitate hematopoiesis in vitro and in vivo: advantages over bone marrow-derived mesenchymal stem cells. *Am J Pathol* 2010; **177**: 547-554 [PMID: 20558580 DOI: 10.2353/ajpath.2010.091042]

35 **Zhang J**, Zhou S, Zhou Y, Feng F, Wang Q, Zhu X, Zhao J, Fu H, Lv M, Ai H, Huang X, Zhang X. Adipose-Derived Mesenchymal Stem Cells (ADSCs) With the Potential to Ameliorate Platelet Recovery, Enhance Megakaryopoiesis, and Inhibit Apoptosis of Bone Marrow Cells in a Mouse Model of Radiation-Induced Thrombocytopenia. *Cell Transplant* 2016; **25**: 261-273 [PMID: 25975417 DOI: 10.3727/096368915X688155]

36 **De Toni F**, Poglio S, Youcef AB, Cousin B, Pflumio F, Bourin P, Casteilla L, Laharrague P. Human adipose-derived stromal cells efficiently support hematopoiesis in vitro and in vivo: a key step for therapeutic studies. *Stem Cells Dev* 2011; **20**: 2127-2138 [PMID: 21388235 DOI: 10.1089/scd.2011.0044]

37 **Heo JH**, Yoon JA, Ahn EK, Kim H, Urm SH, Oak CO, Yu BC, Lee SJ. Intraperitoneal administration of adipose tissue-derived stem cells for the rescue of retinal degeneration in a mouse model *via* indigenous CNTF up-regulation by IL-6. *J Tissue Eng Regen Med* 2018; **12**: e1370-e1382 [PMID: 28715614 DOI: 10.1002/term.2522]

38 **Bartosh TJ**, Ylostalo JH. Preparation of anti-inflammatory mesenchymal stem/precursor cells (MSCs) through sphere formation using hanging-drop culture technique. *Curr Protoc Stem Cell Biol* 2014; **28**: Unit 2B.6. [PMID: 24510769 DOI: 10.1002/9780470151808.sc02b06s28]

39 **Imai Y**, Ibata I, Ito D, Ohsawa K, Kohsaka S. A novel gene iba1 in the major histocompatibility complex class III region encoding an EF hand protein expressed in a monocytic lineage. *Biochem Biophys Res Commun* 1996; **224**: 855-862 [PMID: 8713135 DOI: 10.1006/bbrc.1996.1112]

40 **Li Y**, Kong N, Li Z, Tian R, Liu X, Liu G, Wang K, Yang P. Bone marrow macrophage M2 polarization and adipose-derived stem cells osteogenic differentiation synergistically promote rehabilitation of bone damage. *J Cell Biochem* 2019; **120**: 19891-19901 [PMID: 31338874 DOI: 10.1002/jcb.29297]

41 **Shim S**, Lee SB, Lee JG, Jang WS, Lee SJ, Park S, Lee SS. Mitigating effects of hUCB-MSCs on the hematopoietic syndrome resulting from total body irradiation. *Exp Hematol* 2013; **41**: 346-53.e2 [PMID: 23333483 DOI: 10.1016/j.exphem.2013.01.002]

42 **Ma S**, Xie N, Li W, Yuan B, Shi Y, Wang Y. Immunobiology of mesenchymal stem cells. *Cell Death Differ* 2014; **21**: 216-225 [PMID: 24185619 DOI: 10.1038/cdd.2013.158]

43 **Xie Z**, Hao H, Tong C, Cheng Y, Liu J, Pang Y, Si Y, Guo Y, Zang L, Mu Y, Han W. Human umbilical cord-derived mesenchymal stem cells elicit macrophages into an anti-inflammatory phenotype to alleviate insulin resistance in type 2 diabetic rats. *Stem Cells* 2016; **34**: 627-639 [PMID: 26523620 DOI: 10.1002/stem.2238]

44 **Ylöstalo JH**, Bartosh TJ, Coble K, Prockop DJ. Human mesenchymal stem/stromal cells cultured as spheroids are self-activated to produce prostaglandin E2 that directs stimulated macrophages into an anti-inflammatory phenotype. *Stem Cells* 2012; **30**: 2283-2296 [PMID: 22865689 DOI: 10.1002/stem.1191]

45 **Choi H**, Lee RH, Bazhanov N, Oh JY, Prockop DJ. Anti-inflammatory protein TSG-6 secreted by activated MSCs attenuates zymosan-induced mouse peritonitis by decreasing TLR2/NF-κB signaling in resident macrophages. *Blood* 2011; **118**: 330-338 [PMID: 21551236 DOI: 10.1182/blood-2010-12-327353]

46 **Aggarwal S**, Pittenger MF. Human mesenchymal stem cells modulate allogeneic immune cell responses. *Blood* 2005; **105**: 1815-1822 [PMID: 15494428 DOI: 10.1182/blood-2004-04-1559]

47 **Dong LH**, Jiang YY, Liu YJ, Cui S, Xia CC, Qu C, Jiang X, Qu YQ, Chang PY, Liu F. The anti-fibrotic effects of mesenchymal stem cells on irradiated lungs *via* stimulating endogenous secretion of HGF and PGE2. *Sci Rep* 2015; **5**: 8713 [PMID: 25736907 DOI: 10.1038/srep08713]

48 **Baldridge MT**, King KY, Boles NC, Weksberg DC, Goodell MA. Quiescent haematopoietic stem cells are activated by IFN-gamma in response to chronic infection. *Nature* 2010; **465**: 793-797 [PMID: 20535209 DOI: 10.1038/nature09135]

49 **Essers MA**, Offner S, Blanco-Bose WE, Waibler Z, Kalinke U, Duchosal MA, Trumpp A. IFNalpha activates dormant haematopoietic stem cells in vivo. *Nature* 2009; **458**: 904-908 [PMID: 19212321 DOI: 10.1038/nature07815]

50 **Rezzoug F**, Huang Y, Tanner MK, Wysoczynski M, Schanie CL, Chilton PM, Ratajczak MZ, Fugier-Vivier IJ, Ildstad ST. TNF-alpha is critical to facilitate hemopoietic stem cell engraftment and function. *J Immunol* 2008; **180**: 49-57 [PMID: 18097003 DOI: 10.4049/jimmunol.180.1.49]

51 **Rebel VI**, Hartnett S, Hill GR, Lazo-Kallanian SB, Ferrara JL, Sieff CA. Essential role for the p55 tumor necrosis factor receptor in regulating hematopoiesis at a stem cell level. *J Exp Med* 1999; **190**: 1493-1504 [PMID: 10562323 DOI: 10.1084/jem.190.10.1493]

52 **Baldridge MT**, King KY, Goodell MA. Inflammatory signals regulate hematopoietic stem cells. *Trends Immunol* 2011; **32**: 57-65 [PMID: 21233016 DOI: 10.1016/j.it.2010.12.003]

53 **Corre J**, Planat-Benard V, Corberand JX, Pénicaud L, Casteilla L, Laharrague P. Human bone marrow adipocytes support complete myeloid and lymphoid differentiation from human CD34 cells. *Br J Haematol* 2004; **127**: 344-347 [PMID: 15491297 DOI: 10.1111/j.1365-2141.2004.05198.x]

54 **Nishiwaki S**, Nakayama T, Saito S, Mizuno H, Ozaki T, Takahashi Y, Maruyama S, Nishida T, Murata M, Kojima S, Naoe T. Efficacy and safety of human adipose tissue-derived mesenchymal stem cells for supporting hematopoiesis. *Int J Hematol* 2012; **96**: 295-300 [PMID: 22782260 DOI: 10.1007/s12185-012-1140-8]

55 **Regan-Komito D**, Swann JW, Demetriou P, Cohen ES, Horwood NJ, Sansom SN, Griseri T. GM-CSF drives dysregulated hematopoietic stem cell activity and pathogenic extramedullary myelopoiesis in experimental spondyloarthritis. *Nat Commun* 2020; **11**: 155 [PMID: 31919358 DOI: 10.1038/s41467-019-13853-4]

56 **Sánchez-Martín L**, Estecha A, Samaniego R, Sánchez-Ramón S, Vega MÁ, Sánchez-Mateos P. The chemokine CXCL12 regulates monocyte-macrophage differentiation and RUNX3 expression. *Blood* 2011; **117**: 88-97 [PMID: 20930067 DOI: 10.1182/blood-2009-12-258186]

57 **Mauer J**, Chaurasia B, Goldau J, Vogt MC, Ruud J, Nguyen KD, Theurich S, Hausen AC, Schmitz J, Brönneke HS, Estevez E, Allen TL, Mesaros A, Partridge L, Febbraio MA, Chawla A, Wunderlich FT, Brüning JC. Signaling by IL-6 promotes alternative activation of macrophages to limit endotoxemia and obesity-associated resistance to insulin. *Nat Immunol* 2014; **15**: 423-430 [PMID: 24681566 DOI: 10.1038/ni.2865]

58 **Dayan V**, Yannarelli G, Billia F, Filomeno P, Wang XH, Davies JE, Keating A. Mesenchymal stromal cells mediate a switch to alternatively activated monocytes/macrophages after acute myocardial infarction. *Basic Res Cardiol* 2011; **106**: 1299-1310 [PMID: 21901289 DOI: 10.1007/s00395-011-0221-9]

59 **Zannettino AC**, Paton S, Arthur A, Khor F, Itescu S, Gimble JM, Gronthos S. Multipotential human adipose-derived stromal stem cells exhibit a perivascular phenotype in vitro and in vivo. *J Cell Physiol* 2008; **214**: 413-421 [PMID: 17654479 DOI: 10.1002/jcp.21210]

60 **Hoogduijn MJ**, Crop MJ, Peeters AM, Van Osch GJ, Balk AH, Ijzermans JN, Weimar W, Baan CC. Human heart, spleen, and perirenal fat-derived mesenchymal stem cells have immunomodulatory capacities. *Stem Cells Dev* 2007; **16**: 597-604 [PMID: 17784833 DOI: 10.1089/scd.2006.0110]

61 **Oh W**, Kim DS, Yang YS, Lee JK. Immunological properties of umbilical cord blood-derived mesenchymal stromal cells. *Cell Immunol* 2008; **251**: 116-123 [PMID: 18495100 DOI: 10.1016/j.cellimm.2008.04.003]

62 **Su WR**, Zhang QZ, Shi SH, Nguyen AL, Le AD. Human gingiva-derived mesenchymal stromal cells attenuate contact hypersensitivity *via* prostaglandin E2-dependent mechanisms. *Stem Cells* 2011; **29**: 1849-1860 [PMID: 21987520 DOI: 10.1002/stem.738]

63 **Alio del Barrio JL**, Chiesa M, Garagorri N, Garcia-Urquia N, Fernandez-Delgado J, Bataille L, Rodriguez A, Arnalich-Montiel F, Zarnowski T, Álvarez de Toledo JP, Alio JL, De Miguel MP. Acellular human corneal matrix sheets seeded with human adipose-derived mesenchymal stem cells integrate functionally in an experimental animal model. *Exp Eye Res* 2015; **132**: 91-100 [PMID: 25625506 DOI: 10.1016/j.exer.2015.01.020]

64 **Mosna F**, Sensebé L, Krampera M. Human bone marrow and adipose tissue mesenchymal stem cells: a user's guide. *Stem Cells Dev* 2010; **19**: 1449-1470 [PMID: 20486777 DOI: 10.1089/scd.2010.0140]

65 **He Q**, Ye Z, Zhou Y, Tan WS. Comparative study of mesenchymal stem cells from rat bone marrow and adipose tissue. *Turk J Biol* 2018; **42**: 477-489 [PMID: 30983864 DOI: 10.3906/biy-1802-52]

66 **Li CY**, Wu XY, Tong JB, Yang XX, Zhao JL, Zheng QF, Zhao GB, Ma ZJ. Comparative analysis of human mesenchymal stem cells from bone marrow and adipose tissue under xeno-free conditions for cell therapy. *Stem Cell Res Ther* 2015; **6**: 55 [PMID: 25884704 DOI: 10.1186/s13287-015-0066-5]

67 **Hu Y**, Lou B, Wu X, Wu R, Wang H, Gao L, Pi J, Xu Y. Comparative Study on *In Vitro* Culture of Mouse Bone Marrow Mesenchymal Stem Cells. *Stem Cells Int* 2018; **2018**: 6704583 [PMID: 29760732 DOI: 10.1155/2018/6704583]

68 **Jin HJ**, Bae YK, Kim M, Kwon SJ, Jeon HB, Choi SJ, Kim SW, Yang YS, Oh W, Chang JW. Comparative analysis of human mesenchymal stem cells from bone marrow, adipose tissue, and umbilical cord blood as sources of cell therapy. *Int J Mol Sci* 2013; **14**: 17986-18001 [PMID: 24005862 DOI: 10.3390/ijms140917986]

69 **Rebelatto CK**, Aguiar AM, Moretão MP, Senegaglia AC, Hansen P, Barchiki F, Oliveira J, Martins J, Kuligovski C, Mansur F, Christofis A, Amaral VF, Brofman PS, Goldenberg S, Nakao LS, Correa A. Dissimilar differentiation of mesenchymal stem cells from bone marrow, umbilical cord blood, and adipose tissue. *Exp Biol Med (Maywood)* 2008; **233**: 901-913 [PMID: 18445775 DOI: 10.3181/0712-RM-356]

70 **Zhao C**, Zhang L, Kong W, Liang J, Xu X, Wu H, Feng X, Hua B, Wang H, Sun L. Umbilical Cord-Derived Mesenchymal Stem Cells Inhibit Cadherin-11 Expression by Fibroblast-Like Synoviocytes in Rheumatoid Arthritis. *J Immunol Res* 2015; **2015**: 137695 [PMID: 26090476 DOI: 10.1155/2015/137695]

World Journal of Stem Cells

Submit a Manuscript: https://www.f6publishing.com

World J Stem Cells 2022 March 26; 14(3): 264-266

DOI: 10.4252/wjsc.v14.i3.264

ISSN 1948-0210 (online)

LETTER TO THE EDITOR

Mesenchymal stem/stromal cells as adjuvant therapy in COVID-19-associated acute lung injury and cytokine storm: Importance of cell identification

Jeanne Adiwinata Pawitan

Specialty type: Cell and tissue engineering

Provenance and peer review: Invited article; Externally peer reviewed.

Peer-review model: Single blind

Peer-review report's scientific quality classification

Grade A (Excellent): A
Grade B (Very good): B
Grade C (Good): C
Grade D (Fair): 0
Grade E (Poor): 0

P-Reviewer: Cai J, China; Tan JK, Malaysia; Tazegul G, Turkey

Received: September 11, 2021
Peer-review started: September 11, 2021
First decision: November 17, 2021
Revised: November 23, 2021
Accepted: March 6, 2022
Article in press: March 6, 2022
Published online: March 26, 2022

Jeanne Adiwinata Pawitan, Department of Histology, Faculty of Medicine, Universitas Indonesia, Jakarta 10430, DKI Jaya, Indonesia

Jeanne Adiwinata Pawitan, Stem Cell Medical Technology Integrated Service Unit, Dr. Cipto Mangunkusumo General Hospital/Faculty of Medicine Universitas Indonesia, Jakarta 10430, DKI Jaya, Indonesia

Jeanne Adiwinata Pawitan, Stem Cell and Tissue Engineering Research Center, Indonesia Medical Education and Research Institute (IMERI), Faculty of Medicine Universitas Indonesia, Jakarta 10430, DKI Jaya, Indonesia

Corresponding author: Jeanne Adiwinata Pawitan, MD, PhD, Professor, Department of Histology, Faculty of Medicine, Universitas Indonesia, Gedung Anatomi, Jl. Salemba 6, Jakarta 10430, DKI Jaya, Indonesia. jeanneadiwip@gmail.com

Abstract

Theoretically, mesenchymal stem cells (MSCs) are very promising as adjuvant therapy to alleviate coronavirus disease 2019 (COVID-19)-associated acute lung injury and cytokine storm. Several published studies, which used MSCs to alleviate COVID-19-associated acute lung injury and cytokine storm, reported promising results. However, the evidence came from a case report, case series, and clinical trials with a limited number of participants. Therefore, more studies are needed to get robust proof of MSC beneficial effects.

Key Words: COVID-19; Mesenchymal stem cells; Pneumonia; Cytokine storm; Acute respiratory distress syndrome

Core Tip: Several published studies, which used mesenchymal stem cells (MSCs) to alleviate coronavirus disease 2019-associated acute lung injury and cytokine storm, reported promising results. However, the evidence came from a case report, case series, and clinical trials with a limited number of participants. Therefore, more robust proof is needed. The studies and ongoing clinical trials used MSCs from various sources, and theoretically angiotensin-converting enzyme 2 negative subsets are preferable. Therefore, in future reporting of clinical trial results, the complete identity of the MSCs needs to be defined.

Citation: Pawitan JA. Mesenchymal stem/stromal cells as adjuvant therapy in COVID-19-associated acute lung injury and cytokine storm: Importance of cell identification. *World J Stem Cells* 2022; 14(3): 264-266
URL: https://www.wjgnet.com/1948-0210/full/v14/i3/264.htm
DOI: https://dx.doi.org/10.4252/wjsc.v14.i3.264

TO THE EDITOR

I read with interest a minireview by Zhang *et al*[1], who elaborately discussed the prospects of mesenchymal stem/stromal cells (MSCs) in coronavirus disease 2019 (COVID-19)-associated acute lung injury/acute respiratory distress syndrome. In the beginning, the authors pointed out two recently reported MSC based therapies to deal with cytokine storm and pulmonary damage. The first report was by Leng *et al*[2], which enrolled 7 MSC treated subjects and 3 controls. The report showed favorable prognosis in terms of clinical recovery and serum cytokine profile. The second report of MSC based therapy for COVID-19 was a case report by Liang *et al*[3] that reported a favorable outcome.

Though the two reports showed favorable outcomes, I highly support the opinion of Zhang *et al*[1] that the systematic elaboration of the therapeutics and underlying mechanism is far from satisfactory. The first report, which enrolled only a few subjects, showed that the treatment and control group were unequal in terms of age of the patients and severity of disease. The second report is a case report of only 1 patient[2,3], which provides the lowest level of evidence. There were several other reports that were not assessed by the authors. A case series of 12 patients by Terry[4] used two intravenous infusions of bone marrow-derived MSCs (Ryoncil® from Mesoblast). The results showed that 75% of patients who were previously refractory to other experimental therapies were free from ventilators within 10 d, and overall survival was 83%. Further, a recent randomized clinical trial from Indonesia, which enrolled 40 patients, gave umbilical cord (UC)-derived MSCs, and the results showed that the survival rate in the treatment group was 2.5 times higher than in the control group. However, when only patients with comorbidities were assessed, the survival rate of the treatment group was 4.5 times compared to controls. Moreover, there was a significant decrease in interleukin-6 in the recovered patients, and this result was in line with the anti-inflammatory property of MSCs[5]. Interestingly, there are 70 clinical trials at various stages, which are ongoing, and these trials are using MSCs from various sources[1].

It is interesting to note that Zhang *et al*[1] pointed out the superiority of angiotensin-converting enzyme 2 (ACE2) negative subsets of UC-derived MSCs that were used by Leng *et al*[2]. Other studies that used MSCs for COVID-19 did not use ACE2 negative subsets of MSCs[3-5]. A study showed that ACE2 expression was significantly higher in adipose tissue and bone marrow-derived MSCs compared to UC or placenta-derived MSCs. In addition, culture conditions and passage also had an impact on ACE2 expression levels. At higher passages (3-5 passages) both UC and placenta-derived MSCs expressed higher levels of ACE2[6]. I highly support the opinion of Zhang *et al*[1] that highly bioactive subpopulations from the heterogeneous MSCs need to be identified[1]. Therefore, future studies that will use MSCs need to completely report the source, culture conditions, passage, identity, and properties of the MSCs that are used.

FOOTNOTES

Author contributions: Pawitan JA designed the research, performed the research, analyzed data, wrote the letter, and revised the letter.

Conflict-of-interest statement: Jeanne Adiwinata Pawitan has no conflict of interest.

Country/Territory of origin: Indonesia

ORCID number: Jeanne Adiwinata Pawitan 0000-0002-6551-5238.

S-Editor: Fan JR
L-Editor: Filipodia
P-Editor: Fan JR

REFERENCES

1 **Zhang LS**, Yu Y, Yu H, Han ZC. Therapeutic prospects of mesenchymal stem/stromal cells in COVID-19 associated pulmonary diseases: From bench to bedside. *World J Stem Cells* 2021; **13**: 1058-1071 [PMID: 34567425 DOI: 10.4252/wjsc.v13.i8.1058]

2 **Leng Z**, Zhu R, Hou W, Feng Y, Yang Y, Han Q, Shan G, Meng F, Du D, Wang S, Fan J, Wang W, Deng L, Shi H, Li H, Hu Z, Zhang F, Gao J, Liu H, Li X, Zhao Y, Yin K, He X, Gao Z, Wang Y, Yang B, Jin R, Stambler I, Lim LW, Su H, Moskalev A, Cano A, Chakrabarti S, Min KJ, Ellison-Hughes G, Caruso C, Jin K, Zhao RC. Transplantation of ACE2^{-} Mesenchymal Stem Cells Improves the Outcome of Patients with COVID-19 Pneumonia. *Aging Dis* 2020; **11**: 216-228 [PMID: 32257537 DOI: 10.14336/AD.2020.0228]

3 **Liang B**, Chen J, Li T, Wu H, Yang W, Li Y, Li J, Yu C, Nie F, Ma Z, Yang M, Xiao M, Nie P, Gao Y, Qian C, Hu M. Clinical remission of a critically ill COVID-19 patient treated by human umbilical cord mesenchymal stem cells: A case report. *Medicine (Baltimore)* 2020; **99**: e21429 [PMID: 32756149 DOI: 10.1097/MD.0000000000021429]

4 **Terry M**. Mesoblast's stem cell therapy shows 83% survival in ventilator-dependent covid-19 patients. Biospace; 2020. [cited 10 July 2022]. Available from: https://www.biospace.com/article/mesoblast-ltd-s-stem-cell-therapy-shows-83-percent-survival-in-covid-19-patients/#:~:text=Melbourne%2C%20Australia%20and%20New%20York,stem%20cell%20candidate%20Ryoncil%20(remestemcel)

5 **Dilogo IH**, Aditianingsih D, Sugiarto A, Burhan E, Damayanti T, Sitompul PA, Mariana N, Antarianto RD, Liem IK, Kispa T, Mujadid F, Novialdi N, Luviah E, Kurniawati T, Lubis AMT, Rahmatika D. Umbilical cord mesenchymal stromal cells as critical COVID-19 adjuvant therapy: A randomized controlled trial. *Stem Cells Transl Med* 2021; **10**: 1279-1287 [PMID: 34102020 DOI: 10.1002/sctm.21-0046]

6 **Desterke C**, Griscelli F, Imeri J, Marcoux P, Lemonnier T, Latsis T, Turhan AG, Bennaceur-Griscelli A. Molecular investigation of adequate sources of mesenchymal stem cells for cell therapy of COVID-19-associated organ failure. *Stem Cells Transl Med* 2021; **10**: 568-571 [PMID: 33237619 DOI: 10.1002/sctm.20-0189]

Published by **Baishideng Publishing Group Inc**
7041 Koll Center Parkway, Suite 160, Pleasanton, CA 94566, USA
Telephone: +1-925-3991568
E-mail: bpgoffice@wjgnet.com
Help Desk: https://www.f6publishing.com/helpdesk
https://www.wjgnet.com